

EPA-600/4-81-001  
February 1981

REMOTE MONITORING OF ORGANIC CARBON IN SURFACE WATERS

by

Michael Bristow and David Nielsen  
Environmental Monitoring Systems Laboratory  
U.S. Environmental Protection Agency  
Las Vegas, Nevada

ENVIRONMENTAL MONITORING SYSTEMS LABORATORY  
OFFICE OF RESEARCH AND DEVELOPMENT  
U.S. ENVIRONMENTAL PROTECTION AGENCY  
LAS VEGAS, NEVADA 89114

EPA-600/4-81-001  
February 1981

REMOTE MONITORING OF ORGANIC CARBON IN SURFACE WATERS

by

Michael Bristow and David Nielsen  
Environmental Monitoring Systems Laboratory  
U.S. Environmental Protection Agency  
Las Vegas, Nevada

ENVIRONMENTAL MONITORING SYSTEMS LABORATORY  
OFFICE OF RESEARCH AND DEVELOPMENT  
U.S. ENVIRONMENTAL PROTECTION AGENCY  
LAS VEGAS, NEVADA 89114

## DISCLAIMER

This report has been reviewed by the Environmental Monitoring Systems Laboratory, U.S. Environmental Protection Agency, and approved for publication. Mention of trade names or commercial products does not constitute endorsement or recommendation for use.

# CONTENTS

	<u>Page</u>
Figures. . . . .	v
Tables . . . . .	vii
Abbreviations and Symbols. . . . .	viii
1. Introduction . . . . .	1
2. Conclusions. . . . .	3
3. Recommendations. . . . .	4
4. Review . . . . .	5
Existing methodology for determining total organics in surface waters . . . . .	5
Possible methods for remote monitoring total organics in surface waters . . . . .	7
5. Previous Laboratory Studies on the Fluorescence of Natural Waters. . . . .	9
6. Effects of Optical Attenuation on Water Fluorescence Measurements. . . . .	13
Raman correction of airborne fluorescence measurements. . . . .	17
Raman correction of laboratory fluorescence measurements. . . . .	20
7. Sample Collection, Analysis and Preservation . . . . .	21
Sample sources. . . . .	21
Organic carbon analyses . . . . .	22
Fluorescence analyses . . . . .	23
Preservation and preparation of fluorescence samples. . . . .	28
8. Data Analysis. . . . .	36
Linear correlation results. . . . .	36
Multiple correlation effects. . . . .	59
9. Differences between Laser Fluorosensor and Spectrofluorometer Measurements of $F_R/R$ . . . . .	60

## CONTENTS (Continued)

	<u>Page</u>
10. Discussion . . . . .	67
Inherent limitations in the $F_{\lambda}/R$ - DOC correlation method. . . . .	67
Calibration of airborne $F_R/R$ data in terms of DOC concentration . . . . .	70
Improvements in experimental methodology. . . . .	73
Detailed presentation of conclusions. . . . .	74
References . . . . .	77

## FIGURES

	<u>Page</u>
1 Principle of operation of airborne laser fluorosensor. . . . .	14
2 Corrected fluorescence emission spectra for lake and ultra pure water samples . . . . .	15
3 Optical diagram of corrected-spectra spectrofluorometer (Perkin-Elmer MPF4). . . . .	25
4 Transmission curve for Cation-X liquid filter. . . . .	26
5 Schematic showing water fluorescence and Raman emission parameters obtained from spectra produced using a laboratory spectrofluorometer. . . . .	27
6 Variation of $F_{\max}/R$ with time for different preservation and preparation procedures as applied to identical subsamples. CV is the coefficient of variation ( $S/\bar{x}$ ) . . . . .	30
7 Variation of DOC (mg/l) with $F_{\max}/R$ for 158 samples. . . . .	37
8 Variation of DOC (mg/l) with $F_R/R$ for 158 samples. . . . .	38
9 Variation of TOC (mg/l) with $F_{\max}/R$ for 158 samples. . . . .	39
10 Variation of TOC (mg/l) with $F_R/R$ for 158 samples. . . . .	40
11 Variation of linear correlation coefficient, $r$ , with wavelength for $F_{\lambda}/R$ versus DOC, $F_{\lambda}/R$ versus TOC, $F_{\lambda}/R$ versus POC and $F_{\lambda}/R$ versus turbidity. . . . .	46
12 Variation of turbidity (NTU) with bandwidth of fluorescence emission spectrum, BW (nm), for 110 samples. . . . .	49
13 Variation of DOC (mg/l) with $F_{\max}/F_R$ for 158 samples . . . . .	54
14 Variation of DOC (mg/l) with central wavelength of fluorescence emission band, $\lambda_{\text{cen}}$ (nm), for 155 samples. . . . .	55

	<u>Page</u>
15 Variation of central wavelength of fluorescence emission band, $\lambda_{cen}$ (nm), with $F_{max}/F_R$ . . . . .	56
16 Changes in fluorescence spectrum parameters produced by progressively diluting an Atchafalaya River sample (#E-1) with high-purity water . . . . .	57
17 Optical layout for laboratory simulation of airborne laser fluorosensor for monitoring surface water organics . . . . .	61
18 Emission spectrum showing [OH]-stretch water Raman band from high-purity water sample at 381 nm, excited by $N_2$ laser at 337 nm . . . . .	62
19 Variation of $F_R/R$ from simulated laser fluorosensor measurements with comparable values measured using a laboratory spectrofluorometer for a variety of field samples. . . .	63

## TABLES

	<u>Page</u>
1 Summary of Published Fluorescence/Organic Carbon Correlation Data. . . . .	12
2 Correlation Coefficients for Fluorescence Emission Parameters versus Water Quality Parameters . . . . .	42
3 Correlation Coefficients for Relationships Between Water Quality Parameters. . . . .	43
4 Maximum, Mean and Minimum Values for Fluorescence and Water Quality Parameters. . . . .	44



## LIST OF ABBREVIATIONS AND SYMBOLS

### Abbreviations

BOD	-	Biochemical oxygen demand
BW	-	Bandwidth of fluorescence spectrum
CCE	-	Carbon chloroform extract
CHLA	-	Chlorophyll <u>a</u>
COC	-	Colloidal organic carbon
COD	-	Chemical oxygen demand
COND	-	Conductivity
CV	-	Coefficient of variation
DO	-	Dissolved oxygen
DOC	-	Dissolved organic carbon
FWHM	-	Full width at half maximum
GAC	-	Granulated activated carbon
NTU	-	Nephelometric turbidity unit
[OH]	-	Notation for hydroxyl radical
PH	-	Sample pH
POC	-	Particulate organic carbon
RFM	-	Rapid fluorometric method
S	-	Sample standard deviation
TOC	-	Total organic carbon
TRANSP	-	Secchi disc transparency
TURB	-	Turbidity
UV	-	Ultraviolet
$\bar{x}$	-	Sample mean

### Subscripts

C	-	Central wavelength, per computer printout. Same as CEN.
CEN	-	Central wavelength
L	-	Laser (excitation) wavelength
LFS	-	Laser fluorosensor value
M	-	Maximum wavelength, per computer printout. Same as MAX.
MAX	-	Maximum wavelength
R	-	Raman wavelength
SPF	-	Spectrofluorometer value
T	-	Value at T°C
f	-	Fluorescent substance
W	-	Water
$\lambda$	-	Fluorescence wavelength
O	-	Value at 0°C

## LIST OF ABBREVIATIONS AND SYMBOLS (Continued)

### Superscripts

D	-	Dissolved substance
F	-	Fluorescent substance
NF	-	Nonfluorescent substance
P	-	Particulate substance

### Symbols

A	-	Proportionality constant in Equation 9
C	-	Proportionality constant in Equation 5
DOC	-	Concentration of dissolved organic carbon
F	-	Fluorescence power or intensity
H	-	Elevation of sensor above water surface
K	-	Diffuse attenuation coefficient
L	-	Fluorescence wavelength, per computer printout. Same as $\lambda$ .
N	-	Number of samples
P	-	Laser output power
R	-	Raman power or intensity
T	-	Temperature
b	-	Carbon conversion factor, as defined in Equation 9
d	-	Constant accounting for system and environmental factors
h	-	Depth of sample volume below water surface
i	-	Dimensionless number
k	-	Effective optical attenuation coefficient of water sample
m	-	Temperature coefficient
n	-	Concentration
q	-	Dimensionless number
r	-	Pearson product-moment linear correlation coefficient
s	-	Dimensionless number
t	-	Dimensionless number
y	-	Dimensionless number
$\alpha$	-	Beam attenuation coefficient
$\delta_1$	-	Constant, defined in Equation 4
$\delta_2$	-	Constant, defined in Equation 6
$\delta_3$	-	Constant, defined in Equation 7
$\lambda$	-	Fluorescence wavelength
$\sigma$	-	Excitation cross section
$\tau$	-	Pulse width

## SECTION 1

### INTRODUCTION

Waterborne organic substances are of concern because of their recognized impact on public health, and because of the effects of manmade organics on the aquatic ecosystem. Alarm has been voiced over the presence of toxic and potentially carcinogenic organic materials in drinking water. High concentrations of organics in natural waters can lead to malodorous and toxic conditions which reduce the utility of these waters as a drinking water resource and for recreational purposes. However, a certain concentration of organic substances of natural origin is essential for maintaining a balance in the energy and carbon cycles of the ecosystem, particularly with regard to bacterial growth. Bacteria play an essential role in the biodegradation of organic substances, both natural and manmade. However, the large amounts of oxygen required by this process to degrade high concentrations of organics can lead to severe oxygen depletion with predictable effects on higher aquatic life forms. Alternatively, high concentrations of toxic organics may lead to total elimination of the local biological community.

Organic carbon determinations are routinely accomplished by making laboratory analyses on grab samples. This approach is both time-consuming and costly in terms of manpower and facilities. In addition, because of the relatively long time required to take grab samples from launches or helicopters, it is rarely possible to obtain a synoptic record of organic carbon distribution for a given water surface due to water movement and diurnal effects.

In contrast, both airborne and satellite remote monitoring techniques are capable of rapidly and cost effectively providing data for certain water quality parameters from large areas of water surface without influencing the nature of the sample. The principal limitation of remote sensing in its present form is the inability to provide information from below the surface layer. For active as well as passive sensors operating in the optical region, the depth of this layer is generally on the order of 0.3 to 30 meters, but is more correctly characterized by the attenuation length, the reciprocal of the optical attenuation coefficient measured at a specific wavelength. The concept of a single characteristic attenuation length makes the assumption that the substances responsible for this attenuation are homogeneously distributed.

The subject of this laboratory study is the feasibility of measuring the concentration of organic carbon in the surface layers of natural waters from an airborne platform. At the present time, no proven remote sensing technique exists that is capable of monitoring, directly or indirectly, the organic carbon content of surface waters. It is therefore intended that the results

of this study will be used in the design of a compact integrated airborne system capable of mapping trends, gradients and anomalies in the distribution of organic carbon in surface waters.

## SECTION 2

### CONCLUSIONS

The results of this laboratory feasibility study demonstrate that the Raman-normalized fluorescence emission induced in surface waters by ultraviolet radiation can be used to provide a unique airborne remote sensing capability for monitoring the concentration of DOC.

Airborne laser fluorosensors that utilize this principle will provide a synoptic survey capability for rapidly and cost effectively producing isopleth maps that show concentrations of surface water DOC. These maps can be used for delineating gradients, temporal changes and anomalies in the distribution of total dissolved organics in the surface layers of rivers, lakes and coastal waters. Anomalous features in the airborne data that cannot be readily explained on the basis of existing information can then be investigated in more detail either by means of in situ monitoring or by laboratory analyses of grab samples. Specific applications include baseline monitoring of pristine lakes, verification of lake cleanup and restoration, sampling network design, ecosystem modeling, and defining the location and extent of point and nonpoint sources of organic pollution of unknown origin. Sources of organic carbon include, but are not restricted, to harbors, marinas, septic tank leachates, oil refineries and industrial sites adjacent to waterways, pulp and paper mill effluents, feed lot runoff, municipal sewage effluents, agricultural and silviculture activities, and surface runoff containing organic materials from both living and decayed natural vegetation. (See Section 10 for a detailed presentation of conclusions).

### SECTION 3

#### RECOMMENDATIONS

Factors to be considered when designing an airborne laser fluorosensor for monitoring dissolved organic carbon (DOC) are:

(i) The Raman normalized fluorescence signal should be used in preference to the uncorrected fluorescence signal as an indicator of DOC.

(ii) The Raman normalized fluorescence emission measured at the water Raman wavelength should be used in preference to the maximum value of the Raman normalized fluorescence emission as the parameter characterizing surface water DOC.

(iii) Careful consideration should be given to conflicting requirements when choosing a (laser) wavelength for exciting fluorescence in waterborne organics.

With regard to the operation of an airborne laser fluorosensor it is suggested that:

(i) The airborne fluorescence data should be regarded as a more reliable indicator of surface water DOC than of total organic carbon (TOC), because of the unpredictable and relatively nonfluorescent nature of the particulate organic fraction (POC), where  $TOC = DOC + POC$ .

(ii) The airborne measurements of the Raman normalized fluorescence emission should be calibrated directly in terms of DOC by making a small number of selected ground truth measurements of DOC on samples collected under the sensor flight path concurrent with the airborne survey.

(iii) The ground truth samples for DOC analysis should be prepared with precleaned silver membrane filters, treated with high purity acid and sealed into glass ampoules in those situations where samples cannot be analyzed directly at the field collection site.

## SECTION 4

### REVIEW

#### EXISTING METHODOLOGY FOR DETERMINING TOTAL ORGANICS IN SURFACE WATERS

Dissolved, colloidal and suspended particulate organic matter in lake and river water, which is predominantly natural in origin, can generally be classified under the headings of humic, fulvic and hyalomelanic acids of uncertain structure, with the addition of smaller percentages of polysaccharides, peptides and tannins (Rook, 1977). Although not toxic in low concentrations, there is evidence that these substances can act as carriers for more toxic manmade pollutants, both inorganic (Schnitzer, 1971) and organic (Ogner and Schnitzer, 1970). Evidence now exists that humic and fulvic acids in surface waters act as carriers of trace metals (Nriagu and Coker, 1980). Waters which are highly enriched in organics contain, in addition to the above mentioned substances, significant concentrations of small biodegradable molecules, sulphonated lignins, sulphonated aromatics and chlorinated hydrocarbons (Rook, 1977).

Recently, much concern has been expressed over the presence of trace amounts of halogenated hydrocarbons detected in drinking water (Trussell and Umphres, 1978). A prime example is chloroform, a trihalomethane, which is frequently present in parts per billion concentrations. It is now generally accepted that this substance is a carcinogen in animals (Tardiff, 1977). It is also recognized that chlorinated hydrocarbons are produced during routine chlorination from natural dissolved organics such as humic and fulvic acids, free fatty acids, alcohols, etc., that are present in the source waters (Rook, 1977; Youssefi et al., 1978).

Another group of organics known as polynuclear aromatic hydrocarbons has been detected in the water environment. These substances, usually formed in combustion or other high temperature processes, are also considered to be highly carcinogenic, e.g. 3,4-benzpyrene (Andelman and Suess, 1970). Although their solubility in water is extremely low, these substances are suspected of being transported by adsorption onto colloidal aggregates of natural organics or of becoming solubilized by detergents or similar substances.

Waterborne organics, whether dissolved or particulate, can be categorized as originating from either point or nonpoint sources. Typical point sources are municipal sewage effluents, industrial discharges and waste waters, and mineral oil pollution from harbors, marinas, oil tankers, shipping and oil refineries. Nonpoint sources generally can be broken down into three categories. The first category encompasses runoff waters from highways, construction sites, natural vegetation, lands under silviculture and

agriculture, and landfills such as those associated with mining activities. Second, groundwater leachates from sources such as septic tank facilities introduce organics into surface waters. Third, the atmosphere introduces organics into surface waters, through the medium of rainwater and fallout of atmospheric particulates (Wakeham, 1977), and also in the form of airborne litterfall (Gasith and Hasler, 1976).

Total organic carbon (TOC) and its dissolved component (DOC) are now generally accepted as the primary measurement parameters for gauging the organic carbon content of a water sample. They are nonspecific water quality indicators which provide an accurate indication of the concentration of total organics present in a water sample (Kehoe, 1977).

As indicators of waterborne organic carbon, TOC and DOC have distinct advantages over other parameters such as biochemical oxygen demand (BOD) and chemical oxygen demand (COD) that have been widely used for this purpose in the past (Kehoe, 1977; Dishman, 1979). The BOD and COD water quality tests involve measuring the oxygen consumed during a controlled biochemical or chemical oxidation process and then calculating the corresponding concentration of organic carbon. The TOC and DOC measurements can be readily made within a few minutes by automated or semiautomated instrumentation (Goulden, 1976; Michalek et al., 1977; Dishman, 1979), whereas the BOD and COD measurements take respectively five days and approximately two to three hours to accomplish by means of wet chemistry. The BOD test fails to account for that fraction of the organic carbon that is not biodegradable; in many situations this can be a significant fraction of the total. In addition, the BOD test is susceptible to a number of problems including the effects of biological seed acclimatization, pH and toxic substances, and fails to oxidize certain organic materials. Similarly, the COD test also fails to oxidize certain refractory organics, and is sensitive to the presence of inorganic compounds that are capable of consuming available oxygen.

On the other hand, the TOC and DOC methods are relatively free of interferences and are capable of nearly 100 percent organic carbon recovery. Possibly the principal advantage of the TOC and DOC methods over the BOD and COD methods are their ability to encompass the complete range of concentrations from grossly polluted waters and discharge effluents through to high quality waters ( $<1$  mg/l); at an organic carbon concentration of 1 mg/l, accuracy of the TOC method should be better than  $\pm 5$  percent. By contrast, BOD and COD values are not reliable below 10 mg/l. It is therefore not surprising that universal relationships between TOC and BOD or TOC and COD do not exist, although high correlations between TOC and either BOD or COD for specific waste or fresh waters have been obtained (Stevens and Symons, 1974; Chandler et al., 1976; Dishman, 1979; Constable and McBean, 1979). It should therefore be emphasized that, in general, the BOD and COD measurements are unreliable as indicators of organic carbon unless a correlation can be established for a specific water type. Similarly, the TOC and DOC measurements should not be utilized to indicate oxygen demand unless specific relationships have been established with either BOD or COD.

In a study of the variation of TOC for Lake Superior, Maier and Swain (1978) have indicated that the use of BOD as a measure of waterborne organics



is so insensitive that early signs of irreversible damage to water quality might go undetected. Similarly, in a 5-year study of the Rhine in West Germany, DOC was found to be a significantly more sensitive indicator of clean-up progress than was COD, particularly when variations in river flow rate were taken into account (Sontheimer, 1977).

The ability to remotely monitor TOC over extensive areas would therefore be advantageous not only because of its cost effectiveness in relation to direct sampling methods, but also because it is possibly the only way in which a synoptic record can be obtained at a single time. On a single airborne mission over a given water body, a remote sensing device for monitoring organic carbon could make the equivalent of several million TOC analyses on surface water samples within a period of one hour. By use of relatively cheap microprocessor technology these airborne data could then be converted in near real time into a map of the water surface showing isopleths of surface water organic carbon concentration. Such a map would be used as a general purpose screening or survey tool for locating and monitoring anomalies, gradients, point and nonpoint sources, and, in particular, sources of unknown origin. TOC surveys such as that conducted by Maier and Swain (1978) for Lake Superior, would be an ideal application for a device of this kind. In addition, such maps might be used for designing sampling networks or for indicating how best to further investigate, by direct sampling methods, sources of waterborne organics of known or unknown origin.

#### POSSIBLE METHODS FOR REMOTE MONITORING TOTAL ORGANICS IN SURFACE WATERS

Currently, passive remote sensing in the form of multispectral scanner imagery has achieved only limited success in predicting the concentration of water quality parameters. Much effort has been expended on formulating interpretation schemes for extracting information on concentration of phytoplanktonic chlorophyll *a* (Miller et al., 1977; Morel and Prieur, 1977; Wilson et al., 1978; Johnson, 1978) and suspended sediment (Johnson et al., 1977; Bowker and Witte, 1977; Sydor et al., 1978) in surface waters. Empirical regression models based on extensive concurrent ground truth data must be devised for each application in order to reliably interpret the satellite or airborne data. This is necessary because of the overlap in the spectral reflectance characteristics of suspended sediment and phytoplankton in the visible and near infrared spectral regions. Provided that the concentration of one substance remains dominant, then the model is likely to hold, but this can be quickly undermined by significant fluctuations in algal production (especially at the surface) and suspended sediment runoff that occur on a seasonal basis. Extrapolation of a given interpretation model to data from a different geographical location is generally not feasible because each waterbody has its own peculiar distribution of phytoplankton and suspended sediment types with their own specific optical absorption and scattering properties.

An attempt to remotely monitor organics in surface waters has been made by Davis and Fosbury (1973). They were able to correlate the optical density of black and white multispectral photography with a number of water quality parameters. A correlation coefficient of -0.60 was obtained between TOC

ground truth data and film optical density from flights over the Houston Ship Channel. No attempts were made to calibrate film density with respect to TOC concentration. Clearly, if such an approach is to be developed, the effects of atmospheric backscatter, atmospheric transmission and sky reflection would need to be eliminated and corrections made for the effects of chlorophyll and suspended sediment. It is possible that this correlation is more circumstantial than causal due to the fact that for this one measurement, the solar backscatter was predominantly from material that was organic in origin. However, situations frequently exist where this is not true.

More recently airborne lidar devices employing a laser induced fluorescence approach have shown promise in the area of water quality monitoring. These devices, known collectively as laser fluorosensors, have been used to detect surface water oil spills (Kim and Hickman, 1975; O'Neil et al., 1975; Bristow, 1978), and to generate fluorescence emission spectra that are characteristic of the oil slick (Fantasia and Ingrao, 1974; O'Neil et al., 1980). In addition, they have been successfully used to remotely profile surface waters for chlorophyll a present in phytoplankton (Bristow et al., 1979; Farmer et al., 1979), and for the lignin effluents from pulp and paper mills (O'Neil et al., 1975; Bristow, 1978). This latter application is of particular relevance to the present study as it represents a special category of a highly fluorescent dissolved organic material that can be readily detected using an airborne laser fluorosensor.

Although no attempt has yet been made to use the laser fluorosensor method for remotely sensing total organics in surface waters, a number of studies in the published literature indicate the existence of a relationship between the concentration of total organics in a given sample and the intensity of the UV excited fluorescence emission. The following chapter reviews the results of these studies with the specific purpose of gauging the potential of any such relationship as a means for remotely monitoring waterborne organic carbon.

## SECTION 5

### PREVIOUS LABORATORY STUDIES ON THE FLUORESCENCE OF NATURAL WATERS

The existence of the blue, UV-induced fluorescence emission from natural, drinking and polluted waters has been known for many years (Dienert, 1910; Radley and Grant, 1935; DeMent and Dake, 1942). McLean and Speas (1946) proposed fluorometric screening of well drinking water for the presence of bacterial contamination. Work on the fluorescence of sea water has been reviewed by Kalle (1966), Duurmsa (1974) and Jerlov (1976). This fluorescence is shown to be restricted principally to coastal waters; deep ocean water is known to have a very low organic content and to exhibit relatively weak fluorescence emission. The exact chemical formulations of the substances responsible for this sea water fluorescence are not well understood although they are known to be relatively stable. Consequently, this fluorescence emission can be used to monitor the mixing of river and coastal water with deep ocean water. In addition, these substances are known to be part of a much larger group of sea water organics known collectively as gelbstoffe (yellow stuff). The main sources for these organics are runoff from land introduced principally as river water, rain water, and from in situ formation through the activity and decay of biological matter.

Earlier work on the fluorescence of fresh waters has been reviewed by Smart et al. (1976). Organics of natural origin enter lake and river water in the same manner as for sea water and can generally be classified as humic, fulvic and hymatomelanic acids. Black and Christman (1963), Seal et al. (1964), Levesque (1972) and Hall and Lee (1974) have investigated the fluorescence spectra of humic compounds present in soil and colored waters and also the influence that pH has on the wavelength and intensity of this emission.

A quantitative fluorescence technique for monitoring dissolved waterborne organics has been developed and is being used for gauging the adsorption efficiency and lifetime of activated carbon columns used for removing dissolved organics in drinking water treatment plants (Sylvia, 1973; Sylvia et al., 1974; 1977; Montalvo and Lee, 1976). This technique, called the rapid fluorometric method (RFM), is based on the existence of a strong correlation between the fluorescence emission intensity excited in drinking water samples from a single source and the weight of dissolved organics adsorbed from the same sample water by a granulated activated carbon (GAC) sample; these trapped organics are dissolved from the activated carbon using chloroform and the resultant carbon chloroform extract (CCE) determined gravimetrically. Although about six man hours of time are required for each GAC and CCE determination, the whole process can take at least eight days to perform (Buelow et al. 1973), whereas the RFM measurement can be made in a few

minutes. It should be noted that, because of the lengthy sample preparation time, and because the adsorption and extraction processes are not 100 percent efficient (Stevens and Symons, 1974), the GAC/CCE measurement has not found favor as an indicator of waterborne dissolved organics.

A number of studies have been published on methods for determining the concentration of pulp and paper mill effluents by performing fluorescence analyses on either grab or in situ water samples. These effluents contain high concentrations of dissolved organic substances, many of which are considered hazardous to the aquatic environment due to their high toxicity and tendency to produce conditions of high oxygen demand (Walden, 1976). Christman and Minear (1967), Thruston (1970), Wilander, Kvarnas and Lindell (1974) and Almgren et al. (1975) have established the fluorescence properties for lignosulphonate effluents from sulfite process mills. Likewise, Baumgartner et al. (1971) have established the fluorescence properties for kraft mill effluents. For specific locations it has been shown that the intensity of the UV-induced fluorescence emission at a specific wavelength is highly correlated with the effluent concentration, thereby providing the basis for a rapid in situ tracer method for determining the concentration of these effluents. Fluorescence emission from humic substances present in these same waters was found to occur at longer wavelengths, and as such, did not constitute a significant source of interference (Almgren et al., 1975). Airborne laser fluorosensors have been successfully used to monitor the presence and extent of lignosulphonate effluents in surface waters (O'Neil et al., 1975; Bristow, 1978). In addition, it was shown that the intensity of the fluorescence emission from the organics in the relatively unpolluted waters upstream from these effluent outfalls could be detected with good sensitivity using existing technology (Bristow, 1978).

Fluorescence techniques have also been applied to in situ monitoring of the dispersal of septic tank leachates in near-shore surface waters. Kerfoot and Brainard (1978) measured the concentration of leachates using the ratio of fluorescence to ionic conductivity as the pollutant indicator. System calibration was achieved by measuring this ratio for a leachate sample of known concentration. The fluorescence signal was considered to be due to the presence of fluorescent detergent whiteners, surfactants and natural degradation products that are persistent under conditions of darkness and low dissolved oxygen.

In all of the above water fluorescence studies, no attempts were made to relate this UV-induced fluorescence emission to established water quality parameters indicative of organic carbon, such as BOD, COD, TOC and DOC. However, more recently the results of a number of studies have become available in which data relating the UV-induced fluorescence emission of water samples to either TOC or DOC are presented.

Zimmerman and Bandy (1975) and Huro et al. (1977) examined the relationships between fluorescence and DOC and between fluorescence and TOC, respectively, for marine waters, whereas Lakshman (1975), Measures et al. (1975) and Smart et al. (1976) compared sample fluorescence to TOC for a variety of different fresh water types.

The measurements of Symons et al. (1975) were somewhat different and, as such, nonrepresentative in that they examined drinking water samples from 30 cities in the United States rather than natural waters. In addition, they were careful to note that their measurements encompassed only the nonvolatile fraction of TOC, as the generally small volatile fraction was driven off with the inorganic  $\text{CO}_2$  when purging the acidified samples. As no mention is made in the other studies cited above of preparations to monitor the organic carbon level of the headspace above the sealed samples, it can be assumed that the reported TOC and DOC measurements were also made on the nonvolatile fraction of the samples.

The correlation data for these studies are summarized in Table 1 together with information on the emission and excitation wavelengths employed in the fluorescence analyses. Also shown are the data of Sylvia et al. (1974, 1977) in which sample fluorescence is compared to the CCE accumulated in a GAC column in a drinking water treatment plant. Reasons why the correlation coefficients obtained in these studies vary over a range from 0.46 to 0.99 for the comparisons between the fluorescence and organic carbon data are not immediately apparent. The most likely explanation is that the ratio of fluorescent to nonfluorescent organics is not a constant, but varies due to changes in the concentration and nature of the fluorescent organics that are unrelated to the changes in the TOC and DOC concentrations.

It is notable that in the studies by Zimmerman and Bandy (1975) and by Measures et al. (1975), which are aimed at an airborne laser fluorosensor application for monitoring waterborne organics, the fluorescence emission data were normalized by means of the concurrent water Raman emission signal. This normalization procedure corrects for the attenuation of the fluorescence signal caused by the presence of both dissolved and particulate matter present in the sample.

The present laboratory study was therefore initiated with the purpose of conducting an investigation of the relationships between the fluorescence characteristics of surface waters and the widely accepted organic carbon water quality parameters TOC and DOC, and of establishing the possibility of using these characteristics as a means for remotely monitoring total organics from an airborne platform. In particular, attention will be paid to finding the best water fluorescence parameter for this purpose and to investigating the merits of the Raman normalization procedure as a means of correcting both the laboratory and airborne measured fluorescence data for the effects of optical attenuation.

This study is presented in four parts. The first part (Chapter 6) deals with the effects of optical attenuation on the fluorescence data, and with the Raman normalization procedure. The second part (Chapter 7) describes the experimental methodology with some emphasis being placed on methods for storing and preparing water samples for fluorescence analysis. The third part (Chapter 8) examines the correlations obtained between water quality parameters that are a measure of organic carbon and various fluorescence emission parameters. The fourth part (Chapter 9) is an investigation of problems that are encountered when attempting to apply fluorescence-DOC regression data established in this or similar laboratory studies to the interpretation of fluorescence data obtained using an airborne laser fluorosensor in terms of surface water DOC.

TABLE 1. SUMMARY OF PUBLISHED FLUORESCENCE/ORGANIC CARBON CORRELATION DATA

Reference	Organic Carbon Parameter	Fluorescence Parameters		Raman Corrected	Sample Source	Number of Samples	Linear Correlation Coefficient
		Excitation Wavelength (nm)	Emission Wavelength (nm)				
Sylvia et al., 1974	Carbon Chloroform Extract	340	390	No	From granulated activated carbon column in drinking water treatment plant	52	0.96
Sylvia et al., 1977	Carbon Chloroform Extract	340	390	No	From granulated activated carbon column in drinking water treatment plant	80	0.93
Zimmerman and Bandy, 1975	DOC	337	Max.	Yes	Fresh and marine estuarine waters	39	0.71*
Lakshman, 1975	TOC	365	460	No	Agricultural runoff and water extracts from manure	9	0.98
Symons et al., 1975	Non Volatile TOC	340	390	No	Drinking water from 80 cities in USA	73	0.69*
Symons et al., 1975	Non Volatile TOC	310	Total Emission	No	Drinking water from 80 cities in USA	80	0.66*
Measures et al., 1975	TOC	337	Max.	Yes	Creek and river water	7	0.73
Smart et al., 1976	TOC	365	510	No	Miscellaneous	24	0.98
Smart et al., 1976	TOC	365	510	No	Freeway runoff	17	0.46
Smart et al., 1976	TOC	365	510	No	Creek water	34	0.87
Huro et al., 1977	TOC	340	450	No	Coastal marine water	15	0.99

\* Estimated by present authors from graphical data

## SECTION 6

### EFFECTS OF OPTICAL ATTENUATION ON WATER FLUORESCENCE MEASUREMENTS

Airborne laser fluorosensors use high power, pulsed, blue or ultraviolet (UV) lasers to excite fluorescence emission in a sample volume in the water surface. A fraction of this multidirectional emission is collected by a large aperture telescope and converted into an electrical signal by an optical detector. This fluorescence signal, in conjunction with aircraft navigation data, can be used to prepare contour maps showing the variation in concentration of the specific water quality parameter under investigation. The principle of operation for the laser fluorosensor is illustrated in Figure 1 in which the airborne platform is usually flown at a height of several hundred meters above the water surface. The volume of water interrogated by the system is approximately defined by the diameter of the laser excitation spot on the water surface and the penetration depth of the laser beam. For a homogeneous vertical distribution of dissolved and particulate matter in the sample column, this depth can be represented by the characteristic optical attenuation length. Assuming that the attenuation lengths at the laser and fluorescence wavelengths are approximately equal, then it can be shown that  $(1 - 1/e^2)$ , i.e. 86.5%, of the fluorescence radiation received by an airborne laser fluorosensor is emitted from the first attenuation length (e.g. see Friedman and Hickman, 1972).

The spectral nature of this laser-induced fluorescence emission from typical surface waters can be readily demonstrated using a proprietary laboratory spectrofluorometer. The two emission spectra shown in Figure 2 were obtained on high purity and lake water samples using a laboratory spectrofluorometer (Perkin Elmer MPF-4), which has a corrected spectra attachment that eliminates spectral artifacts that would otherwise be introduced by the emission and excitation monochromators, the xenon excitation lamp and the photomultiplier detector. Excitation at 337 nm was employed as it lies close to the wavelength producing the maximum fluorescence emission in fresh water samples, and also because it corresponds to that of the widely available pulsed nitrogen laser. This type of laser has already been used in an airborne laser fluorosensor system capable of monitoring the fluorescence of natural waters with good sensitivity (Bristow, 1978), albeit in the absence of a solar background signal.

These water fluorescence spectra exhibit two features of interest. First, the lake water sample exhibits a broad blue fluorescence band peaked in the region of 430 nm whereas the spectrum for the high purity sample is essentially fluorescence free. Treatment of water samples by passage through an activated charcoal trap to remove organics also eliminates essentially all of this fluorescence signal (Sylvia, 1973; Montalvo and Lee, 1976), suggesting

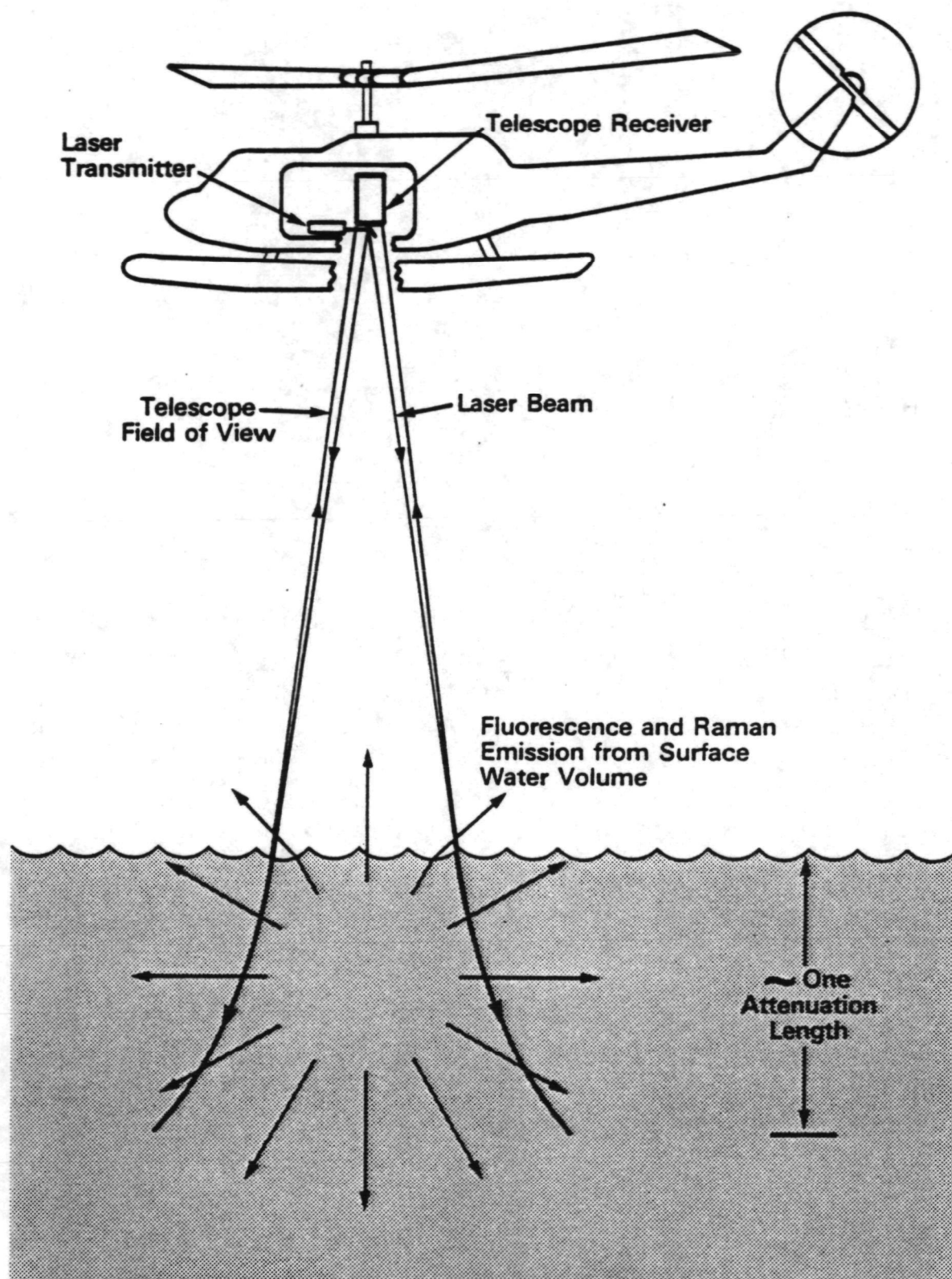


Figure 1. Principle of operation of airborne laser fluorosensor.



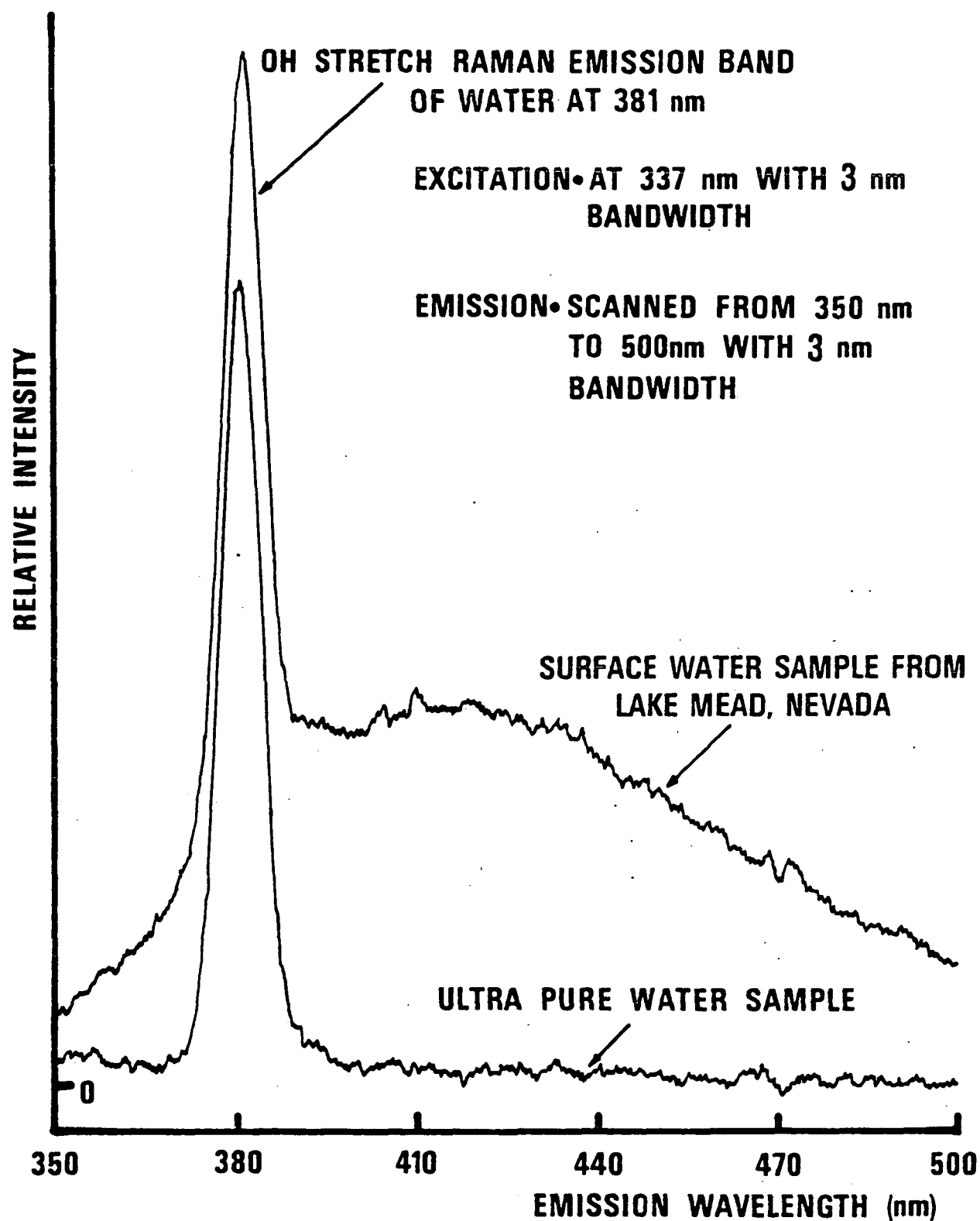


Figure 2. Corrected fluorescence emission spectra for lake and ultra-pure water samples.

that fluorescent inorganics make a negligible contribution to the fluorescence of natural waters. The sample obtained from Lake Mead in Nevada, is known to be low in organics having a TOC level on the order of 1 mg/l. This suggests that a fluorescence signal that can be measured with high sensitivity from samples low in TOC might be usable as an indicator of surface water organics provided that the fluorescence and organic carbon parameters can be related in a meaningful way.

The other spectral feature, an intense, relatively narrow, constant amplitude band located at 381 nm and superimposed on the fluorescence spectrum, is the Raman emission for the OH vibrational stretching mode of water. Unlike fluorescence emission, (Stokes) Raman emission is always displaced by a constant frequency shift to the longwave side of the excitation wavelength. For water in the liquid phase, this frequency shift is  $3,418 \text{ cm}^{-1}$ , which, for excitation at 337 nm, corresponds to Raman emission at 381 nm. Although the intensity and spectral shape of the water Raman band are known to be weakly dependent on water temperature and salinity (Walrafen, 1967; Chang and Young, 1974), changes that can be anticipated in these parameters for fresh water environments are not expected to affect the integrated emission intensity for the whole Raman band.

For high purity samples or those relatively low in dissolved and particulate matter, e.g., most drinking waters, and for a constant excitation intensity, the amplitude of the Raman signal emitted from a short (1 cm) pathlength sample remains essentially constant. Stated another way, self-absorption of the fluorescence and Raman radiation by the sample is negligible over a 1-cm pathlength. However, in the presence of more significant concentrations of dissolved and particulate matter, the intensity of this Raman signal will be attenuated by absorption and scattering losses. In the case of the fluorescence signal, changes in intensity may be due either to this optical attenuation or to changes in concentration of the fluorescent substances under investigation thereby introducing ambiguities into the interpretation of the fluorescence data. This attenuation can be significant in the case of samples high in dissolved organics with the result that the attenuated fluorescence signal will indicate a lower value of TOC than is actually present.

As will be shown, significant attenuation of the fluorescence emission due to self-absorption can occur in 1-cm thick laboratory samples that contain high levels of organics. In an airborne laser fluorosensor application, the effective volume of sample being interrogated will depend critically on the penetration depth of the laser beam through the surface water. As this depth or attenuation length may vary over a range from, say, 0.1 to 10 meters or more for a given water body, very large errors can be incurred in the measured fluorescence signal. Consequently, as the Raman signal is a property of water alone, and as the concentration of water is constant for all but grossly polluted waters, observed variations in its intensity will be due to variations in the optical attenuation coefficients at the laser and Raman wavelengths. The Raman signal can therefore be used as an internal reference standard with which to monitor the effect of changes in these attenuation coefficients on the concurrent fluorescence signal.

Although self evident, it should be emphasized that the water Raman signal used to monitor changes in sample optical attenuation is emitted from essentially the same sample volume and at the same time as the fluorescence signal. This is an important consideration in a remote sensing application when it is realized that marked changes in the attenuation properties of surface waters can occur over distances of a few meters.

## RAMAN CORRECTION OF AIRBORNE FLUORESCENCE MEASUREMENTS

By taking the ratio of the remotely sensed fluorescence emission intensity or power level to the corresponding Raman value, a parameter is obtained that, to a first approximation, varies only as the concentration of the homogeneously distributed fluorophor (fluorescent substance) and is independent of changes in the optical attenuation coefficients at the laser (excitation), fluorescence and Raman wavelengths. Use of this Raman correction technique has been proposed and successfully demonstrated by Bristow et al. (1979) in a similar airborne remote sensing application, which involved monitoring the concentration of surface water chlorophyll a. It was shown that the remotely sensed fluorescence power at any wavelength  $\lambda$  can be given by a general expression of the form:

$$F_{\lambda} = \left( \frac{P}{H^2} \right) \frac{n_f \sigma_f d_{\lambda}}{(k_{\lambda} + k_L)} \quad (1)$$

where  $P$  is the power of the laser excitation source at wavelength  $\lambda_L$ ,  $H$  is the fluorescent target to collector lens distance,  $n_f$  is the concentration of the fluorophor under investigation,  $\sigma_f$  is the fluorescence conversion efficiency (excitation cross section) of the fluorophor,  $d_{\lambda}$  is a constant accounting for known or measurable environmental and system factors, and  $k_{\lambda}$  and  $k_L$  are the effective optical attenuation coefficients at the fluorescence and excitation wavelengths respectively. A number of assumptions are made in the determination of this expression and these are discussed by Browell (1977) and Bristow et al. (1979). In the present context, three of these assumptions are noteworthy. First,  $F_{\lambda}$  is the emitted fluorescence power integrated over a sample of infinite depth or thickness. In reality, this means that the total water depth must be significantly larger than the optical attenuation lengths given by  $(k_{\lambda})^{-1}$  and  $(k_L)^{-1}$ . Second, at a given sampling location, the concentrations of all dissolved and particulate waterborne substances whether fluorescent or nonfluorescent that influence the values of  $k_{\lambda}$  and  $k_L$  are assumed to remain constant in the vertical dimension such that  $k_{\lambda}$  and  $k_L$  also remain constant. Third, the integration of the fluorescence power over an infinitely thick sample requires that  $\sigma_f$  remain constant over this sample volume. However, for Equation 1 to be valid in a given remote sensing application,  $\sigma_f$  must also remain constant for all sample locations. In the present application, the validity of this assumption will depend critically on the constancy of the percentage contribution of each fluorophor to the overall mixture of fluorophors over the extent of a given water body. This subject will be examined further in the discussion.

A similar expression can be written for the remotely sensed water Raman power,  $R$ , measured at wavelength,  $\lambda_R$ , such that:

$$R = \left( \frac{P}{H^2} \right) \frac{n_W \sigma_W d_R}{(k_R + k_L)} \quad (2)$$

where  $n_W$  is the concentration of water, which for all natural waters is a constant,  $\sigma_W$  is the Raman excitation cross-section for the [OH]-vibrational stretching mode of water,  $d_R$  is a constant similar to  $d_\lambda$ , and  $k_R$  is the effective optical attenuation coefficient at the Raman emission wavelength. Using Equations 1 and 2, an expression for the power ratio  $F_\lambda/R$  is obtained where:

$$\frac{F_\lambda}{R} = \frac{n_f \sigma_f d_\lambda}{n_W \sigma_W d_R} \left( \frac{k_L + k_R}{k_L + k_\lambda} \right) \quad (3)$$

As  $\sigma_f$ ,  $d_\lambda$ ,  $n_W$ ,  $\sigma_W$  and  $d_R$  are all considered to be constant, this expression can be simplified to read:

$$\frac{F_\lambda}{R} = n_f \delta_1 \left( \frac{k_L + k_R}{k_L + k_\lambda} \right) \quad (4)$$

where  $\delta_1$  is a new constant encompassing all of the above mentioned factors, and  $(k_L + k_R)/(k_L + k_\lambda)$  is a factor representing residual attenuation effects due to differential spectral absorption and scattering. The expression 'differential spectral absorption and scattering' refers to the changes in the magnitude of these optical loss mechanisms that exist between any two (or more) wavelengths, and by implication, indicates that they are wavelength dependent. Clearly, for this expression to be useful in the interpretation of remote sensing data,  $(k_L + k_R)/(k_L + k_\lambda)$  must remain constant or, at the most, change only slowly when significant changes occur in the individual  $k$  values. Preliminary airborne laser fluorosensor measurements (Bristow et al., 1979; Bristow, 1980\*) have shown that  $F_\lambda/R$  provides a better indication of changes in chlorophyll *a* concentration than does  $F_\lambda$ , suggesting that, to a first approximation,  $(k_L + k_R)/(k_L + k_\lambda)$  can be treated as a constant. Equation (4) can then be simplified to read:

$$\frac{F_\lambda}{R} = n_f C \quad (5)$$

\* Bristow, 1980, U.S. Environmental Protection Agency, unpublished data.

where C is an unknown constant that can best be determined from Equation 5 using a number of airborne measurements of  $F_\lambda/R$  together with concurrent ground truth measurements of  $n_f$  obtained on samples from a series of preselected reference sites under the sensor flightpath. In this situation,  $n_f$  will correspond to the concentration of organic fluorophors, which is closely related to total organics as represented by TOC (or DOC).

With the proposed UV laser excitation at 337 nm, Raman emission at 381 nm and fluorescence emission at (say) 430 nm, significant differences in the magnitude and behavior of the corresponding k values for similar water types can be expected (Jerlov, 1976). However, all concern over the validity of the assumption that  $(k_L + k_R)/(k_L + k_\lambda)$  remains constant can be eliminated by making both the Raman and fluorescence measurements at the same wavelength; in this case,  $(k_L + k_R)/(k_L + k_\lambda)$  becomes equal to unity.

In applications to remotely monitor the concentration of total organics, three significant advantages are to be gained by normalizing the fluorescence signal with the concurrent water Raman signal:

- (i) Raman normalization corrects for the attenuation of the fluorescence signal due to the presence of either inorganic or organic particulate and dissolved matter. For airborne applications over deep waters, the effective sample length is determined by the optical attenuation length, which may vary over a range of 100 to 1 or more. Correspondingly large corrections to the fluorosensor data are then required. In addition, as the factor  $(k_L + k_R)/(k_L + k_\lambda)$  is assumed to be a constant, no information is required concerning the analytical model needed to describe the effective optical attenuation coefficients,  $k_\lambda$ . Some controversy exists over whether the beam attenuation coefficient, the diffuse attenuation coefficient, or some intermediate form is most applicable to the laser fluorosensor situation (Browell, 1977).
- (ii) Raman normalization of the fluorescence data eliminates problems due to both short-term (within mission) and long-term changes in system sensitivity that have an equal influence on both the fluorescence and Raman signals. Such changes include but are not restricted to pulse-to-pulse fluctuations and long term drift in laser output power, line voltage changes and amplifier gain drift.
- (iii) As both the fluorescence and Raman signals exhibit a  $1/H^2$  dependence on changes in aircraft altitude, H, above the water surface target, the ratio  $F_\lambda/R$  is independent of these changes.

It should be mentioned that (i) and (ii) apply equally to remote sensing, in situ or laboratory applications for measuring water fluorescence, although for (i), attenuation effects in 1-cm pathlength samples will be relatively small requiring corrections to the fluorescence signal no greater than 50 percent.

Although not related to the present airborne laser fluorosensor application it is suggested that the measured values of R can also be used to

measure  $k_\lambda$  which in this case is the mean of  $k_R$  and  $k_L$  appearing in Equation 2. Both  $P$  and  $H$  are measurable, and  $n_w$ ,  $w$  and  $d_R$  are constant so that  $k_\lambda$  varies as  $R^{-1}$ , where  $k_\lambda = (k_L + k_R)/2$  is equivalent to the effective attenuation coefficient for some wavelength intermediate between  $\lambda_L$  and  $\lambda_R$ . The proportionality constant relating  $k_\lambda$  to  $R^{-1}$  can be determined by making a number of in situ measurements of  $k_R$  and  $k_L$  together with corresponding airborne measurements of  $R$  at the same reference locations as proposed for establishing constant  $C$  in Equation 5. Implementation of this proposal raises the question as to whether  $k_R$  and  $k_L$  are better described by the beam attenuation coefficient or by the diffuse attenuation coefficient. By arranging that an airborne mission encounter a sufficiently wide range of  $k_\lambda$  values, it may be possible to determine which of these two coefficients is a more suitable model of optical attenuation in a laser fluorosensor application.

## RAMAN CORRECTION OF LABORATORY FLUORESCENCE MEASUREMENTS

The laboratory measured values of  $F_\lambda/R$  are subject to the same secondary effects of differential spectral absorption and scattering as are the airborne measured values, but, because of the  $90^\circ$  scattering angle employed in laboratory spectrofluorometers of the type used in this study, Equations 1 through 5 are not applicable. In such an instrument, the fluorescence emission, excited in a small focal volume of sample, is viewed at  $90^\circ$  to the excitation beam in contrast to the  $0^\circ$  scattering angle employed in a remote sensing configuration. Consequently, the emission emanates from a single point at a fixed depth below the surface of an optically thin sample (typically in a 1-cm square sample cell) rather than being integrated over an infinitely deep sample volume. For emission from a point source at a fixed depth, it is easily shown (e.g. see Friedman and Hickman, 1972) that  $F_\lambda/R$  can be given by an expression of the form:

$$F_\lambda/R = n_f \delta_2 \exp \{h (k_R - k_\lambda)\} \quad (6)$$

where  $\delta_2$  is a constant analogous to  $\delta_1$  in Equation 5, and  $h$  is the sample depth, which, in this case, is the distance from the inner surface of the sample cell wall to the focal volume located at the center of the cell. In the same manner as for the remote sensing application, differential spectral attenuation effects, represented by the exponential term in Equation 6, can be eliminated by making the fluorescence measurements at the Raman band wavelength. In this case, the exponential term becomes equal to unity, and  $F_R/R = n_f \delta_2$ , which is analogous to Equation 5.

On the basis of the foregoing discussion, the fluorescence to Raman ratio,  $F_\lambda/R$ , would appear to be an ideal candidate parameter for remotely characterizing the fluorescence emission of surface waters due to its relative independence from environmental and system factors. The merits of this and other dimensionless fluorescence parameters for use as remote sensing indicators of TOC (or DOC) will therefore be examined in some detail in Chapter 8.

## SECTION 7

### SAMPLE COLLECTION, ANALYSIS AND PRESERVATION

#### SAMPLE SOURCES

A total of 161 water samples was collected for analysis. In order to avoid surface debris and oil films but, at the same time, obtain samples representative of the water surface, 1-liter samples were obtained at a depth of 1 m. This master sample was then stirred, and split into three nominally identical subsamples for the TOC, DOC and fluorescence analyses, which were stored in 100-ml polyethylene bottles.

Fifty samples, relatively low in organics, were obtained from Lake Mead and Lake Mohave, both manmade reservoirs on the Colorado River bordering Arizona and Nevada that can vary between oligotrophic and mesotrophic conditions on a seasonal basis. Although the bulk of the water is derived from the Colorado River, Lake Mead is also supplied by the Muddy River, the Virgin River and Las Vegas Wash. The latter source, a nutrient-rich stream contaminated with industrial and municipal sewage wastewater from the Las Vegas region, enters Lake Mead through Las Vegas Bay, the receiving end of which exhibits eutrophic conditions for a large part of the year. Even though the flow rate for Las Vegas Wash is only 0.5 percent of that for the Colorado River, it is the principal source of the pollutants in Lake Mead, and is especially rich in nitrogen and phosphorus. Lake Mohave, further down the Colorado River, receives all of its water from Lake Mead.

The largest set of samples, totaling 107 and ranging widely in organic content, was obtained from the Atchafalaya River Basin which is a large shallow depression located within the deltaic plain of the Mississippi River in southern Louisiana. Approximately 30 percent of the total flow of the Mississippi River enters the Basin through the Old River Control Structure where it joins with the flow from the Red River to form the Atchafalaya River. A major feature of the region is the Atchafalaya Basin Floodway, which is defined by a system of levees used to contain periodic inundation by the Mississippi River. The majority of samples were obtained from sites within the levees and were often highly colored, containing relatively high levels of particulate and dissolved organic matter. It is these conditions that are responsible for the detritus-based food chain of the waters in the floodway. In addition the limited light penetration into these turbid waters has a restraining influence on phytoplankton growth with chlorophyll a levels generally less than 10  $\mu\text{g/l}$ . In contrast, 20 samples collected from swamplands outside the levees were generally characterized by lower levels of particulate and dissolved organic matter but by higher levels of chlorophyll a. The Mississippi River also introduces significant levels of manmade

organics into the floodwaters, some of which are not readily biodegradable. Pesticides and runoff from agricultural activities in and adjacent to the Basin have been observed to have detrimental effects on fish populations, and as such, also make contributions to the overall level of organics. Although there are over 100 oil- and gas-producing wells within this basin, there is little evidence to suggest that they constitute a significant pollution threat at the present time.

In addition, four drinking and high purity water samples were included in the survey with a view to extending the range of measured values.

## ORGANIC CARBON ANALYSES

The samples for TOC and DOC analysis were acidified to pH  $\leq 2$  by the addition of HCl in order both to drive off inorganic carbon in the form of  $\text{CO}_2$  and to attenuate bacterial activity, and then, prior to analysis, were stored in the dark at  $4^\circ\text{C}$ . All TOC and DOC analyses were made with the TOC analyzer (Envirotech Dohrmann DC-52) operating in the low level, high sensitivity sparge mode using  $10\ \mu\text{l}$ -sample injections. Reproducibility of the measurements was established by making 30 replicate measurements on a Lake Mead sample relatively low in organic carbon. The mean values were  $2.86 \pm 0.10\ \text{mg/l}$  for TOC and  $0.91 \pm 0.05\ \text{mg/l}$  for DOC, where the uncertainty represents the 95 percent confidence limits for the means. The DOC values were obtained in the same manner as for the TOC values except that the particulate matter was removed prior to analysis by passing the samples through Whatman GF/F glass fiber filters. For particles  $0.7\ \mu\text{m}$  or larger in size, it is claimed that these filters have a 98 percent retention efficiency (Averso, 1976). Glass fiber filters were selected because they are known to contain very low concentrations of organic carbon (Parker, 1967; Sharp, 1974), and because cellulosic membrane filters, such as the Millipore HA,  $0.45\text{-}\mu\text{m}$  pore size filter that is frequently used for separating particulate and soluble materials in water quality work, have been shown to introduce significant amounts of organic carbon into the filtrate (Guillard and Wangersky, 1958; Cahn, 1967; Parker, 1967; Hwang et al. 1979). Comparable silver membrane filters (Selas, Flotronics Division, Huntingdon Valley, Pa.) were rejected in relation to glass fiber filters because of their higher cost, higher carbon content (Gordon and Sutcliffe, 1974; Sharp, 1974), low filtration speed (Parker, 1967) and unpredictable load capacity (Sheldon, 1972). In addition, Salonen (1979) has recently shown that silver membrane filters have a loading capacity that is several times lower than that for glass fiber filters with comparable retention efficiency. The POC data were obtained by subtracting the measured DOC values from the corresponding TOC values.

Sparging or purging the samples prior to analysis with an inert gas drives off any residual  $\text{CO}_2$  produced during acidification, but, in the process, also drives off volatile organic substances. The TOC and DOC values measured in this work should therefore be understood to represent the less-volatile fraction of their respective total values. Generally, for surface waters, volatile organics constitute only a small percentage of the total organics present (MacKinnon, 1979). In addition, the loss of volatiles



during sparging should not significantly effect the correlation with the fluorescence data, as these volatile substances are generally non-aromatic having low molecular weight, and, as such, are unlikely to exhibit significant fluorescence.

DOC and TOC blanks subsequently run on high purity water samples stored in glass containers as against polyethylene containers, with and without acidification, indicated a carbon background for the acid of about 0.4 mg/l. This acid background value was therefore subtracted from all measured TOC and DOC values. Similar tests to determine the background contribution from the polyethylene sample bottles indicated an approximate increase in carbon background on the order of 0.05 mg per day but with a large bottle-to-bottle variability. However, as the samples were usually analyzed within a five-day period, corrections for the polyethylene background were not made, partly because of its generally small value and partly because of the uncertainty in establishing a precise value. As such, this sample-bottle background level constitutes a potential source of error in the TOC and DOC data.

For the 158 samples analyzed, TOC values ranged from 0.2 to 44 mg/l with a mean value of 7.21 mg/l, DOC values ranged from 0.2 to 19 mg/l with a mean value of 4.02 mg/l and POC values ranged from 0 to 27 mg/l with a mean value of 3.47 mg/l. Although the mean value for DOC is marginally greater than that for POC, many samples had POC values considerably larger than the corresponding DOC values, and for the 50 samples from Lakes Mead and Mohave, the mean value for POC (1.48 mg/l) was 40 percent higher than the mean value for DOC (1.05 mg/l).

## FLUORESCENCE ANALYSES

As the ultimate purpose of this feasibility study is to establish a method for remotely detecting the concentration of total organics for in situ surface water samples using fluorometric techniques, every effort was made to ensure that the grab samples for fluorescence analysis remained as representative of the true field conditions as was practicably possible. Clearly, remote sensing operations do not allow for any form of sample preparation or conditioning. A number of measures were therefore taken in order to ensure that the integrity of the fluorescence properties of the grab samples was maintained during the period between collection and analysis. Procedures that minimize the changes in sample fluorescence properties with time are discussed in the following section. In at least one case, viz., that of temperature, replication of field conditions was not possible. This was of concern because it has been shown that the fluorescence emission is temperature dependent (Smart et al., 1976). The effects of temperature on the remote sensing of fluorescence emission is also discussed in the following section. For the purposes of the laboratory correlation study, the fluorescence measurements were made at a temperature of  $21^{\circ} \pm 1^{\circ}\text{C}$ .

All fluorometric measurements were made using a proprietary spectrofluorometer (Perkin Elmer MPF4) capable of producing fluorescence spectra on a relative quanta scale that have been corrected for the spectral artifacts introduced by the xenon excitation lamp, the excitation and emission

grating monochromators and the photomultiplier detector (Porro et al., 1973). The optical layout for this instrument is shown in Figure 3. Corrected spectra can be made over the wavelength range from 290 nm to 704 nm. Additional features are the high sensitivity cell holder that has back reflectors providing a four-fold signal increase; high-gain red-sensitive emission and reference photomultipliers (Hamamatsu R928), and a Cation-X short-wavelength cutoff filter. This filter is used to prevent the 337-nm excitation radiation that is scattered by sample particulates from reaching the emission detector, and interfering with the measurements in the 350-nm to 380-nm region. The Cation-X liquid filter consists of a 2-gm/l aqueous solution of 2,7-dimethyl-3,6-diazacyclohepta-1,6-diene iodide (Eastern Chemical Company, Hauppauge, N.Y.). The transmission curve for the 2-1/2-mm thick liquid filter, held between fluorescence-free, fused quartz plates, is shown in Figure 4 and is essentially flat for the working region above 360 nm. In addition, this liquid filter appears to be essentially non-fluorescent in contrast to many proprietary colored glass short wavelength cutoff filters (Bristow, 1979).

Water fluorescence emission spectra, as typified by those shown in Figure 2, were obtained by exciting the sample at 337 nm and scanning the emission spectrum from 350 nm to 500 nm. A fixed excitation wavelength of 337 nm was employed throughout this study partly because this wavelength generally lies close to that producing the maximum fluorescence emission from fresh water samples, and partly because of the wide availability of the reliable pulsed  $N_2$  laser, which operates at this wavelength and which is considered suitable for remote sensing laser fluorosensor applications. Use of an alternate wavelength such as that corresponding to the pulsed XeF excimer laser at 351 nm should not make any significant changes to the conclusions obtained in this study. Both excitation and emission monochromators were used with spectral slit widths adjusted to an equivalent bandwidth of 3 nm in order to optimize the resolution of the OH-stretch water Raman band at 381 nm, also shown in Figure 2. A fluorescence emission spectrum was produced for each water sample, and the six fluorescence characteristics, indicated in Figure 5 were obtained in each case.  $F_{max}$  is the fluorescence emission intensity at the peak of the spectrum and generally lies in the 415-nm to 440-nm region.  $R$  is the peak intensity of the Raman band at 381 nm and  $F_R$  is the corresponding fluorescence emission intensity at this wavelength. The  $R$  and  $F_R$  components of the total emission intensity at 381 nm are separated by interpolation, using a third-order polynomial curve-fitting procedure, which utilizes the fluorescence intensity values at 362.5 nm, 370 nm, 397.5 nm and 407.5 nm. The other fluorescence spectrum characteristics are BW, the full bandwidth at half height (FWHM),  $\lambda_{max}$ , the wavelength at the peak intensity, and  $\lambda_{cen}$ , the wavelength at the center of the fluorescence band as determined from the midpoint of BW. Due to the broad and relatively flat nature of these spectra, the exact value of  $\lambda_{max}$  was often difficult to establish, and as a result,  $\lambda_{cen}$  was preferred as the characteristic wavelength. In addition,  $F_\lambda$ , the fluorescence intensity at wavelength  $\lambda$ , was measured every 10 nm from 350 nm to 500 nm. From these latter data, it was possible to establish  $F_{av}$ , the mean fluorescence intensity for the spectrum between 350 nm and 500 nm, which is a measure of the total or integrated emission between these wavelength limits.

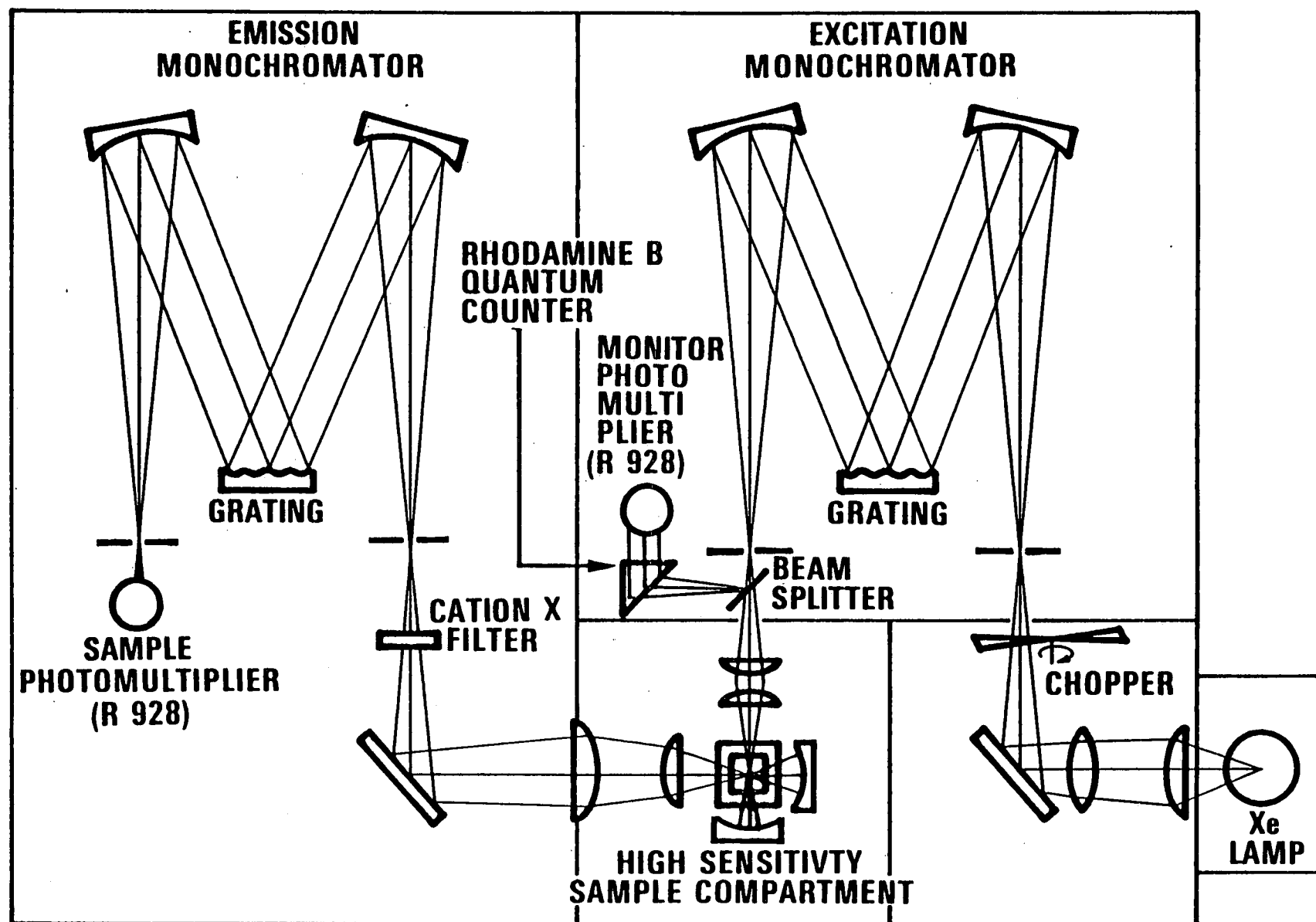


Figure 3. Optical diagram of corrected-spectra spectrofluorometer (Perkin-Elmer MPF4).

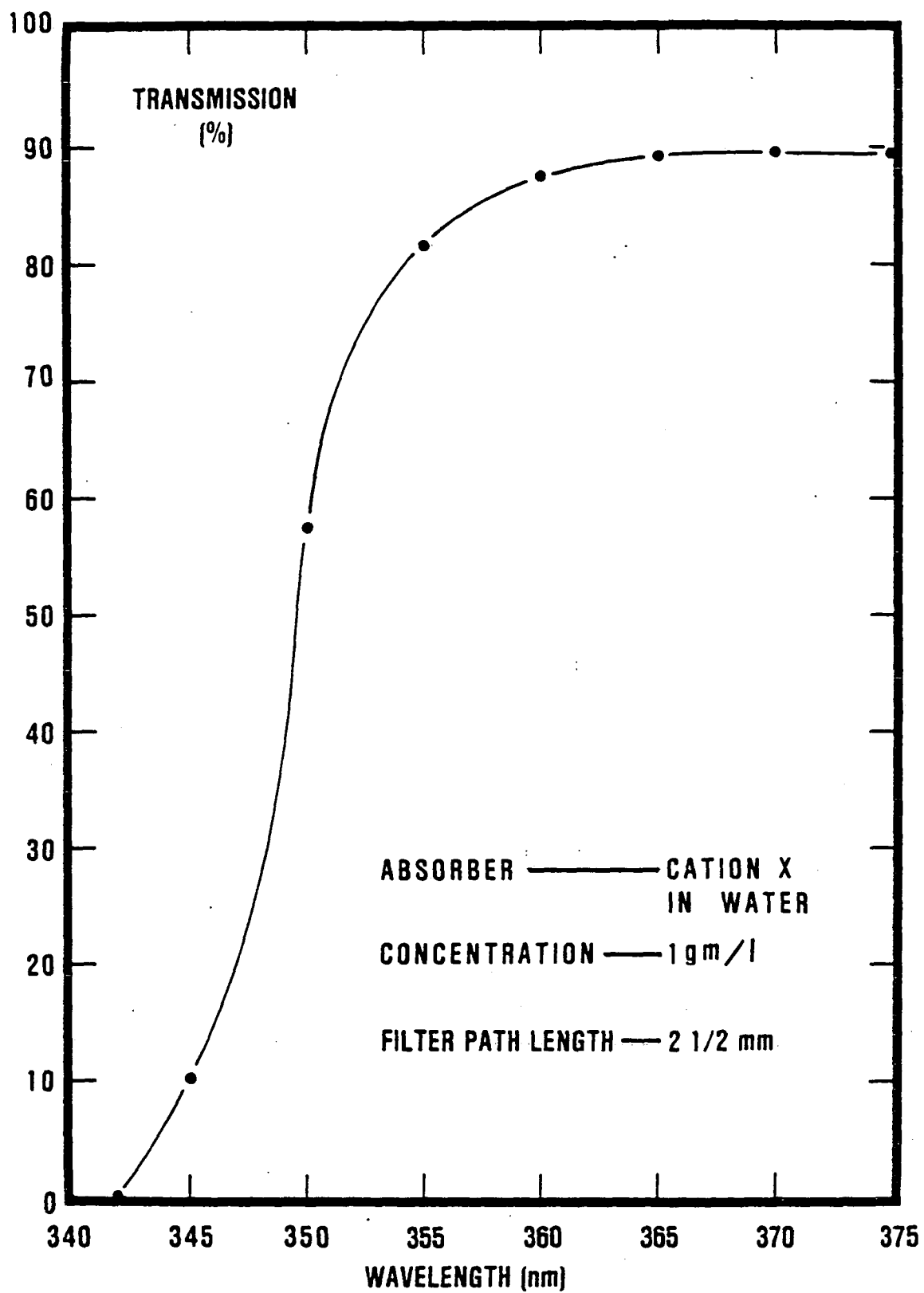


Figure 4. Transmission curve for Cation-X liquid filter.

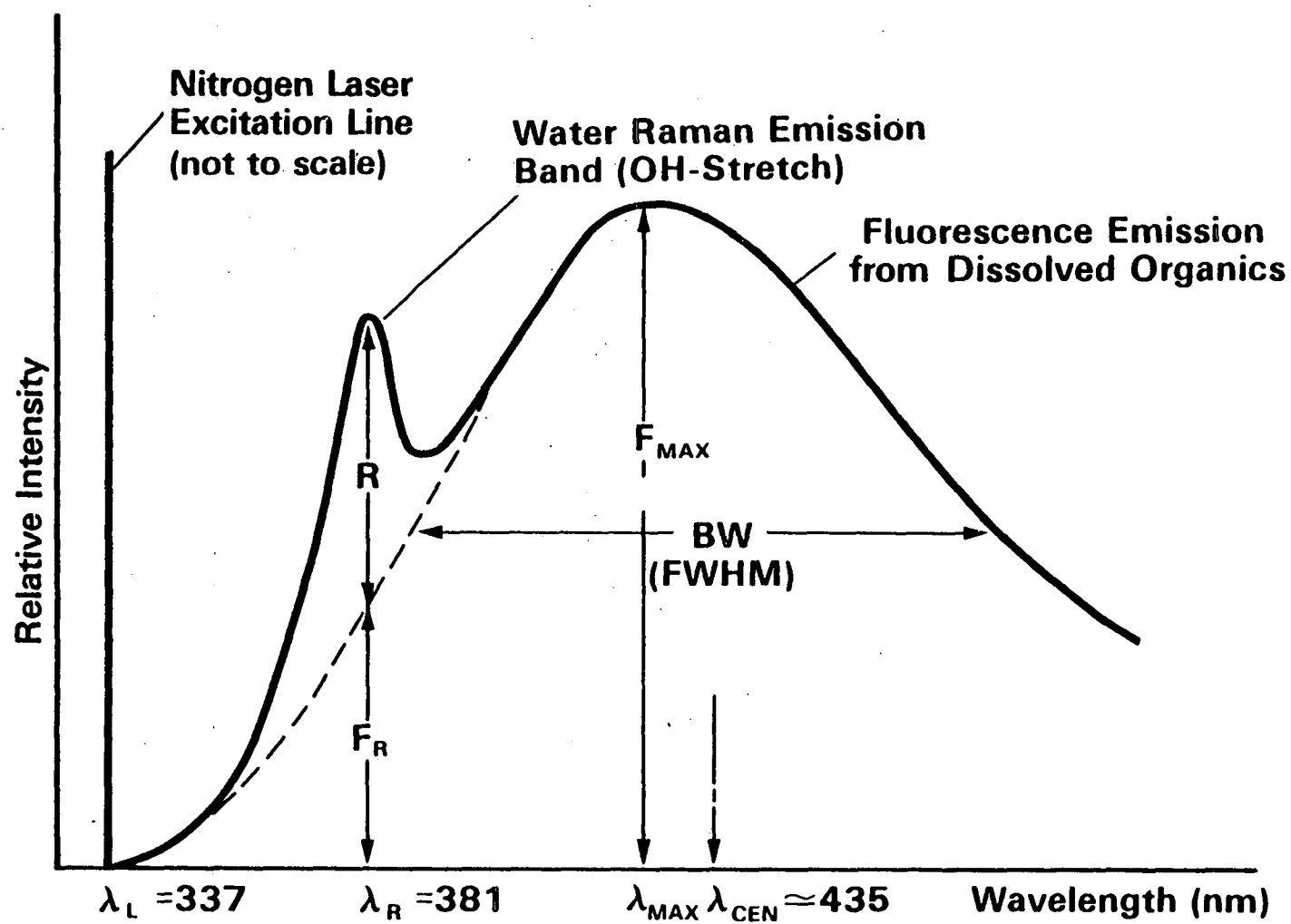


Figure 5. Schematic showing water fluorescence and Raman emission parameters obtained from spectra produced using a laboratory spectrofluorometer.

Reproducibility of the fluorescence data was established by making 10 replicate measurements of  $F_{\max}/R$  and  $F_R/R$  on the same unfiltered Lake Mead sample as was used for evaluating the reproducibility of the TOC and DOC measurements. The means were  $0.68 \pm 0.01$  for  $F_{\max}/R$  and  $0.48 \pm 0.01$  for  $F_R/R$ , where the uncertainty represents the 95 percent confidence limits for the means.

## PRESERVATION AND PREPARATION OF FLUORESCENCE SAMPLES

The time taken for each fluorometric measurement was on the order of 20 minutes, so that a complete fluorescence analysis of the 161 samples takes at least 7 days. In addition, a 1-to-2 day delay was generally incurred before the fluorescence analysis could be started due to the time taken to collect and ship the ice-chilled samples from the field site in Louisiana to the laboratory in Las Vegas, Nevada. Questions were therefore raised concerning sample contamination and integrity during this shipping and storage period, and the effects that any such changes might have on the fluorescence data. Sample contamination by the polyethylene bottles and the possible effects of continued bacterial activity, oxidation, photodecomposition and colloidal aggregate formation were of principal concern. Tests were therefore conducted with the purpose of establishing a sample preservation and storage procedure that minimizes changes to the sample fluorescence properties.

Contamination of the samples by hydrocarbons leached from the polyethylene storage bottles is known to influence the UV absorption spectra of pure water (Delhez, 1960), and, in the present study, has been shown to contribute a carbon background on the order of 0.05 mg/day. The effect of the bottles on the fluorescence measurements was investigated by examining the fluorescence of an ultrapure water sample stored in an unused 100-ml polyethylene bottle each day over a 4-day period.  $F_{\max}/R$  remained close to zero, suggesting that the organics that are leached from the polyethylene bottles over this period are essentially nonfluorescent.

In order to investigate the effects of storage and preparation on sample integrity, tests were performed on identical subsamples of a single master sample from the Atchafalaya River Basin that were stored, preserved and prepared according to seven different procedures over a 14-day period. In all of these procedures, the fraction of subsample that was drawn off each day was brought up to the laboratory ambient temperature ( $21 \pm 1^\circ\text{C}$ ) just prior to the fluorescence analysis. This was done because Smart et al. (1976) have shown that the fluorescence of natural waters is moderately sensitive to water temperature. The seven sample preservation and storage procedures are as follows:

- (i) Subsample stored in the dark at  $4^\circ\text{C}$  and vigorously shaken by hand each day just prior to drawing off fraction for fluorescence analysis.
- (ii) Subsample kept at laboratory temperature and under fluorescent lighting during normal working hours, and vigorously shaken by hand each day just prior to drawing off fraction for fluorescence analysis.

- (iii) Same as (i), but subsample not shaken.
- (vi) Same as (i), but subsample agitated with an ultrasonic (20-kHz) probe just prior to drawing off fraction for fluorescence analysis rather than hand shaken.
- (v) Same as (i) but, in addition, subsample initially acidified with HCl to  $\text{pH} \leq 2$ .
- (vi) Same as (i) but, in addition, subsample heated to 130°F for 1 hour just prior to drawing off fraction for fluorescence analysis.
- (vii) Same as (i) but, in addition, the fraction drawn off for fluorescence analysis was passed through a 0.3  $\mu\text{m}$  pore-size cellulosic membrane filter (Millipore MF-PH).

The results of these tests are summarized graphically in Figure 6 as plots of  $F_{\text{max}}/R$  against time. Procedure (iv), for which the samples were stored in the dark at 4°C and agitated with an ultrasonic probe prior to analysis, exhibited the least variability and drift over the 4-day measurement period. Ultrasonic agitation was limited in both duration and power level to ensure that the sample temperature never rose above ambient by more than a few degrees. This precaution was taken to avoid the possibility of locally overheating the sample thereby causing thermal damage to the fluorescent organics.

The coefficient of variation ( $S/\bar{x}$ ) for  $F_{\text{max}}/R$  for procedure (iv) over the 14-day period was 2.1 percent, suggesting that no significant changes have occurred with the fluorescent organics for samples preserved and treated in this manner. All 161 samples for fluorescence analysis that were examined in this study were therefore stored and prepared according to procedure (iv). Although the data for samples treated according to (i) are not significantly different from those treated according to (iv) at the 5 percent level, (i) was not employed because of the inherently haphazard nature of hand-shaking as a method for sample homogenization.

It is noteworthy that samples treated according to procedure (iii) in which the samples were stored in the dark at 4°C, but neither shaken nor agitated during storage or preparation, exhibited a lower mean value for  $F_{\text{max}}/R$  together with a higher coefficient of variation than did (i) or (iv). This reduction in  $F_{\text{max}}/R$  is most likely due to either settling-out of fluorescent particulates or to the formation of aggregations from colloidal material. The exact manner by which  $F_{\text{max}}/R$  is reduced is not clear as at least three different optical mechanisms are available that will, in principle, either reduce  $F_{\text{max}}$  or increase  $R$ . First, if either the settled particulates or the aggregated colloidal material is fluorescent, then a reduction in  $F_{\text{max}}$  and hence in  $F_{\text{max}}/R$  will result. Formation of colloidal aggregations effectively reduces the physical and fluorescence excitation cross section of fluorescent colloidal material exposed to the excitation beam thereby reducing the measured values of  $F_{\text{max}}$  and  $F_{\text{max}}/R$  below their true or in situ values. Second, a real or apparent reduction in suspended material

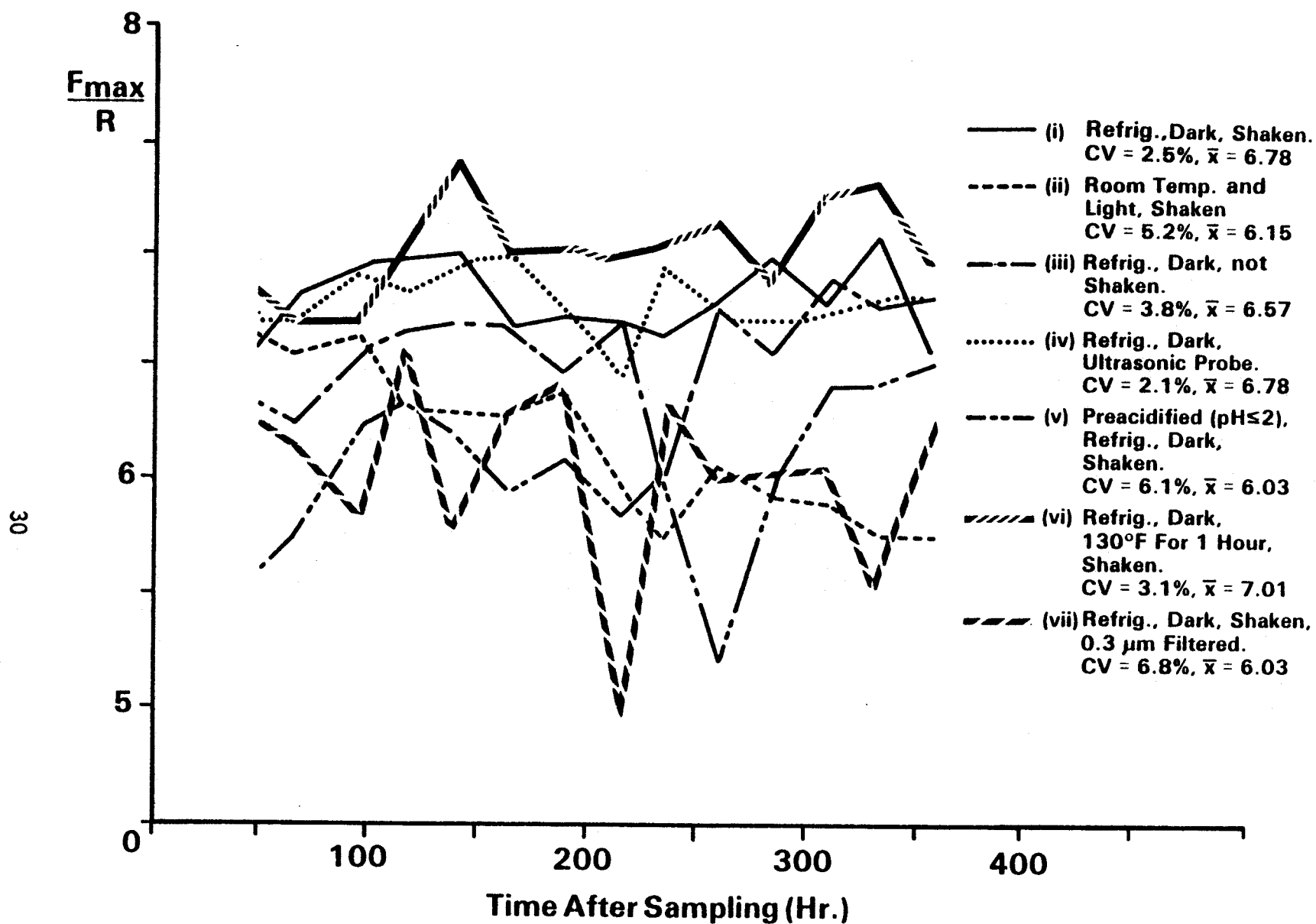


Figure 6. Variation of  $F_{\max}/R$  with time for different preservation and preparation procedures as applied to identical subsamples.  
CV is the coefficient of variation ( $S/\bar{x}$ ).



in the excitation beam will reduce the absorption and scattering losses that are incurred by both the Raman and fluorescence signals. As these losses are stronger in the UV than in the visible, the reduction in the attenuation of R will be greater than that of  $F_{\max}$ . This tends to increase R in relation to  $F_{\max}$ , again resulting in a reduction in the measured value of  $F_{\max}/R$ , but in this case towards, rather than away from, the true value. Third, an undispersed broadband background signal that is known to leak from the excitation monochromator is scattered by both the particulate and colloidal materials into the emission monochromator. This background signal enhances the fluorescence emission without influencing the narrow band Raman emission and therefore acts to increase  $F_{\max}/R$  above its true value. In this case, a reduction in the scattering losses caused by either particulate settling or by aggregate formation will reduce the measured value of  $F_{\max}$ . Again, this results in a reduction in  $F_{\max}/R$ , and also towards its true value.

The relative contributions that each of these optical effects makes towards reducing  $F_{\max}/R$  when compounded with the physical effects of particulate settling or aggregate formation are not apparent from the data for procedure (iii), shown in Figure 6. However, detailed examination of the fluorescence versus DOC correlation data to be presented for the 161 samples of this survey in Chapter 8 will provide some insight into the relative influence that the latter two (side) effects have on the fluorescence measurements.

A plausible explanation for the higher coefficient of variation for the data of procedure (iii) in relation to that for (i) and (iv) is that random amounts of particulate and colloidal materials were drawn off each day from the unstirred subsample thereby inducing fluctuations in the measured values of  $F_{\max}/R$  by means of the optical mechanisms described above.

A number of other interesting trends and effects can be seen in the fluorescence plots shown in Figure 6. The sample preserved according to (ii), i.e., under conditions of ambient temperature and lighting and shaken prior to analysis, exhibited a slow but steady decline in  $F_{\max}/R$  with time away from an initial value that is close to the initial values for (i) and (iv). A likely explanation for this trend is that the fluorescent substances are undergoing degradation due possibly to bacterial activity, photodecomposition or oxidation.

The additional features contained within procedures (v) and (vi) were evaluated with the specific purpose of terminating rather than inhibiting bacterial activity. Procedure (vi), similar to (i) except that the sample was heated to 130°F for 1 hour each day, gave values for the mean of  $F_{\max}/R$  and the coefficient of variation that were slightly higher than that for procedures (i) and (iv), and that exhibited a slight upward trend with time. This suggests that heating the sample to terminate bacterial activity provides no additional advantage over inhibiting bacterial activity by storage in the dark at 4°C and, in addition, may induce a small increase in the fluorescence properties of the sample.

Procedure (v) was found to be unacceptable as a method for terminating bacterial activity both because of the relatively large coefficient of

variation ( $S/\bar{x} = 6.1$  percent), and because the mean value for  $F_{\max}/R$  was significantly lower than that for procedures (i) and (ii). This latter phenomenon has been observed by Smart et al. (1976), who showed that changing sample pH to below 4 produced a marked reduction in the fluorescence of a natural water sample, in relation to unmodified samples having pH values in the range between 6.5 and 8.5.

The fluorescence spectra used to determine the optimum sample preservation procedure and those subsequently obtained for the 161 samples of the survey handled according to procedure (iv), were all made on unfiltered samples. This approach was adopted for the obvious reason that, when performing fluorescence measurements from an airborne platform, one does not have the option to filter the in situ samples. One might then expect  $F_{\max}/R$  for unfiltered samples to show a better correlation with TOC than with DOC or POC on the assumption that both the dissolved and particulate organic materials make significant contributions to the measured value of  $F_{\max}/R$ . With a view to establishing the fluorescence properties of the dissolved fraction, the fluorescence spectra were obtained on a day-to-day basis for a subsample prepared according to procedure (vii), which is identical to procedure (i) except that, in addition, the fraction drawn off each day for fluorescence analysis was passed through a 0.3- $\mu\text{m}$  pore-size cellulosic membrane filter (Millipore MF-PH). As indicated in Figure 6, the mean value of  $F_{\max}/R$  for this data set is about 11 percent below that obtained using procedures (i) and (iv), suggesting that, for this specific sample, the contribution to  $F_{\max}/R$  from the dissolved fraction is on the order of 89 percent. However on a day-to-day basis, the percentage for the fluorescence of the dissolved fraction varied significantly from a high of 96 percent to a low of 77 percent, indicating that other factors are influencing the amount of fluorescent particulate material entering the filtrate in addition to the filter pore size. The coefficient of variation for this data set was 6.8 percent, which is over three times larger than that for procedure (iv).

Concern that the variability in  $F_{\max}/R$  for the filtered samples was due to contamination by elutable organics known to be present in membrane filters (Guillard and Wangersky, 1958; Cahn, 1967; Parker, 1967) was unfounded. Tests performed on high purity water samples indicated that they remained essentially fluorescence free after passage through the filters referred to above suggesting that any soluble organics contributed by the filters are essentially non-fluorescent. A rational explanation for the higher variability in  $F_{\max}/R$  for the filtered samples in relation to the unfiltered samples might be the presence of relatively high concentrations of colloidal material in relation to the truly dissolved and particulate fractions. Much evidence is now available indicating that a significant fraction of TOC present in both marine and fresh waters exists in colloidal form (Reiswig, 1972; Sharp, 1973; Lock et al., 1977), and that the colloidal organic carbon (COC) fraction is generally much larger than the POC fraction (Reiswig, 1972; Wangersky, 1972; Sharp, 1973). The equivalent spherical size range for particles in this intermediate (colloidal) size category can vary continuously from those  $10^{-3}$   $\mu\text{m}$  in diameter, only just larger than truly dissolved and discrete molecules, through to those 1  $\mu\text{m}$  in diameter, more typical of particles that readily settle in water when subjected to a 1-g gravitational field.

Problems arise because of the tendency of COC to adsorb onto the filter materials (Lammers, 1971; Reiswig, 1972; Gordon and Sutcliffe, 1974), even though the size of the colloidal particle may be smaller than the equivalent filter-pore size (Wangersky, 1972). The filtration of samples containing COC may be further complicated by the tendency of colloidal particles to aggregate into larger units (Riley, 1970; Reiswig, 1972; Sharp, 1974) either when the samples are allowed to stand without agitation as occurs during transportation and storage, or directly at the filter surface. As these particles grow in size, the probability that they will penetrate a given glass fiber filter will fall and ultimately approach zero as the particle diameter exceeds the filter characteristic pore size. In this respect, it is significant that the fluorescence data for the subsamples, prepared according to procedure (iv) in which the samples were agitated with an ultrasonic probe just before the fluorescence analysis, exhibited the lowest day-to-day variability. Clearly, if the processes governing the adsorption and aggregation of organic colloidal materials are not fully understood or cannot be easily controlled, then it is conceivable that random amounts of COC may enter the filtrate for a given sample and filter type after a given storage period. Although ultrasonic agitation prior to filtration may help to break up colloidal aggregations, the problem of adsorption onto the filter surface still remains. Partly because of the relatively poor reproducibility of the  $F_{\max}/R$  data obtained from filtered samples, but principally because sample filtration is not relevant to remote sensing of in situ samples, no further attempts were made to measure the fluorescence properties of the dissolved fraction.

The relatively poor reproducibility of the fluorescence data for the filtered samples raised doubts concerning the reliability of the DOC data. Evidence exists that glass fiber filters are able to adsorb significant amounts of COC that would otherwise be expected to pass through a filter of a given pore size (Riley, 1970; Wangersky, 1972; Gordon and Sutcliffe, 1974). This evidence conflicts with claims by the filter manufacturer, who suggest that their glass fiber filters have negligible adsorptive properties (Meakin and Pratt, 1972).

Although it is possible that the glass fiber filters are able to trap a higher percentage of COC material than are other types of filters, resulting in lower DOC values, the reproducibility of the DOC data obtained using these filters appears to be acceptable for this type of measurement. For example, the 30 replicate TOC and DOC analyses performed on a Lake Mead sample gave means and coefficients of variation for TOC of 2.86 mg/l and 9.1 percent, respectively and, for DOC, of 0.91 mg/l and 14.3 percent, respectively. As the spread of the DOC data is not markedly different from that of the TOC data particularly as the DOC value of 0.9 mg/l is close to the usable sensitivity limit of the TOC analyzer, we conclude that the reproducibility of the DOC data has not been significantly impaired by use of the glass fiber filters at least for the samples from Lakes Mead and Mohave. However, as comparable TOC and DOC reproducibility tests were not performed on samples from the Atchafalaya Basin, it cannot be concluded that filter-sample interactions were absent from the DOC measurements made on this group of samples.

Even though the reproducibility of the DOC data obtained using glass fiber filters appears to be within acceptable limits, it cannot be ruled out

that use of nonadsorbing filters might result in a higher correlation between  $F_{\max}/R$  measured on unfiltered samples and DOC than is reported in this study. Silver membrane filters would appear to be an obvious alternative as these filters do not appear to adsorb COC (Wangersky, 1972; Gordon and Sutcliffe, 1974). However, care should be taken with the choice of pore size when using these filters. The 0.45- $\mu\text{m}$  filters are known to contain relatively high and random amounts of carbon that must be removed by precombustion, a process that increases their effective pore size to about 0.8  $\mu\text{m}$  (Riley, 1970; Wangersky, 1975). In contrast, the 0.8- $\mu\text{m}$  and 1.2- $\mu\text{m}$  filters were seen to exhibit lower carbon blanks and maintain their pore size after combustion.

It is therefore recommended that, when preparing samples for DOC or fluorescence analysis using filtration techniques, particularly for waters high in colloidal matter, the samples be filtered using the aforementioned 0.8- $\mu\text{m}$  pore-size silver membrane filter in spite of the drawbacks indicated earlier for this filter type. Use of this specific filter type will therefore combine the DOC and COC fractions into a single overall DOC category that will also include bacteria smaller than 0.8- $\mu\text{m}$  in size, while simultaneously avoiding adsorption effects peculiar to glass fiber filters. In addition, use of this type of filter eliminates problems with the fluorescence measurements caused by optical scattering from large ( $>0.8\text{-}\mu\text{m}$ ) particles. However, it is recommended that colloidal aggregations should be broken up prior to filtration by vigorous agitation, preferably by means of an ultrasonic probe as described earlier.

An alternative approach to this problem is to simply avoid it by not performing analyses on filtered samples. Because the separation of sample organic carbon into the dissolved and particulate fractions by filtration is both arbitrary in terms of the selected particle cutoff size and the filter characteristics, and is possibly unreliable due to the formation of aggregates, Gordon and Sutcliffe (1973) and Sharp (1973) have suggested that filtration not be performed and that TOC be the sole parameter characterizing waterborne organic carbon. In studies of the type reported here, this approach would be undesirable for the simple reason that, as will be shown, the fluorescence parameters exhibit significantly higher correlations with DOC than with TOC. This approach would also appear to be unwise because DOC is a better overall indicator of the concentration of natural (dissolved) organics such as humic and fulvic acids than is TOC. The presence of these substances in source waters is currently of great concern because they are known to be susceptible to conversion into potentially carcinogenic trihalomethanes during routine chlorination in drinking water treatment plants.

Although the adopted sample preservation and storage procedure maintains the laboratory measured values of  $F_{\max}/R$  at an acceptably constant level, it should not be concluded that these values are necessarily the same as those that would be obtained either by using a fresh grab sample or by making an in situ measurement, whether made using either a flow-through fluorometer or an airborne laser fluorosensor.

A number of environmental factors that are known to influence  $F_{\lambda}/R$ , either directly or indirectly, will change as the sample is collected, transported and stored in the laboratory. Some of the factors that are

subject to change are sample temperature, pH, colloidal state, dissolved oxygen level and the viability of algae and bacteria. For example, Smart et al. (1976) have shown that the fluorescence of dissolved organics varies with temperature according to the relationship  $F_T = F_0 \exp(mT)$ , where  $F_T$  is the fluorescence intensity at temperature  $T$ ,  $F_0$  is the corresponding emission at  $0^\circ\text{C}$  and  $m$  is a temperature coefficient that is a constant for a given water type. With  $m = -0.018^\circ\text{C}^{-1}$ , the largest value observed, a  $15^\circ\text{C}$  change in sample temperature produces a 25 percent change in the fluorescence emission intensity.

However all questions concerning sample integrity and changes in  $F_\lambda/R$  that occur between field and laboratory can be avoided if the airborne laser fluorosensor is calibrated to measure TOC or DOC directly. This can be achieved by making an airborne measurement of  $F_\lambda/R$  on an in situ sample together with concurrent ground truth determinations of TOC and DOC for a preselected sampling station site on the water body being surveyed. A conversion factor relating  $F_\lambda/R$  to either TOC or DOC is then obtained directly from Equation 5.

## SECTION 8

### DATA ANALYSIS

Due to the absence of any simple physicochemical relationships between the organic carbon characteristics of a water sample and its corresponding fluorescence emission properties, the approach adopted in analyzing the experimental measurements is strictly statistical with emphasis placed on establishing the existence of a linear relationship between these two groups of data through use of the linear correlation coefficient.

#### LINEAR CORRELATION RESULTS

The emission intensity values  $F_{\max}$ ,  $F_R$ , and  $R$ , obtained on the aforementioned samples using the laboratory spectrofluorometer, were used to calculate the nondimensional ratios  $F_{\max}/R$ ,  $F_R/R$ ,  $F_{\max}/F_R$ ,  $F_{\max}/(R + F_R)$  and  $(F_{\max} - F_R)/R$  for correlation with independent TOC, DOC and POC measurements obtained on corresponding subsamples. Other fluorescence parameters employed in the correlation analyses were the characteristic wavelengths  $\lambda_{\text{cen}}$  and  $\lambda_{\max}$ , the bandwidth  $BW$ , and  $(\lambda_{\text{cen}} - \lambda_{\max})$ . In addition, the fluorescence to Raman ratios  $F_{\lambda}/R$  and  $F_{\text{av}}/R$  were calculated.  $F_{\lambda}$  is the fluorescence emission intensity at any specified wavelength  $\lambda$  and was measured at intervals of 10 nm from 350 nm to 500 nm.  $F_{\text{av}}$  represents the mean fluorescence emission intensity between 350 nm and 500 nm and is obtained from the individual  $F_{\lambda}$  values by means of the relationship

$$F_{\text{av}} = \frac{1}{N} \sum_{i=1}^N F_{\lambda_i}$$

where  $N$  is the number of spectral bands used in the summation. For the present measurements,  $N = 15$ .

Data used to correlate DOC and TOC with  $F_{\max}/R$  and  $F_R/R$  are presented graphically in Figures 7, 8, 9 and 10, which show  $F_{\max}/R$  versus DOC,  $F_R/R$  versus DOC,  $F_{\max}/R$  versus TOC and  $F_R/R$  versus TOC respectively. Examination of the data in these figures indicates the presence of a relatively large and discrete group of data points at the low end of the fluorescence scale. This group represents the 54 samples from Lake Mead and Lake Mohave together with the four drinking and ultra-pure water samples.

The Pearson product-moment linear correlation coefficient,  $r$ , was calculated for all possible pairings between the fluorescence and organic

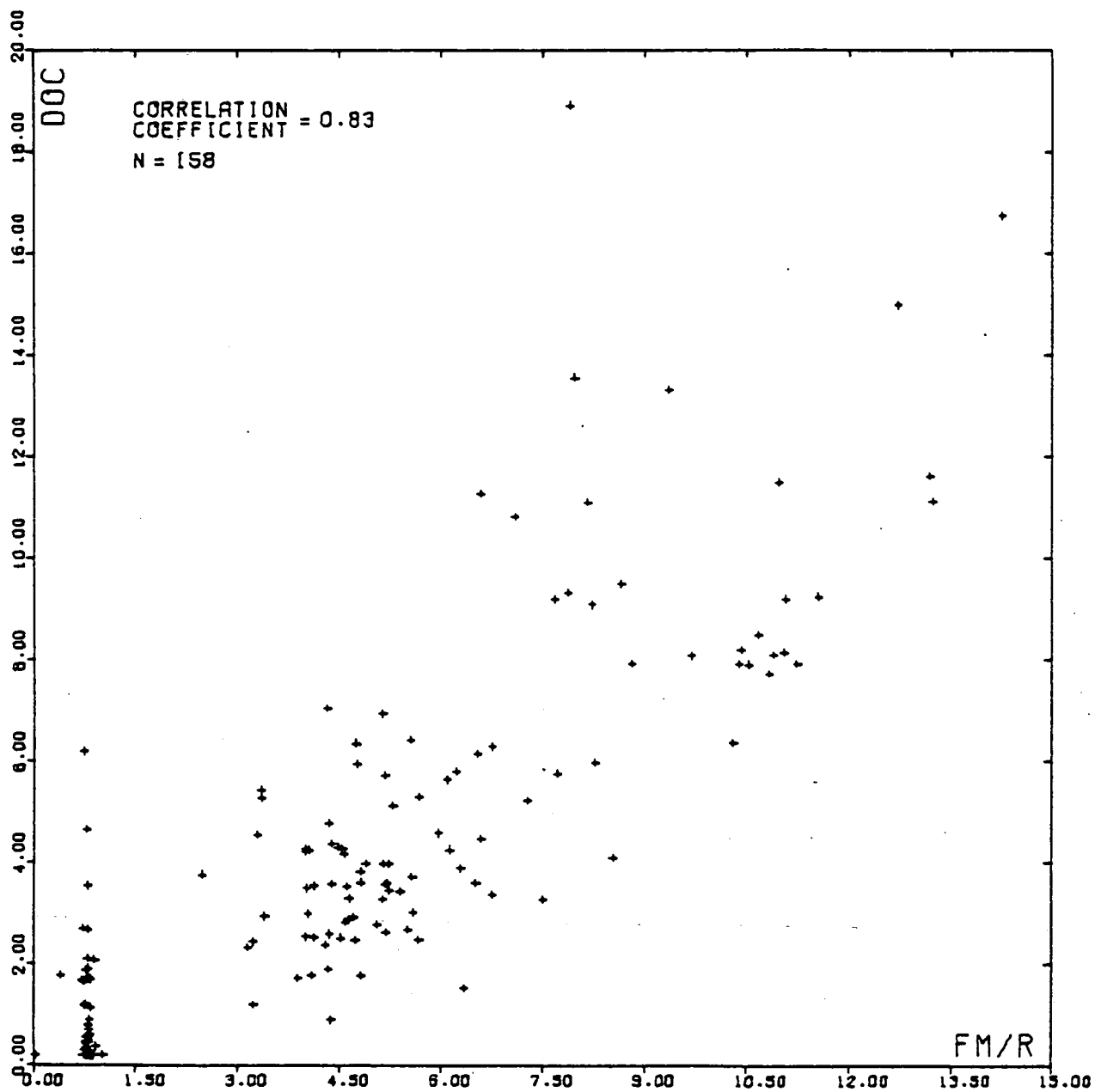


Figure 7. Variation of DOC (mg/l) with  $F_{max}/R$  for 158 samples.

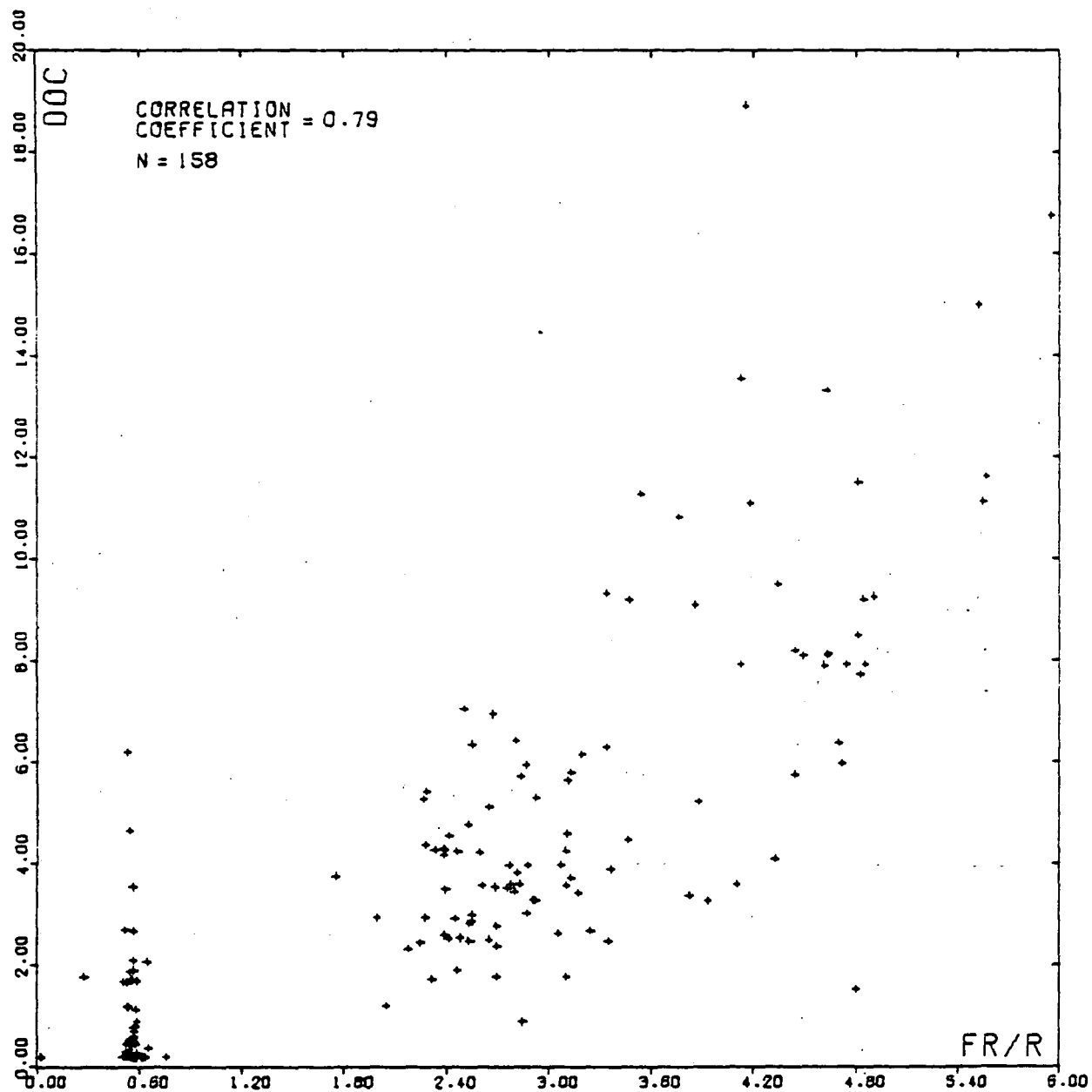


Figure 8. Variation of DOC (mg/l) with  $F_R/R$  for 158 samples.



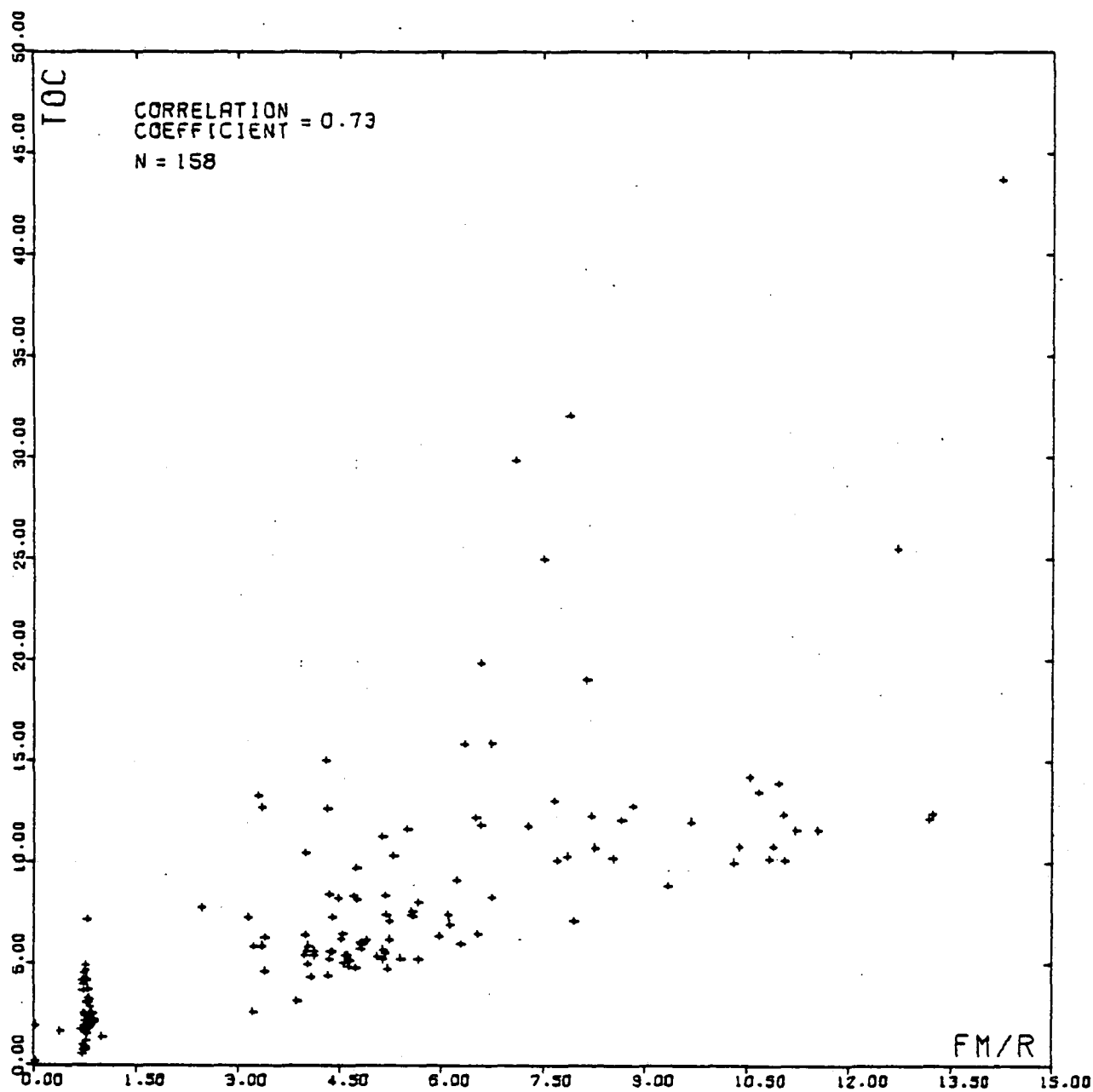


Figure 9. Variation of TOC (mg/l) with  $F_{max}/R$  for 158 samples.

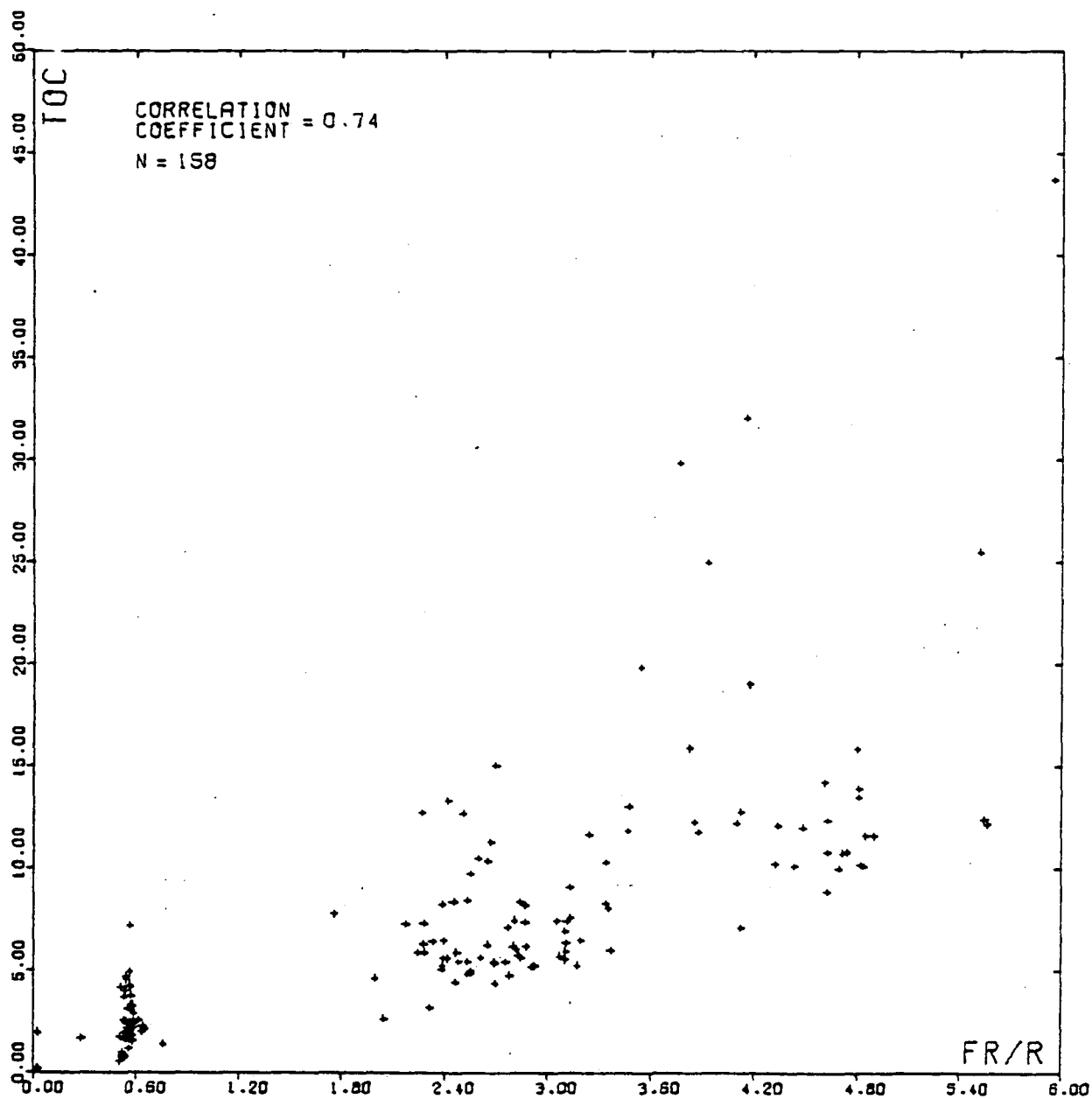


Figure 10. Variation of TOC (mg/l) with  $F_R/R$  for 158 samples.

carbon parameters. These coefficients are shown in Table 2 together with values denoting the upper and lower limits of the 95 percent confidence interval for  $r$  calculated by converting the distribution of  $r$  to normal statistics using Fisher's  $z$  transformation, together with  $N$ , the number of data pairs used in the calculation of  $r$ . All values of  $r \geq \pm 0.27$  with  $N \geq 95$  and  $r \geq \pm 0.22$  with  $N \geq 148$  are significant at the 1 percent level. Similarly, all values of  $r \geq \pm 0.21$  with  $N \geq 95$  and  $r \geq \pm 0.17$  with  $N \geq 148$  are significant at the 5 percent level.

Also compared with these fluorescence parameters are chlorophyll  $a$  (CHLA), pH (PH), dissolved oxygen (DO), conductivity (COND), Secchi disc transparency (TRANSP) and turbidity (TURB). Correlation coefficients relating  $\lambda_{max}$  and  $\lambda_{cen}$  to the other fluorescence intensity ratios are also presented. In addition, an array of coefficients for all possible pairings between the established water quality parameters for which measurements were made, is presented in Table 3. Maximum, mean and minimum value for all the fluorescence and water quality parameters are presented in Table 4 together with the number of measurements made for each parameter.

Discussion of the correlation data is presented in two parts; the first part deals with the relative tendencies of the three organic carbon parameters to correlate with the fluorescence emission data whereas the second part examines the relative merits of the various fluorescence parameters for use as remote sensing indicators of waterborne organic carbon.

Table 2 indicates that DOC is the water quality parameter most highly correlated with the various fluorescence parameters, in particular with  $F_{max}/R$ ,  $F_R/R$ ,  $(F_{max} - F_R)/R$ ,  $F_{max}/F_R$  and  $F_{max}/(R + F_R)$ . A similar conclusion can be drawn from Figure 11, where the coefficients for correlations between  $F_\lambda/R$  and DOC,  $F_\lambda/R$  and TOC,  $F_\lambda/R$  and POC, and  $F_\lambda/R$  and turbidity are plotted as a function of wavelength. At wavelengths of 381 nm and approximately 435 nm,  $F_\lambda/R$  becomes equivalent to  $F_R/R$  and  $F_{max}/R$  respectively. The correlation coefficients for DOC versus the various fluorescence parameters lie in the range from 0.78 to 0.84 whereas the corresponding values for TOC versus the same fluorescence parameters lie in the range from 0.62 to 0.74. By converting the distribution for these  $r$  values to normal statistics using Fisher's  $z$  transformation, a test can be performed to determine whether the correlation coefficient for DOC versus a specific fluorescence parameter belongs to the same population as does the coefficient for TOC versus this same fluorescence parameter. This procedure shows that correlations involving DOC are significantly different from similar correlations involving TOC at the 5 percent level for a sample size of 158.

As DOC is the organic carbon parameter exhibiting the highest correlation with  $F_\lambda/R$  ( $r=0.83$ ) together with a number of other fluorescence parameters, and, as POC shows only a weak correlation with DOC for which  $r=0.44$  (Table 3), one can then predict a poor correlation between POC and  $F_\lambda/R$ ; this is confirmed by the curve for POC versus  $F_\lambda/R$  in Figure 7, for which  $r=0.45$ . This prediction can be made because the fluorescence intensity measurements,  $F_\lambda$ , were obtained on unfiltered samples containing both DOC and POC, so that the relationships between DOC and  $F_\lambda/R$  and between POC and  $F_\lambda/R$  are mutually dependent. A consequence of these observations is that  $TOC (=DOC +$

TABLE 2. CORRELATION COEFFICIENTS FOR FLUORESCENCE EMISSION PARAMETERS VERSUS  
WATER QUALITY PARAMETERS

	FM/P	FR/R	(FM-FR)/R	FM/FR	FM/(R+FR)	LCEN	LMAX	LC-LM	BW	TURB	
UR	.8746	.8440	.8778	.8367	.8366	.8201	.7914	-.1442	.0443	-.0754	DOC
R	.8326	.7929	.8367	.7835	.7813	.7614	.7248	-.2937	-.1126	-.2582	
LR	.7781	.7274	.7834	.7155	.7153	.6870	.6413	-.4301	-.2641	-.4241	
N	(156)	(158)	(158)	(158)	(154)	(155)	(155)	(155)	(155)	(108)	
UR	.7960	.8003	.7737	.7049	.7535	.7066	.7197	-.2282	.2787	.2236	TOC
R	.7314	.7369	.7032	.6176	.6778	.6187	.6349	-.3711	.1281	.0379	
LR	.6503	.6571	.6155	.5118	.5843	.5121	.5314	-.4984	-.0286	-.1504	
N	(156)	(158)	(158)	(158)	(158)	(155)	(155)	(155)	(155)	(107)	
UR	.5396	.5827	.4933	.4084	.4965	.4181	.4757	-.1759	.4124	.4124	PUC
R	.4171	.4677	.3634	.2675	.3672	.2769	.3420	-.3265	.2705	.2415	
LR	.2772	.3342	.2178	.1142	.2220	.1226	.1928	-.4621	.1158	.0541	
N	(151)	(151)	(151)	(151)	(151)	(148)	(148)	(148)	(148)	(104)	
UR	-.0059	.0284	-.0185	.0305	.0224	.0412	-.0442	.2744	.1524	.0261	CHL A
R	-.1956	-.1623	-.2077	-.1603	-.1682	-.1499	-.2321	.0892	-.0386	-.1645	
LR	-.3716	-.3417	-.3825	-.3398	-.3469	-.3303	-.4041	-.1024	-.2268	-.3437	
N	(104)	(104)	(104)	(104)	(104)	(104)	(104)	(104)	(104)	(104)	
UR	-.0482	.0951	-.1222	-.2911	-.1715	-.1733	-.3063	.2427	.4572	.4994	PH
R	-.2385	-.0993	-.3076	-.4580	-.3524	-.3541	-.4711	.0526	.2901	.3394	
LR	-.4122	-.2864	-.4722	-.5979	-.5104	-.5118	-.6085	-.1414	.1033	.1571	
N	(101)	(101)	(101)	(101)	(101)	(101)	(101)	(101)	(101)	(101)	
UR	-.1174	.0060	-.1774	-.3878	-.2824	-.3277	-.3503	.0039	.6126	.6756	DO
R	-.3006	-.1440	-.3553	-.5380	-.4483	-.4672	-.5065	-.1861	.4783	.5572	
LR	-.4640	-.3613	-.5107	-.6604	-.5831	-.6198	-.6353	-.3632	.3173	.4108	
N	(104)	(104)	(104)	(104)	(104)	(104)	(104)	(104)	(104)	(104)	
UR	.0667	.1336	.0331	.0176	.0564	.0557	-.1045	.4074	.0754	.0465	COND
R	-.1314	-.0646	-.1644	-.1795	-.1416	-.1422	-.2948	.2293	-.1228	-.1513	
LR	-.3196	-.2577	-.3495	-.3631	-.3249	-.3295	-.4644	.0345	-.3117	-.3377	
N	( 97)	( 97)	( 97)	( 97)	( 97)	( 97)	( 97)	( 97)	( 97)	( 97)	
UR	.4335	.2945	.4995	.6648	.5734	.5706	.4957	.5255	-.4055	-.5614	TRANSP
R	.2601	.1051	.3369	.5395	.4256	.4222	.3324	.3679	-.5568	-.6820	
LR	.0682	-.0922	.1514	.3846	.2511	.2472	.1465	.1858	-.6784	-.7742	
N	( 98)	( 98)	( 98)	( 98)	( 94)	( 98)	( 98)	( 98)	( 98)	( 98)	
UR	-.0027	.2048	-.1251	-.3676	-.1411	-.2533	.0099	-.5155	.9051	1.0000	TURB
R	-.1873	.0209	-.3029	-.5172	-.3176	-.4185	-.1751	-.6394	.8649	1.0000	
LR	-.3596	-.1645	-.4618	-.6407	-.4745	-.5549	-.3486	-.7370	.8096	1.0000	
N	(110)	(110)	(110)	(110)	(110)	(110)	(110)	(110)	(110)	(110)	
UR	.9400	.9195	.9438	.9739	.9703	1.0000	.9602	-.2346	.0649	-.2533	LCEN
R	.9269	.8917	.9240	.9645	.9597	1.0000	.9460	-.3757	-.0907	-.4185	
LR	.9015	.8549	.8976	.9519	.9454	1.0000	.9270	-.5012	-.2420	-.5599	
N	(158)	(158)	(158)	(158)	(158)	(158)	(158)	(158)	(158)	(110)	
UR	.9344	.9465	.9025	.9272	.9818	.9602	1.0000	-.5577	.2973	.0099	LMAX
R	.9115	.9277	.8691	.9019	.9752	.9460	1.0000	-.6558	.1495	-.1751	
LR	.8811	.9025	.8754	.8684	.9683	.9270	1.0000	-.7359	-.0053	-.3486	
N	(158)	(158)	(158)	(158)	(154)	(158)	(158)	(158)	(158)	(110)	

ur and lr are the upper and lower limits of the 95% confidence interval for the correlation coefficient r. N is the number of samples used to find the correlation coefficient r.

TABLE 3. CORRELATION COEFFICIENTS FOR RELATIONSHIPS BETWEEN WATER QUALITY PARAMETERS

	DOC	TOC	POC	CHL A	PH	DO	COND	TRANSP	TURB	
UR	1.0000									DOC
R	1.0000									
LR	1.0000									
N	(158)									
UR	.8448	1.0000								TOC
R	.7937	1.0000								
LR	.7282	1.0000								
N	(157)	(158)								
UR	.5608	.8981	1.0000							POC
R	.4419	.8627	1.0000							
LR	.3050	.8159	1.0000							
N	(151)	(151)	(151)							
UR	-.0587	.1327	.3160	1.0000						CHL A
R	-.2476	-.0615	.1285	1.0000						
LR	-.4194	-.2511	-.0686	1.0000						
N	(102)	(101)	(98)	(104)						
UR	.0152	.1683	.3314	.5381	1.0000					PH
R	-.1789	-.0270	.1434	.3846	1.0000					
LR	-.3600	-.2204	-.0556	.2065	1.0000					
N	(100)	(99)	(96)	(100)	(101)					
UR	-.0360	.1913	.3552	.2656	.7833	1.0000				DO
R	-.2261	-.0013	.1716	.0788	.6952	1.0000				
LR	-.4005	-.1938	-.0246	-.1136	.5797	1.0000				
N	(102)	(101)	(98)	(103)	(100)	(104)				
UR	.1198	.1942	.3020	.5620	.5505	.3330	1.0000			COND
R	-.0806	-.0054	.1058	.4101	.3934	.1451	1.0000			
LR	-.2746	-.2047	-.0989	.2314	.2094	-.0539	1.0000			
N	(95)	(94)	(91)	(96)	(93)	(96)	(97)			
UR	.4215	.2553	.0708	.1991	-.2004	-.2061	.2486	1.0000		TRANSP
R	.2445	.0599	-.1327	.0028	-.3845	-.3860	.0495	1.0000		
LR	.0494	-.1401	-.3255	-.1938	-.5424	-.5406	-.1536	1.0000		
N	(96)	(95)	(92)	(97)	(94)	(98)	(92)	(94)		
UR	-.0754	.2236	.4124	.0261	.4994	.6756	.0465	-.5614	1.0000	TURB
R	-.2582	.0379	.2415	-.1645	.3394	.5572	-.1513	-.6820	1.0000	
LR	-.4241	-.1504	.0541	-.3437	.1571	.4108	-.3377	-.7742	1.0000	
N	(108)	(107)	(104)	(104)	(101)	(104)	(97)	(98)	(110)	

ur and lr are the upper and lower limits of the 95% confidence interval for the correlation coefficient r. N is the number of samples used to find the correlation coefficient r.

TABLE 4. MAXIMUM, MEAN AND MINIMUM VALUES FOR FLUORESCENCE AND WATER QUALITY PARAMETERS

Parameter	Units	Max. Value	Mean Value	Min. Value	Sample Size
$F_{\max}/R$	-	14.25	4.43	0.02	158
$F_R/R$	-	5.95	2.36	0.02	158
$F_{av}/R$	-	10.71	2.95	0.01	158
$(F_{\max}-F_R)/R$	-	8.30	2.06	0	158
$F_{\max}/F_R$	-	2.40	1.69	0.89	158
$F_{\max}/(R+F_R)$	-	2.05	1.10	0.02	158
$\lambda_{cen}$	nm	447.74	435.82	423.55	155
$\lambda_{\max}$	nm	439.69	427.68	415.63	155
$\lambda_{cen}-\lambda_{\max}$	nm	13.60	8.15	-2.70	155
BW	nm	153.90	122.13	113.30	155
DOC	mg/l	18.91	4.02	0.18	158
TOC	mg/l	43.69	7.21	0.20	158
POC	mg/l	26.95	3.47	0	158
CHLA	$\mu\text{g/l}$	31.30	7.73	0.20	104
pH	pH	8.10	7.34	6.70	101
DO	mg/l	9.60	5.01	0.01	104
COND	$\mu\text{mhos/cm}$	973.00	270.71	87.00	97
TRANSP	m	0.99	0.30	0.10	98
TURB	FTU	220.00	50.07	0.61	110

POC) will show a weaker correlation with  $F_{\lambda}/R$  than will DOC. This is apparent in Figure 11 where the correlation coefficient curves for TOC versus  $F_{\lambda}/R$  and for DOC versus  $F_{\lambda}/R$  have values of about 0.72 and 0.83 respectively in the blue spectral region.

It should be noted that neither the fluorescence data, the organic carbon data, nor the various correlations provide any direct evidence as to whether the fluorescence emission originates from all or part of either the particulate or dissolved substances or from some mixture of both. This ambiguity, which exists in spite of the strong correlation between  $F_{\max}/R$  and DOC ( $r = 0.83$ ) and the weak correlation between  $F_{\max}/R$  and POC ( $r = 0.42$ ), arises because the fluorescence measurements were made exclusively on unfiltered samples. As indicated earlier, filtration of the fluorescence samples was not performed, mainly because airborne monitoring does not allow for any such sample preparation, but also because of the aforementioned difficulties encountered in measuring the fluorescence of filtered samples. Also, sample filtration may produce differences between the laboratory measured values of  $F_{\max}/R$  for the filtered and unfiltered samples due to the elimination of particulates that can produce either scattering losses in  $R$  or an apparent enhancement in  $F_{\max}$  due to scattering of a leaked background signal. These differences are in addition to that caused by the elimination of the fluorescence contribution from particulate organic substances. Further discussion of the influence of these scattering side effects on the fluorescence data are presented below.

As an example of this ambiguity, a scenario can be envisaged in which sample fluorescence originates entirely from a small but significant fraction of the particulate organics that correlates, not with POC, but with DOC. This latter condition is necessary because POC, and DOC have been shown to be poorly correlated ( $r = 0.44$ ). A possible candidate for this material might be COC which is more likely to vary in unison with DOC than with POC, even though COC is included in the POC category by the ability of glass fiber filters to efficiently trap colloidal material by adsorption. This situation is suggested mainly to caution the reader to avoid assuming that the correlations obtained in this work necessarily established causal relationships. Clearly, the relative contributions to  $F_{\max}/R$  from both particulate and dissolved organics can be determined by making fluorescence measurements on filtered samples as well as on unfiltered samples in which the same filter type is used for both the fluorescence and the DOC analyses. Based on the earlier discussion, a non-adsorbing silver membrane filter with a pore size of  $0.8 \mu\text{m}$  would appear to be ideal for this application, so that all COC below this cut-off size will enter the filtrate and be counted as DOC. Alternatively, glass fiber filters might be used throughout, in which case a significant part of the COC fraction will be trapped on the glass filter and hence be counted as POC.

Discussion of the relative merits of the various fluorescence parameters as airborne predictors of waterborne organic carbon are dealt with on a case-by-case basis as follows:

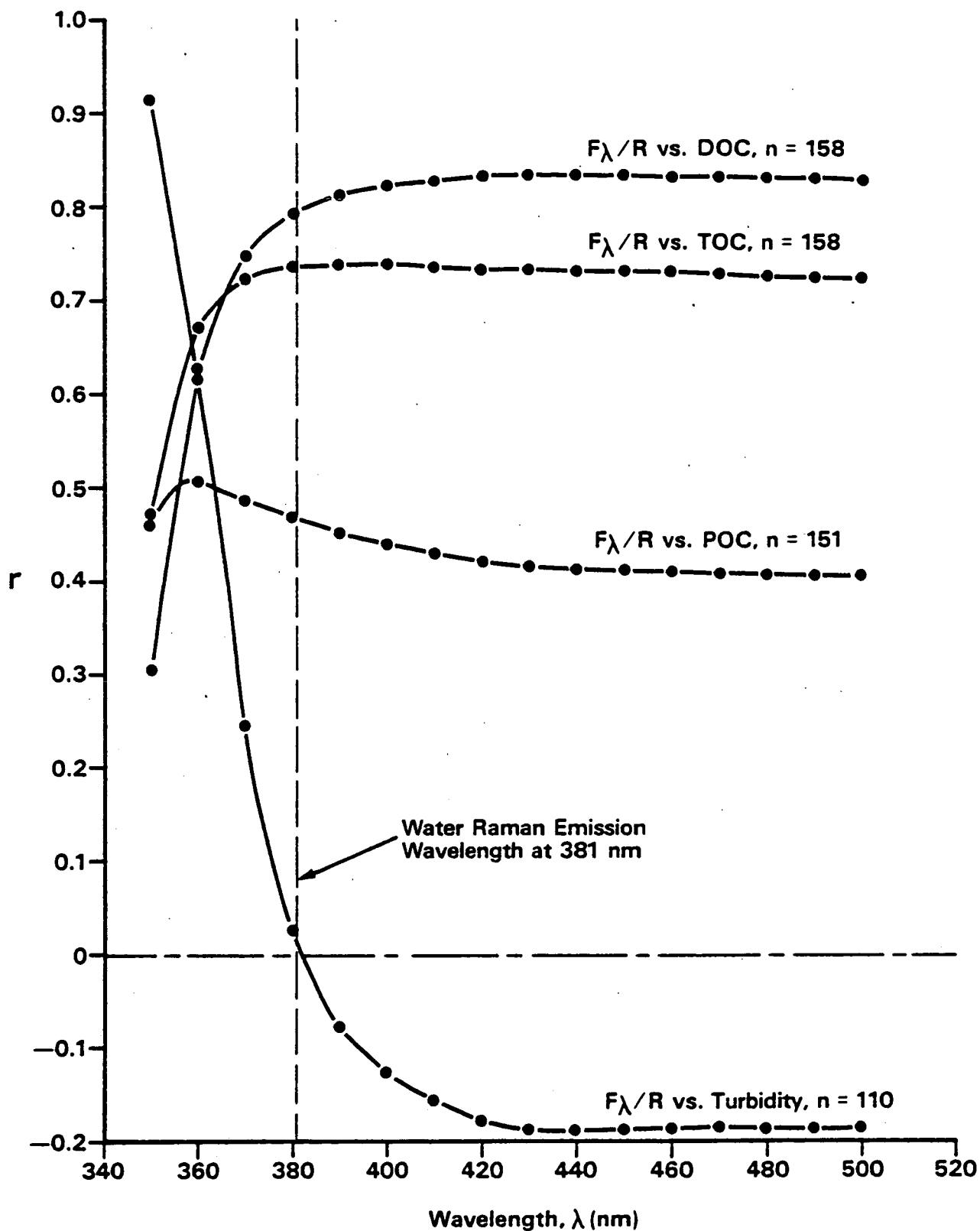


Figure 11. Variation of linear correlation coefficient,  $r$ , with wavelength for  $F_{\lambda}/R$  versus DOC,  $F_{\lambda}/R$  versus TOC,  $F_{\lambda}/R$  versus POC and  $F_{\lambda}/R$  versus turbidity.



(i)  $F_{\max}/R$  and  $F_{\lambda}/R$  above 400 nm

The correlation coefficient curve for  $F_{\lambda}/R$  versus DOC shown in Figure 11 indicates that the optimum value for correlation with DOC occurs in the region of 430 nm; this wavelength corresponds closely to the mean values for the peak ( $\lambda_{\max}$ ) and centre ( $\lambda_{\text{cen}}$ ) wavelengths of the emission spectra respectively as indicated in Table 4. As  $F_{\max}$  is defined to be the fluorescence intensity at  $\lambda_{\max}$ , then  $F_{\max}/R$  would appear to be the optimum value of  $F_{\lambda}/R$  for use as a DOC indicator.

(ii)  $F_{\lambda}/R$  below 400 nm

According to Figure 11, the correlations between  $F_{\lambda}/R$  and either DOC or TOC exhibit a marked decline for wavelengths shorter than 400 nm. Two reasons for this decline are suggested.

It is apparent from the fluorescence emission spectrum for the sample of Lake Mead water shown in Figure 2 that the fluorescence intensity  $F_{\lambda}$  falls rapidly for wavelengths shorter than 380 nm. This will produce an increase in the percentage measurement error for  $F_{\lambda}$ , thereby tending to reduce the correlation between  $F_{\lambda}/R$  and either DOC or TOC.

However, a more plausible explanation for this decline involves an experimental artifact introduced by the spectrofluorometer in conjunction with the effects of sample suspended particulates. In addition to the desired spectral band at 337 nm, the excitation monochromator is known to emit a somewhat broader but considerably weaker band of scattered light. This leaked or background light falls off only gradually over a region several hundred nanometers wide to the long wavelength side of the desired excitation band. As the sample fluorescence is monitored at  $90^{\circ}$  to the excitation beam, this background does not constitute a problem in the absence of a scattering medium such as a suspension of particulates. In reality however, samples were frequently turbid such that a significant fraction of  $F_{\lambda}$  measured in the 350-nm to 380-nm region for these samples was due to this Mie-scattered background light in addition to the desired contribution from the DOC-related fluorescence. The influence of this background signal on  $F_{\lambda}$  is exacerbated by the fact that, in the 350-nm to 360-nm region where this background is the strongest, the sample fluorescence signal is at its weakest as indicated by the spectrum for the Lake Mead sample shown in Figure 2. This background signal therefore increases the measured value of  $F_{\lambda}$  particularly in the short wavelength region while leaving the measurement of  $R$  unchanged; as the Raman intensity  $R$  is superimposed on the fluorescence spectra, its measurement is not affected by the presence of this background signal. The influence of this scattered background was particularly noticeable in the spectra for samples high in suspended particulates as a flattening out of the fluorescence spectrum due to enhancement of  $F_{\lambda}$  in the short wavelength region below 380 nm.

This explanation is confirmed by using sample turbidity as an indicator of suspended particulate concentration and correlating turbidity with  $F_\lambda/R$ . As shown in Figure 11, this correlation becomes strongly positive in the short wavelength region with  $r = +0.92$  at 350 nm. If the suspended particulates were simply attenuating  $F_\lambda$  rather than acting as a source of scattered background light, then the correlation between turbidity and  $F_\lambda/R$  would be strongly negative in contrast to the high positive values obtained for the spectral region below 381 nm.

Another manifestation of the combined effect of the leaked background signal and the suspended particulates on  $F_\lambda$  is provided by the strong correlation ( $r = +0.86$ ) between turbidity and BW, the FWHM bandwidth of the fluorescence spectrum. The distribution of these data points are shown in Figure 12. The bandwidth of 115 nm at zero turbidity probably represents the true limiting value in the absence of the background interference, although the influence of differential absorption effects, to be discussed later, may also be present. As the values of  $F_\lambda$  at shorter wavelengths are enhanced without any significant change occurring at the longer wavelengths, the net effect is such as to increase BW in direct response to increases in the concentration of the suspended particulates as represented by the turbidity measurement.

This background signal, which contributes to the  $F_\lambda$  measurement through the presence of suspended particulates, is therefore considered to be the principal cause for the marked decline in the correlations between  $F_\lambda/R$  and either DOC or TOC at wavelengths below 380 nm. As DOC and turbidity are only weakly correlated ( $r = -0.26$ ), it is concluded that the correlation between  $F_\lambda/R$  and turbidity has been enhanced at short wavelengths at the expense of the correlation between  $F_\lambda/R$  and DOC.

It was possible to eliminate this background from the emission spectra by inserting a 337-nm narrow band interference filter into the excitation beam before it enters the sample cell. However, due to the poor transmission (<20%) of this and other filters available for this spectral region, this expedient produced a significant and unacceptable reduction in  $F_\lambda$  and the corresponding signal-to-noise ratio. The fluorescence analyses of the 161 samples were therefore performed without the use of this filter on the assumption that this background constituted only a small percentage of  $F_\lambda$  in the region of  $\lambda_{max}$ , particularly as the turbid samples were generally also highly fluorescent. However, it is possible that the correlation between  $F_\lambda/R$  (at 381 nm) and DOC, as indicated in Figure 11, has been degraded by this instrumental artifact. Due to the presence of this background, the  $F_\lambda/R$  data in the 350 nm to 370 nm spectral region cannot be considered meaningful in relation to the TOC and DOC data.

In contrast to the effects of the background scattered light, the influence of differential absorption and scattering on  $F_\lambda/R$ , as

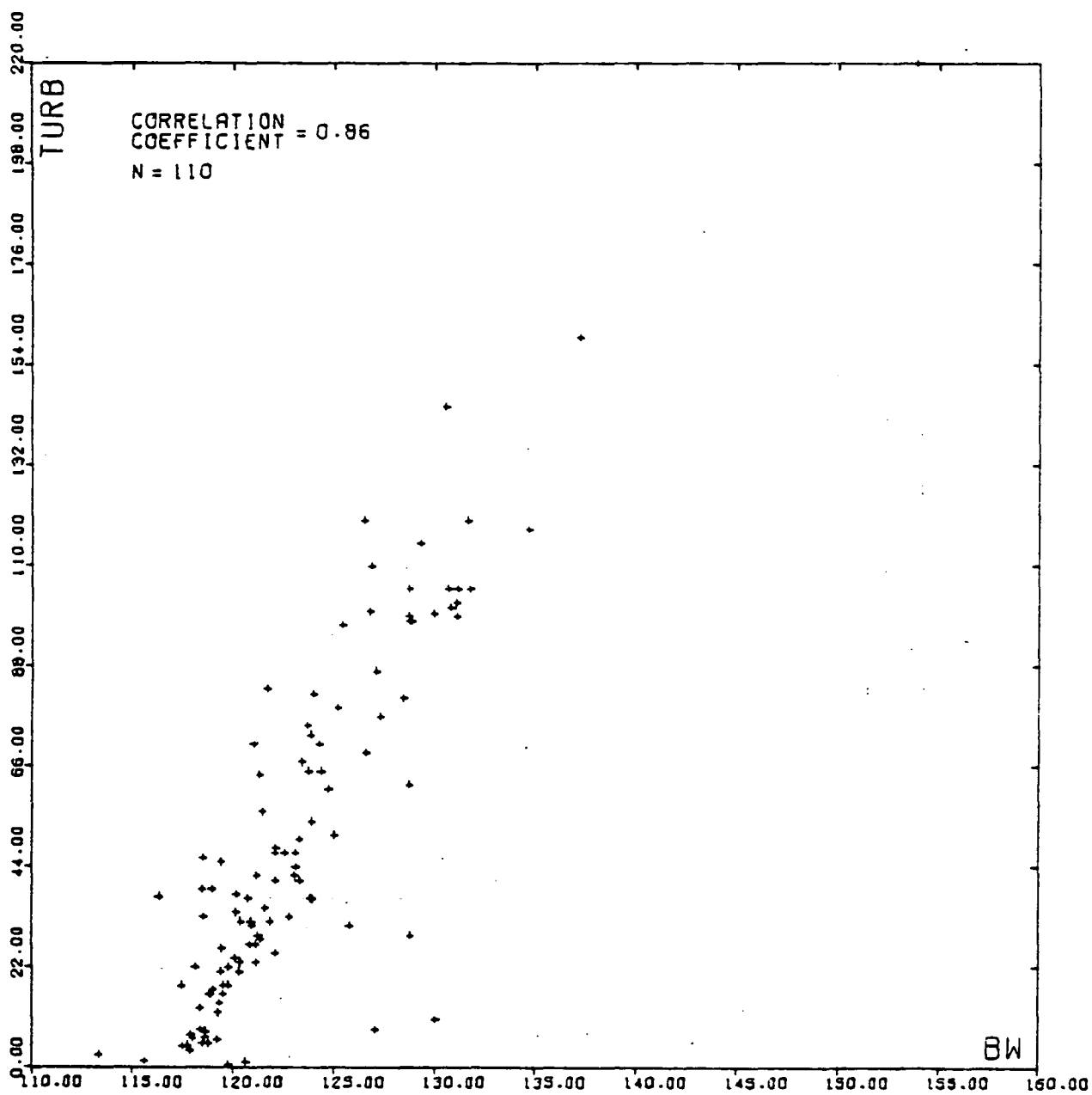


Figure 12. Variation of turbidity (NTU) with bandwidth of fluorescence emission spectrum, BW (nm), for 110 samples.

predicted by the exponential term in Equation 6, and on the correlation between  $F_\lambda/R$  and either DOC or TOC is not apparent in the curves shown in Figure 11.

Optical absorption by natural waters increases rapidly at shorter wavelengths, particularly below 380 nm, and is closely related to the DOC level (Dobbs et al., 1972; Mattson et al., 1974; Briggs et al., 1976; Smart et al., 1976). In this situation, the attenuation coefficients in Equation 6,  $k_R$  and  $k_\lambda$ , will become strongly dependent on  $n_f$  and, by implication, on DOC. Consequently, an increase in DOC, in addition to increasing  $F_\lambda$ , results in attenuation by absorption of both  $F_\lambda$  and the incident excitation beam. Even though differential absorption of  $F_\lambda$  with respect to  $R$  is a nonlinear process governed by the exponential term in Equation 6, its effect, for all but very highly colored waters, is to introduce a second order correction term into the otherwise linear relationship between  $F_\lambda/R$  and DOC. Clearly a trend of this magnitude that is also systematic with DOC will not have a significant influence on the correlation between  $F_\lambda/R$  and DOC, particularly in view of the relatively wide dispersion in the existing data as typified by the distributions shown in Figures 7 and 8. It is therefore likely that the effect of differential absorption is being masked by the scattered background signal that acts to enhance rather than attenuate  $F_\lambda$  (and  $F_\lambda/R$ ) in the spectral region below 380 nm.

Attenuation by Mie scattering from sample suspended sediment is also stronger at shorter wavelengths and is governed by a wavelength dependence of the form  $1/\lambda^y$  where, for waterborne particulates,  $y$  generally has a value in the range between 1 and 2 (Austin, 1974).

With  $y = 1.5$ , this dependence produces a 22% reduction in  $R$  at 381 nm in relation to  $F_\lambda$  at 433 nm, thereby suggesting the existence of a positive correlation between  $F_\lambda/R$  and turbidity for wavelengths above 381 nm. However, the data for this correlation, as shown in Figure 11, indicate a negative correlation on the order of -0.18 for the spectral region above 400 nm. Because this value is not significant at the 5 percent level for a sample size of 110, specific conclusions should not be drawn from these correlation data for this spectral region. For wavelengths shorter than 381 nm, Mie scattering losses in  $F_\lambda$  in relation to  $R$ , should reduce  $F_\lambda/R$  and produce a negative correlation with turbidity in contrast to the positive values shown in Figure 11. Clearly, any tendency in this direction has been masked by the influence of the scattered background signal in this spectral region.

A further trend apparent in Figure 11 is the tendency for the correlation between  $F_\lambda/R$  and POC to increase at shorter wavelengths, reaching a peak at about 360 nm. Two possible reasons for this trend are suggested. First, POC, which is only poorly correlated with DOC ( $r = 0.44$ ) and as such relatively independent of DOC, may make an increasing fluorescence contribution to  $F_\lambda$  at short wavelengths thereby raising the correlation between  $F_\lambda/R$  and POC.

Alternatively, the particulate organic material may be scattering the leaked background light into the emission monochromator in the same manner as the total suspended particulate concentration. With the data presently available, it is not possible to separate out the contributions that these two side effects make to the correlation between  $F_{\lambda}/R$  and POC. The fall-off in the correlation between  $F_{\lambda}/R$  and POC below 360 nm is most likely due to the dominance of the correlation between  $F_{\lambda}/R$  and turbidity in this spectral region caused by scattering of the background signal from suspended particulates.

(iii)  $F_R/R$

Although  $F_R/R$  exhibits a weaker correlation with DOC ( $r = 0.79$ ) than does  $F_{\max}/R$  ( $r = 0.83$ ), there are several reasons why  $F_R/R$  is preferable to  $F_{\max}/R$  for use as an airborne indicator of DOC.

First, the difference between these two coefficients, which is not significant at the 5 percent level for a sample size of 158, is apparently due to an experimental artifact introduced by a scattered background signal that leaks from the excitation monochromator. In the absence of this interference, it can be expected that the correlation between  $F_R/R$  and DOC will approach that obtained between  $F_{\max}/R$  and DOC.

The second reason concerns the influence of differential spectral absorption and scattering on the measurement of  $F_{\max}$  with respect to those of  $F_R$  and  $R$ . As already discussed, these secondary effects cause the fluorescence (and Raman) intensity measurements made at the shorter wavelengths to be attenuated more than those made at the longer wavelengths. Measured values of  $F_{\max}/R$  will therefore exhibit the influences of these side effects in addition to the desired information on DOC concentration. In contrast, both the airborne and laboratory measurements of  $F_R/R$  are free of these differential spectral effects as predicted by Equations 4 and 6 respectively.

A final advantage to using  $F_R/R$  concerns the practicabilities of making these fluorescence measurements with an airborne laser fluorosensor.  $F_R/R$  requires only three intensity measurements, one at 381 nm and one each on either side of the Raman wavelengths in order that  $F_R$  and  $R$  can be separated by the process of linear interpolation. Using the ratio  $F_{\max}/R$  as an indicator for DOC requires the additional measurement of  $F_{\max}$ . This demands that an additional system channel for optical detection, electronic monitoring and data recording be included in the airborne system.

(iv)  $(F_{\max} - F_R)/R$

This parameter was calculated with the purpose of subtracting out any background and interference effects common to both  $F_{\max}/R$

and  $F_R/R$ . The correlation of  $(F_{\max} - F_R)/R$  versus DOC gave a coefficient of +0.84, which is not significantly different from the value of +0.83 for the correlation between  $F_{\max}/R$  and DOC. This correlation is not surprising as  $F_{\max}/R$  and  $F_R/R$  are themselves highly correlated such that their difference will also be highly correlated with DOC provided that  $(F_{\max} - F_R)/R$  is not small in relation to  $F_{\max}/R$  and  $F_R/R$ . This parameter would therefore appear to have no particular advantage over  $F_{\max}/R$  or  $F_R/R$  as an indicator of DOC.

(v)  $F_{\max}/(R + F_R)$

This ratio has the advantage that its calculation requires only two spectral measurements;  $(R + F_R)$  is the total measured intensity at the Raman wavelength so that in this case  $R$  and  $F_R$  do not have to be separated. A requirement for only two discrete spectral measurements would reduce to two the number of detection, monitoring and recording channels required in an airborne laser fluorosensor in relation to the four needed to calculate  $F_{\max}/R$ .

At low DOC levels, fluorescence emission is generally weak with  $F_R \ll R$ , so that the ratio  $F_{\max}/(R + F_R)$  becomes equivalent to  $F_{\max}/R$ . At high DOC levels where  $F_R \gg R$ , the ratio becomes equivalent to  $F_{\max}/F_R$ . The merits of this latter ratio, which is also highly correlated with DOC, are discussed in the following section.

Although there is no conceptual basis for using this parameter as a DOC indicator, it appears to correlate with DOC as well as any of the other fluorescence parameters at the 5 percent significance level. In addition, it has the advantage of requiring only two spectral measurements.

(vi)  $F_{av}/R$

As the curve of  $r$  for DOC versus  $F_{\lambda}/R$  is essentially flat in the 400-nm to 500-nm wavelength region and as the bulk of the fluorescence emission occurs in this spectral region, the correlation of  $F_{av}/R$  versus DOC has a value of 0.81, which, not surprisingly, is essentially the same as the coefficients for DOC versus  $F_{\max}/R$  (0.83) and for DOC versus  $F_{\lambda}/R$  (0.83) in this spectral region. As the calculation of  $F_{av}/R$  requires considerably more spectral data than does  $F_{\max}/R$  or  $F_R/R$ , it offers no particular advantages as an indicator of DOC.

(vii)  $F_{\max}/F_R$  and  $\lambda_{cen}$

If the sole effect of changing the concentration of DOC (or TOC) were to simply change the amplitude of the fluorescence emission spectrum, one could anticipate a zero correlation between DOC and either  $F_{\max}/F_R$  or  $\lambda_{cen}$ . In reality, however, the coefficients for DOC versus  $F_{\max}/F_R$  and DOC versus  $\lambda_{cen}$  were 0.78 and 0.76,

respectively. These correlations exist because the fluorescence spectrum exhibits changes in location and shape in addition to amplitude with change in the DOC level.

This relationship is another manifestation of the influence of differential spectral absorption on the fluorescence measurements. The dependence of  $F_{\max}/F_R$  on the concentration of organic fluorophors,  $n_f$ , measured using a laboratory spectrofluorometer can be predicted by a relationship similar to Equation 6 such that:

$$\frac{F_{\max}}{F_R} = \delta_3 \exp \left\{ h (k_R - k_{\max}) \right\} \quad (7)$$

where  $\delta_3$  is a constant similar to  $\delta_1$  and  $\delta_2$ , and  $k_{\max}$  is the effective optical attenuation coefficient at  $\lambda_{\max}$ . As both  $F_{\max}$  and  $F_R$  are linearly dependent on  $n_f$ ,  $F_{\max}/F_R$  does not exhibit an explicit dependence on  $n_f$  but rather varies by virtue of the fact that the attenuation coefficient  $k_R$  and  $k_{\max}$  are both strongly dependent on  $n_f$ . Implicit in this discussion, is the assumption that  $n_f$  is closely related to DOC.

The experimental data relating DOC to either  $F_{\max}/F_R$  or  $\lambda_{\text{cen}}$  are presented in Figures 13 and 14 respectively. The trend in both cases is consistent with increasing sample self-absorption of the short (UV) wavelength component,  $F_R$ , in relation to the longer (blue) wavelength component,  $F_{\max}$ , with increasing sample DOC. Increasing DOC causes  $F_{\max}/F_R$  to increase and  $\lambda_{\text{cen}}$  to shift to longer wavelengths. Predictably,  $F_{\max}/F_R$  and  $\lambda_{\text{cen}}$  are highly correlated, with  $r = + 0.96$ ; the variation of  $\lambda_{\text{cen}}$  with  $F_{\max}/F_R$  is shown graphically in Figure 15.

The limiting value for  $F_{\max}/F_R$  of approximately 1.35 for vanishingly small DOC levels is presumably characteristic of spectra unbiased by differential self-absorption effects. Similarly, the limiting value of  $\lambda_{\text{cen}}$  for small DOC levels is approximately 427 nm.

Further evidence confirming the action of differential self absorption on  $F_{\lambda}$  was obtained by progressively diluting a single sample high in organics and low in suspended sediment with ultra-pure water. The variations in  $F_{\max}/R$ ,  $F_R/R$ ,  $F_{\max}/F_R$  and  $\lambda_{\text{cen}}$  with percentage dilution are presented in Figure 16.  $F_{\max}/R$  and  $F_R/R$  predictably fall to zero for a 100 percent pure-water sample, whereas  $\lambda_{\text{cen}}$  and  $F_{\max}/F_R$  fall to their limiting values typical of a sample low in DOC and therefore negligible self-absorption over a 1-cm pathlength.

These same values of  $F_{\max}/F_R$  and  $\lambda_{\text{cen}}$  for the diluted sample are also presented in Figure 15 together with the individual

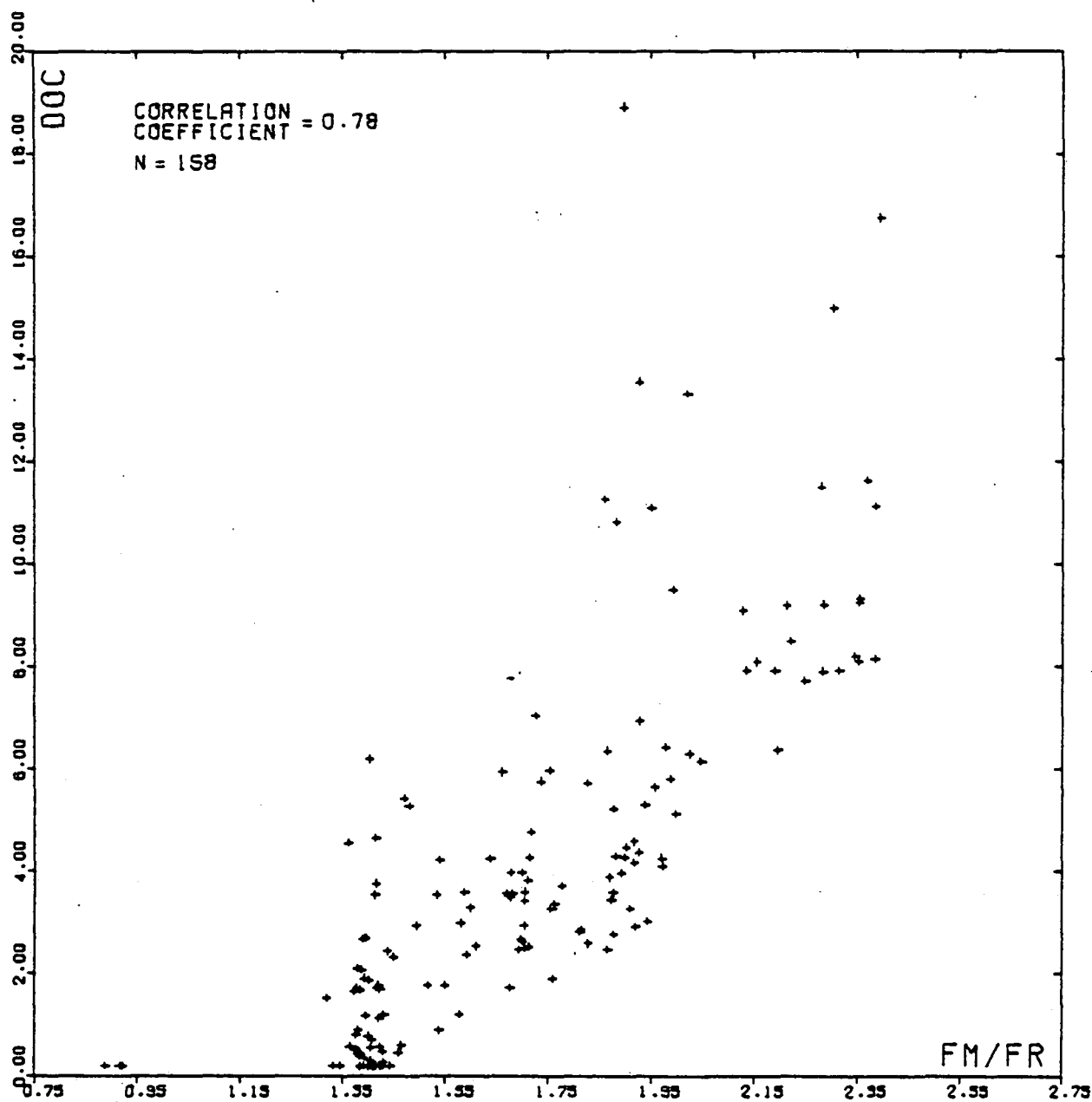


Figure 13. Variation of DOC (mg/l) with  $F_{max}/F_R$  for 158 samples.



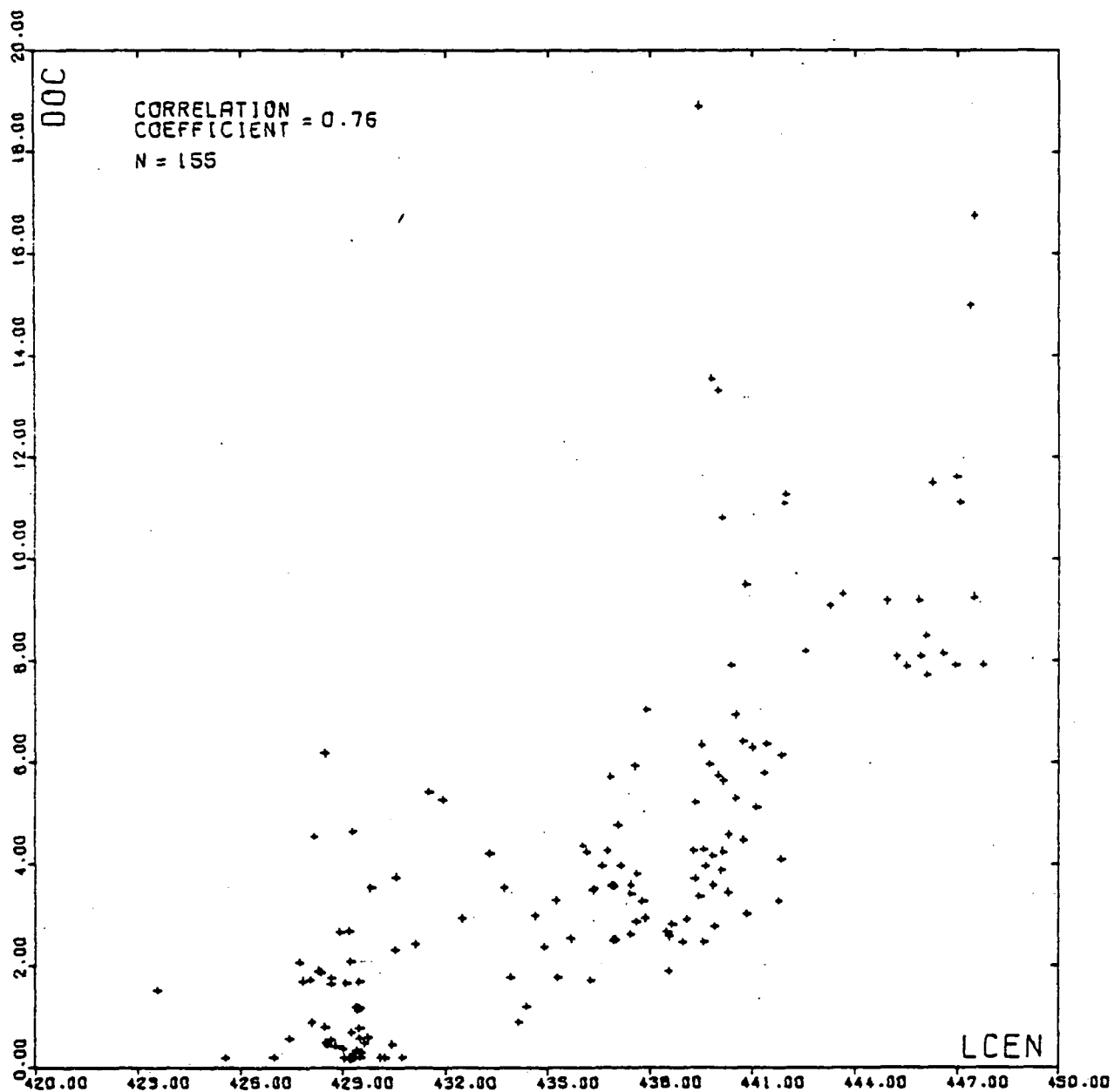


Figure 14. Variation of DOC (mg/l) with central wavelength of fluorescence emission band,  $\lambda_{cen}$  (nm), for 155 samples.

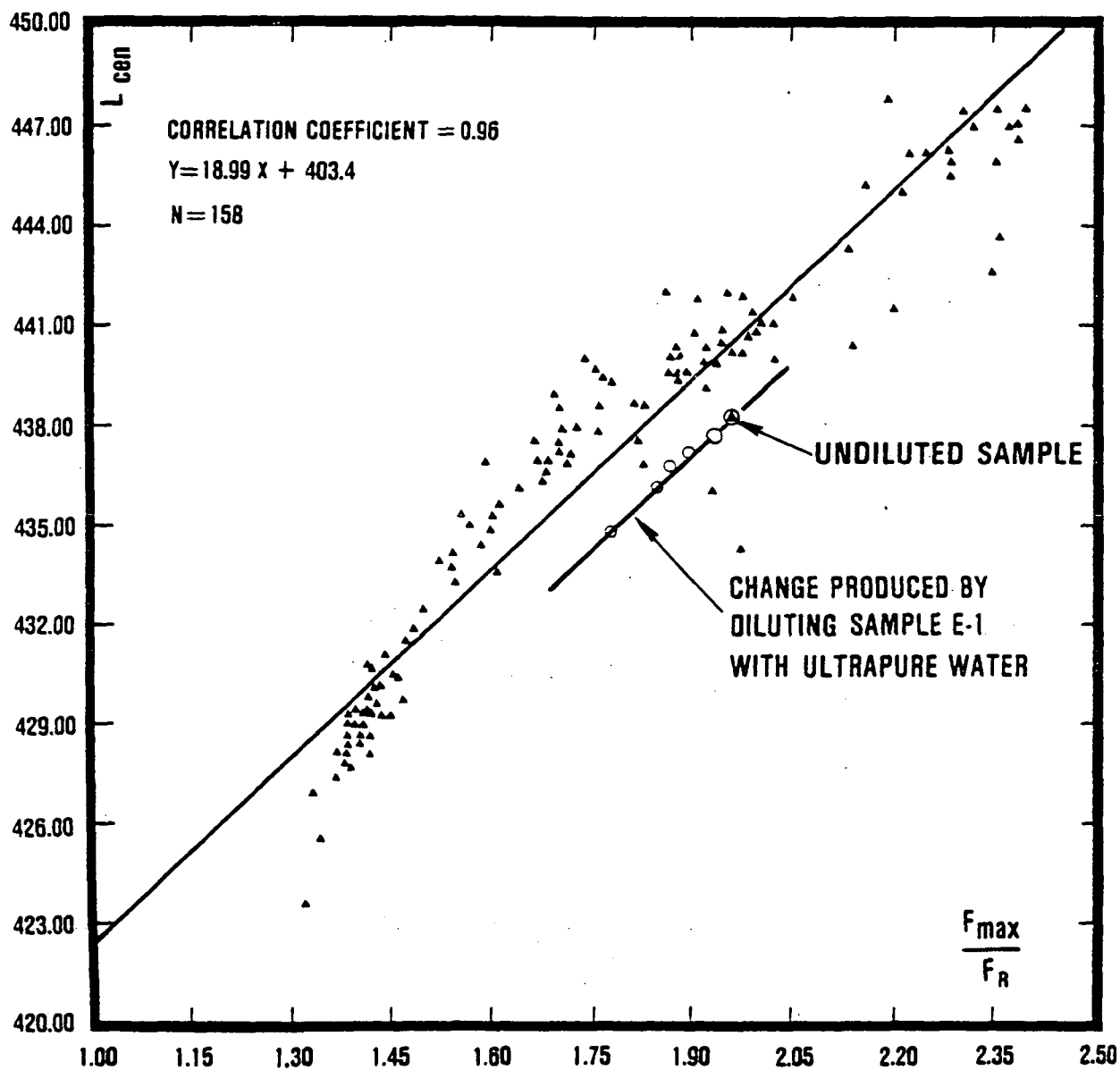


Figure 15. Variation of central wavelength of fluorescence emission band,  $\lambda_{cen}$  (nm), with  $F_{max}/F_R$ . Also shown are data obtained by progressively diluting a single Atchafalaya River sample (#E-1) with high-purity water.

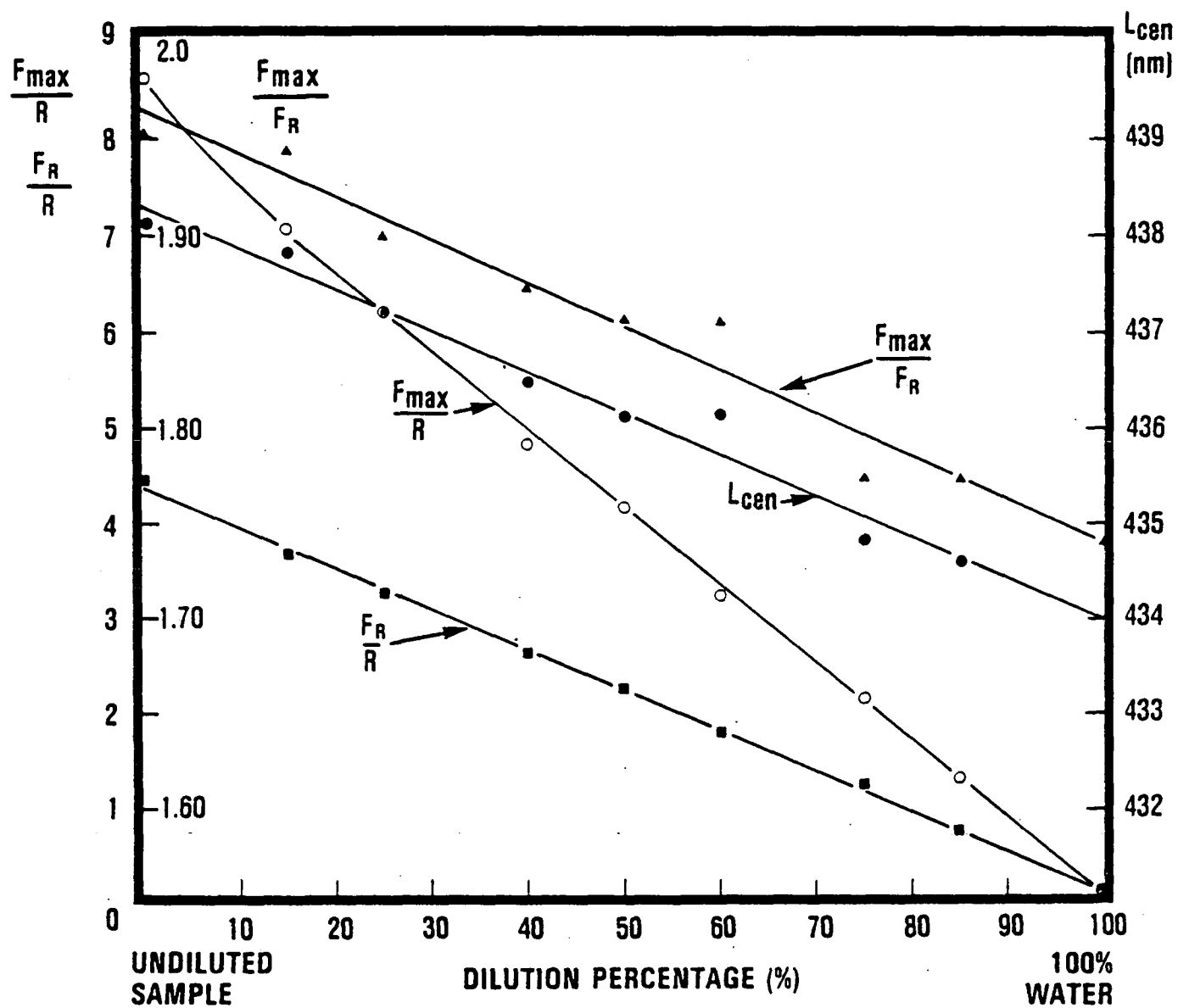


Figure 16. Changes in fluorescence spectrum parameters produced by progressively diluting an Atchafalaya River sample ( E-1) with high-purity water.

values for the 158 undiluted samples. The slope of the linear regression line of DOC on  $F_{\max}/F_R$  for the 158 undiluted samples was 19.0 and that for the dilution data is essentially identical at 19.1. From this observation, it is concluded that the change in  $F_{\max}/F_R$  and the shift in  $\lambda_{\text{cen}}$  with change in DOC concentration is due to optical self-absorption of the fluorescence emission by the sample rather than to any differences in the chemical or physical properties of the dissolved organics between samples. In addition  $F_{\max}/F_R$ , like  $F_{\lambda}/R$  for  $\lambda < 381$  nm, is influenced by the leaked background light which is scattered by sample suspended particulates. Table 2 indicates a correlation of -0.52 for  $F_{\max}/F_R$  versus turbidity suggesting that  $F_R$  is being enhanced in relation to  $F_{\max}$  by the scattered background signal.

$F_{\max}/F_R$  also exhibited significant correlations with pH and DO (dissolved oxygen) giving coefficients of -0.46 and -0.54 respectively. Although these correlations do not establish cause and effect relationships, it is possible that changes in these parameters might influence the shape and location of the fluorescence spectra. In particular, Smart et al. (1976) have demonstrated that changing sample pH to values greater than 9 or to less than 4 can have a marked effect on the overall emission intensity whereas changes of pH within this band had only a small effect on sample fluorescence. As the maximum and minimum values of pH encountered in this study were 8.10 and 6.70 respectively as shown in Table 4, one can expect the effect of pH on  $F_{\max}/F_R$  to be minimal. The negative correlation between pH and  $F_{\max}/F_R$  would seem to imply that increasing pH either increases  $F_R$  in relation to  $F_{\max}$  or shifts the whole fluorescence spectrum to shorter wavelengths. No further investigations of the influence of pH on  $F_{\lambda}$  were conducted partly because water pH cannot be measured from an airborne platform and partly because its effect on the correlations between DOC and the more important ratios,  $F_{\max}/R$  and  $F_R/R$ , was, at the most, only marginally significant (see Table 2).

Unlike fluorescence parameters such as  $F_{\max}/R$  that are subject to interference from differential absorption,  $F_{\max}/F_R$  is uniquely dependent on this phenomena for its existence as a DOC indicator. However, like  $F_{\max}/R$ , it is susceptible to scattering interference from suspended sediment and, similarly, requires four spectral measurements for its determination.

Although  $\lambda_{\text{cen}}$  appears to be equally good as an indicator of DOC as is  $F_{\max}/F_R$ , its measurement would probably require at least six spectral measurements in the 400-nm to 450-nm region for its accurate determination.  $F_{\max}/F_R$  and  $\lambda_{\text{cen}}$  would therefore appear to offer no special advantages over  $F_R/R$  as indicators of DOC while incurring several disadvantages.

## MULTIPLE CORRELATION EFFECTS

Multiple linear correlation effects between specific fluorescence properties and an array of water quality parameters were also investigated with a view to determining the cause of the residual variation,  $(1-r^2)$ , not explained by a simple two-parameter linear relationship between the fluorescence and organic carbon parameters. Table 3, an array of linear correlation coefficients for relationships between water quality parameters, indicates the presence of a number of correlations significant at the 5-percent level. In particular, correlations between DOC and either chlorophyll a, dissolved oxygen or turbidity gave coefficients of -0.25, -0.23, and -0.26 respectively. Correlations between the fluorescence and water quality parameters are given in Table 2. The most significant correlations were seen to be those between  $F_{\max}/F_R$  and either dissolved oxygen, pH or turbidity, for which the coefficients were -0.54, -0.46 and -0.52 respectively.

Multiple linear regression analysis was applied to all data sets complete in fluorescence and organic carbon parameters together with chlorophyll a, pH, dissolved oxygen, conductivity and turbidity. A total of 87 samples from the Atchafalaya River Basin for which complete data sets existed was used in the analysis. The multiple correlation analysis employed a stepwise regression procedure for maximizing the multiple correlation coefficient (Dixon, 1975). Multiple correlation coefficients for  $F_{\max}/R$  or  $F_R/R$  versus the array of water quality parameters, including TOC, DOC and POC, not surprisingly indicated the principal water quality parameter to be DOC with very small increments from dissolved oxygen, chlorophyll a, turbidity and pH. For example the coefficient for  $F_{\max}/R$  versus DOC is +0.773, increasing to +0.787 by adding in dissolved oxygen and to +0.791 by adding in chlorophyll a.

Only multiple correlations with  $F_{\max}/F_R$  appeared to show any real improvement over the two-parameter linear correlation model. The multiple correlation coefficient for  $F_{\max}/F_R$  versus DOC is +0.69, increasing to +0.82 by adding in turbidity, to +0.85 by adding in dissolved oxygen, and to +0.86 by adding in conductivity. However, the influence of turbidity can be discounted as it has been shown to be caused by an instrumental artifact whereby a leaked background light signal is scattered into the detector by suspended sediment.

Clearly, the influence of these additional water quality parameters other than turbidity on the relationships between DOC and the various fluorescence parameters are not significant, suggesting that other reasons must be found to explain why these correlations are less than ideal. This subject will be examined in more detail in the discussion (Chapter 10).

## SECTION 9

### DIFFERENCES BETWEEN LASER FLUOROSENSOR AND SPECTROFLUOROMETER MEASUREMENTS OF $F_R/R$

Utilization of the fluorescence-organic carbon regression data to predict TOC or DOC values from airborne fluorometric measurements assumes that the fluorescence ratios measured using the laboratory spectrofluorometer, in particular  $F_{\max}/R$  and  $F_R/R$ , are directly equivalent to those values measured using an airborne laser fluorosensor. With a view to testing this assumption, an experiment was conducted in which  $F_R/R$  was measured for a representative group of 10 samples selected from the 161 samples of the survey using both the spectrofluorometer and a laboratory laser fluorosensor that simulates the optical characteristics of an airborne system.  $F_R/R$  was chosen for the comparison rather than  $F_{\max}/R$  in order to avoid possible interferences from differential absorption and scattering effects.

The simulated laser fluorosensor, shown schematically in Figure 17, used a pulsed  $N_2$  laser excitation source, and was configured so as to monitor the fluorescence and Raman emission in the  $180^\circ$  scattering mode; the  $180^\circ$  scattering angle used in this laboratory simulation and the  $0^\circ$  scattering angle used in airborne measurements for viewing the water Raman emission are exactly equivalent (Gilson and Hendra, 1970). The effects of laser beam polarization and emission monochromator polarization artifacts on the laser fluorosensor measurements of  $F_R/R$  were eliminated by depolarizing the laser excitation beam and the fluorescence emission using compensated quartz-wedge polarization scramblers, as shown in Figure 17. The pulsed emission from the samples was dispersed through a scanning monochromator with 0.8 nm spectral resolution and detected with a fast response photomultiplier (Hamamatsu R928). Using a sampling oscilloscope in the non-scanning mode, the peak of the pulse was converted into a steady signal level and used to produce stripchart recordings of the emission spectra by scanning the monochromator from 350 nm to 500 nm. By careful choice of electronic low-pass filter cutoff frequency and monochromator scanning rate, a considerable enhancement in the signal-to-noise ratio was achieved for spectra recorded in this manner. The [OH]-stretch water Raman band for a high purity water sample recorded with this simulated laser fluorosensor is shown in Figure 18. The width of this band (FWHM) at  $20^\circ\text{C}$  was 6.4 nm, which is close to the value of 6.3 nm estimated from the measurements of Walrafen (1967) made at  $20^\circ\text{C}$ .

The values of  $F_R/R$  for the 10 samples obtained using both spectrofluorometer (SPF) and laser fluorosensor (LFS) systems are plotted against one another in Figure 19. The two sets of data are related by the approximate relationship:

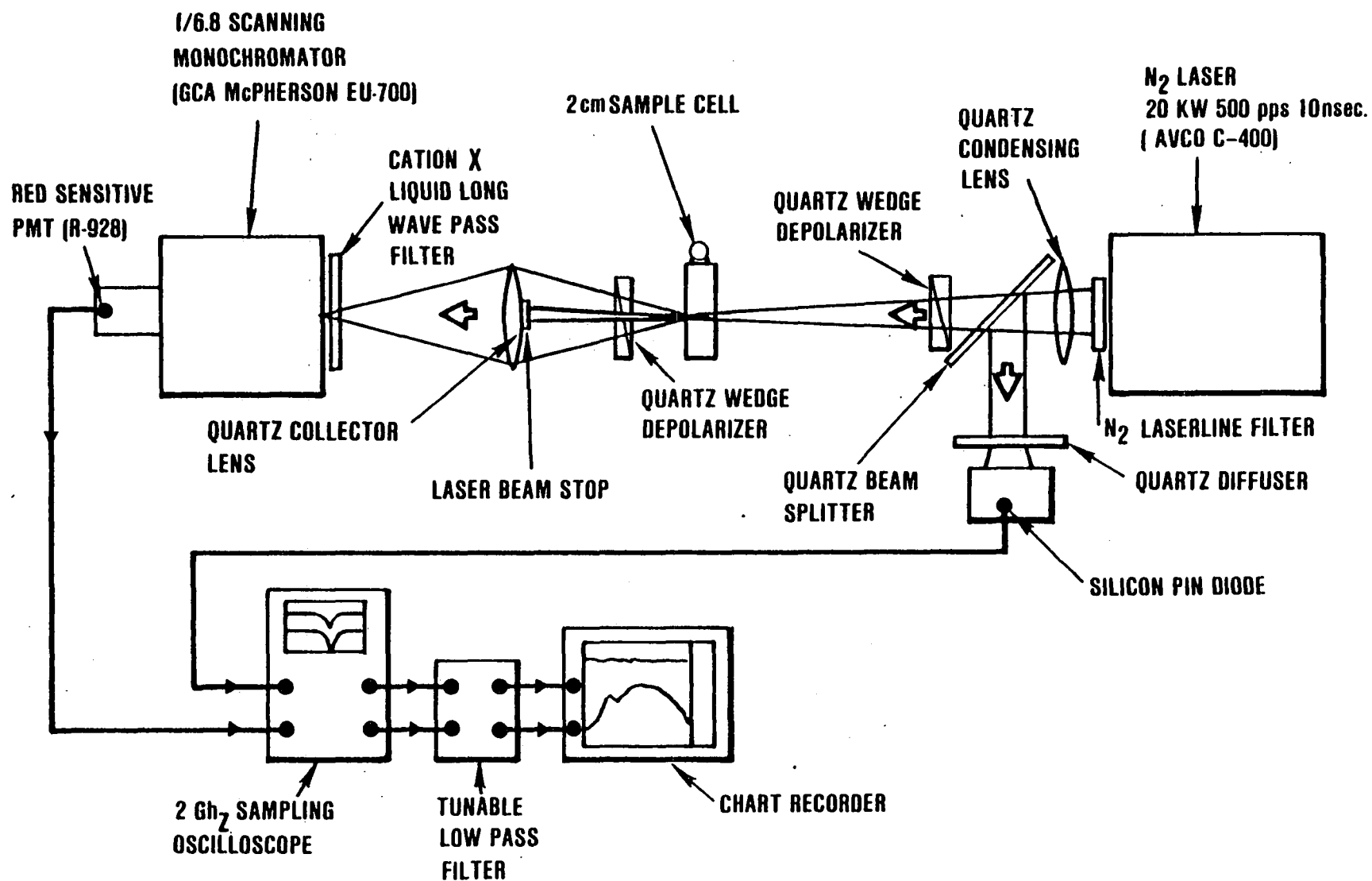


Figure 17. Optical layout for laboratory simulation of airborne laser fluorosensor for monitoring surface water organics.

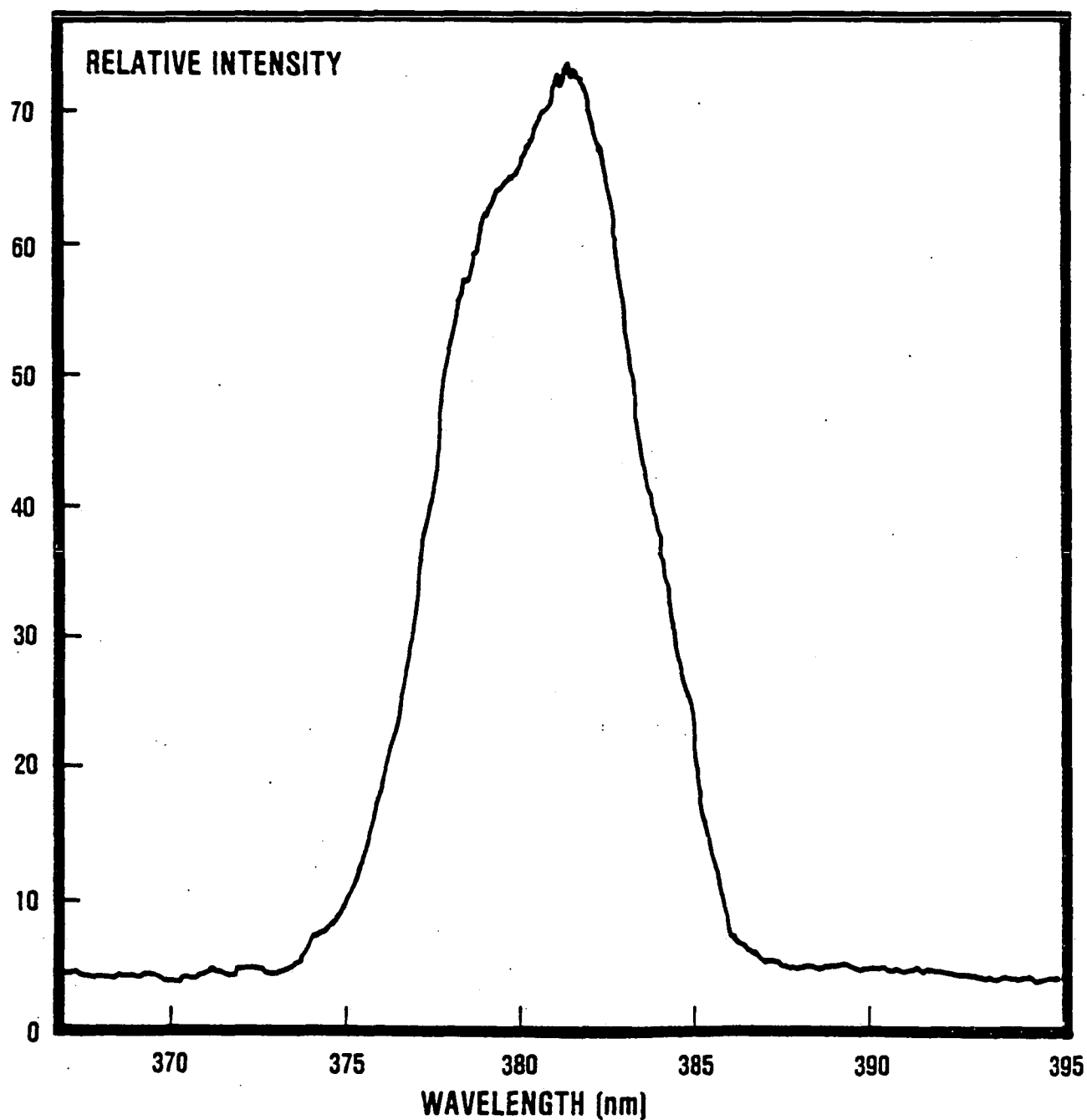


Figure 18. Emission spectrum showing [OH]-stretch water Raman band from high-purity water sample at 381 nm, excited by N<sub>2</sub> laser at 337 nm.



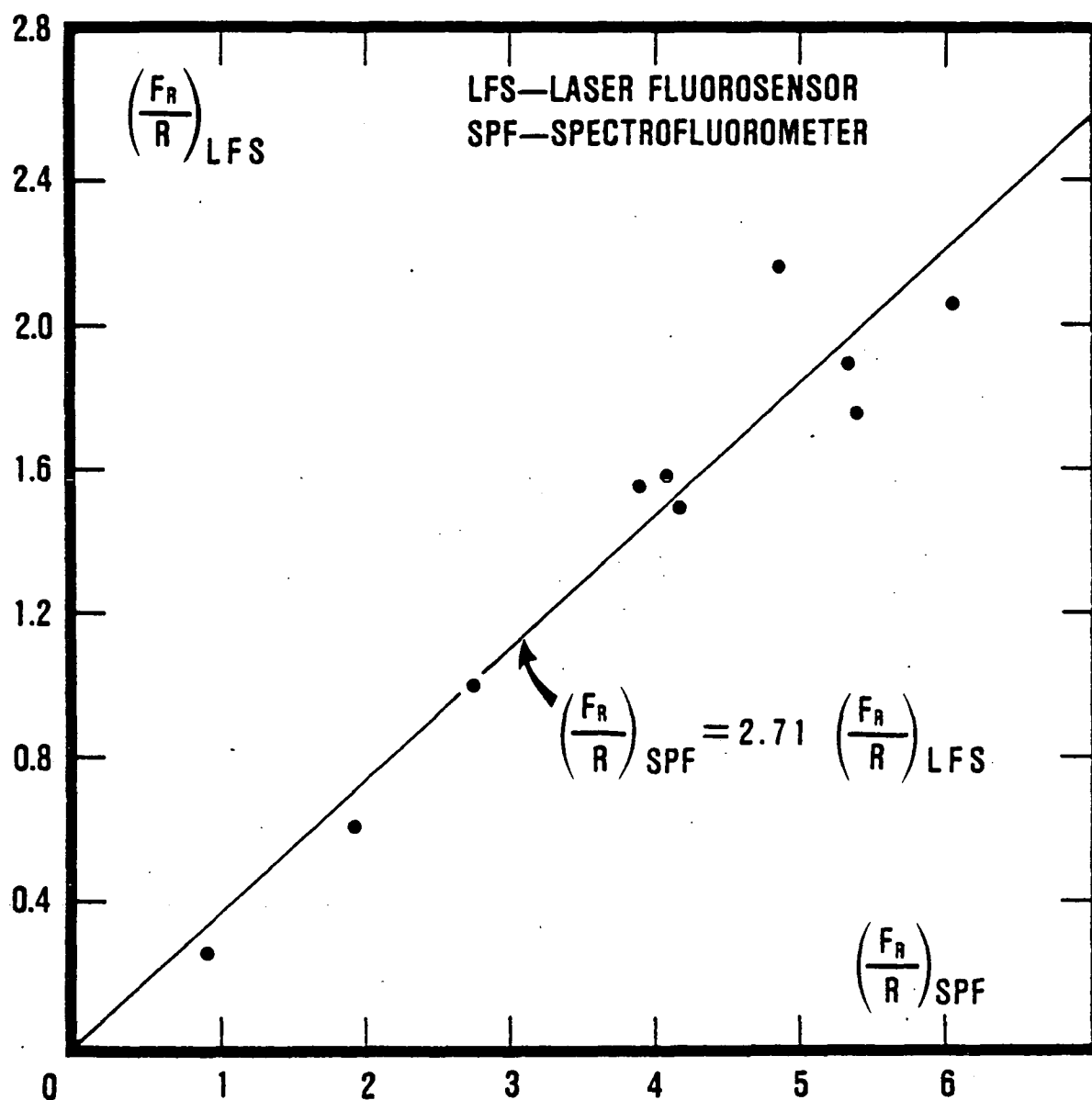


Figure 19. Variation of  $F_R/R$  from simulated laser fluorosensor measurements with comparable values measured using a laboratory spectrofluorometer for a variety of field samples.

$$(F_R/R)_{SPF} = 2.71 (F_R/R)_{LFS}$$

(8)

The deviation of the individual data points from the regression line, given by Equation 8, was found to be reproducible for a given sample and is considered to be due principally to scattering artifacts introduced into the measurement of  $(F_R/R)_{SPF}$  by sample-to-sample variability in the concentration of suspended particulates. As already discussed, suspended particulates scatter an undispersed background signal, which is known to leak from the excitation monochromator into the emission monochromator. This background signal increases both the measured values of  $(F_R)_{SPF}$  and the calculated values of  $(F_R/R)_{SPF}$  above their true values. In addition, sample particulates also produce partial depolarization of the Raman emission, which, in conjunction with the polarization sensitivity of the emission monochromator, can produce changes in the measured values of  $(R)_{SPF}$  and hence in the calculated values of  $(F_R/R)_{SPF}$ .

A number of factors are known to be responsible for the large value of the ratio of  $F_R/R$  measured with the spectrofluorometer in relation to that measured with the laser fluorosensor. These factors are discussed below and wherever possible, correction factors are calculated with a view to reducing this ratio toward unity:

(i) Spectrofluorometer Spectral Resolution

Although the spectrofluorometer has a limiting spectral resolution of 0.2 nm, signal-to-noise requirements dictate the use of excitation and emission slit widths equivalent to 3 nm when monitoring the relatively weak water fluorescence and Raman signals. The true bandwidth at FWHM for the [OH]-stretch Raman band at 381 nm when excited at 337 nm is 6.3 nm (Walrafen, 1967), whereas the bandwidth measured using 3 nm-wide excitation and emission slits is on the order of 7.2 nm (Figure 2). By progressively reducing the slit width towards zero, the true Raman bandwidth of 6.2 nm was obtained, together with a 30 percent increase in the Raman band amplitude, but with a considerable reduction in the signal-to-noise ratio. Correction factors of 1.3 and  $1.3^{-1}$  should therefore be applied to the measured values of  $R_{SPF}$  and  $(F_R/R)_{SPF}$  respectively.

(ii) Spectrofluorometer Risetime

Due to the combined effects of spectrofluorometer wavelength scanning rate, finite chart recorder slewing rate and electronic low-pass filter bandwidth, a full scale (10 inches) chart deflection signal for the Raman band is attenuated by about 5 percent. The corresponding multiplicative correction factor is 1.05 falling to 1 as the signal amplitude is reduced to zero. Correction factors of up to 1.05 and  $1.05^{-1}$  should therefore be applied to the measured values of  $(R)_{SPF}$  and  $(F_R/R)_{SPF}$  respectively depending on the relative amplitude of  $(R)_{SPF}$ .

(iii) Laser Fluorosensor Induced Sample Photodecomposition

Photodecomposition of the dissolved organics by the focused UV laser beam was generally found to reduce  $(F_R)_{LFS}$  by about 5 percent during the time taken to perform a spectral scan of a fresh sample. A correction factor of 1.05 should therefore be applied to the measured values of  $(R)_{LFS}$  and  $(F_R/R)_{LFS}$ . Clearly, sample photodecomposition effects will not occur during the airborne operation of a laser fluorosensor as the water surface sample volume would be exposed to only a single laser pulse of considerably lower energy and power densities than exist for the laboratory laser fluorosensor measurements.

(iv) Laser Fluorosensor Fluorescence Decay Time

In contrast to the spectrofluorometer, which uses a constant output excitation source, the laser is pulsed with pulsewidth on the same order as the fluorescence lifetime of the dissolved organics. Consequently the fluorescence pulse observed from the water samples will be stretched-out such that the peak amplitude is attenuated in relation to that for the laser excitation pulse. As the Raman emission process is essentially instantaneous, the Raman pulse follows the profile of the laser excitation pulse so that its peak amplitude is unattenuated. To a first approximation, the effects of fluorescence pulse-stretching on the amplitude of  $(F_R)_{LFS}$  can be estimated by multiplying  $(F_R)_{LFS}$  and  $(F_R/R)_{LFS}$  by  $(\tau_f/\tau_L)$ , the ratio of the fluorescence to laser pulsewidths at FWHM.  $\tau_f$  was measured to be about 13 nsec for the majority of samples examined and  $\tau_L$  was about 10 nsec, so that  $(\tau_f/\tau_L) = 1.3$ . This correction procedure is based on the assumption that both the fluorescence and Raman pulses are Gaussian in shape and concurrent in time during the oscilloscope pulse height measurement.

(v) Polarization Artifacts

Liquid water consists of two spectroscopically distinct forms in thermal equilibrium. These polymeric and monomeric types influence the [OH] molecular bond strength and ultimately the nature of the [OH]-stretch Raman emission (Chang and Young, 1974). In particular, the spectral characteristics of the Raman emission are highly dependent on both the polarization state of the excitation radiation and on the scattering configuration used to view the emission (Gilson and Hendra, 1970). The partial polarization effect introduced by the diffraction grating monochromators and the 90°-scattering configuration of the spectrofluorometer are therefore not compatible with the format envisioned for an airborne laser fluorosensor. An airborne laser fluorosensor of necessity operates in a downlooking mode, which constitutes a 0°-scattering angle, and will likely employ an essentially unpolarized N<sub>2</sub> laser as the excitation source. Consequently, the combined effects of Raman band depolarization, the polarization sensitivity of the excitation and emission

monochromators and the 90°-scattering configuration employed by the spectrofluorometer make it difficult to estimate an equivalent laser fluorosensor value for  $F_R/R$  from the values measured using a spectrofluorometer.

By combining all of the above correction factors into a single factor, viz.,  $(1.3 \times 1.05 \times 1.30 \times 1.05)^{-1}$ , the constant in Equation (3) can be reduced from 2.71 to 1.45. It is suggested that the deviation of this new ratio or conversion factor from unity is due principally to the polarization artifacts known to influence the spectrofluorometer determination of  $R$ .

On the basis of the foregoing discussion, it is clear that the laboratory spectrofluorometer and airborne laserfluorosensor determinations of  $F_R/R$  are not equivalent and that different laboratory and airborne systems will produce different values for the conversion constant in Equation 8. In addition, measurements of  $F_R/R$  made on identical samples but using different spectrofluorometers will also be different due to the different spectral, temporal and polarization artifacts introduced by each instrument into the measurement of  $R$ .

## SECTION 10

### DISCUSSION

#### INHERENT LIMITATIONS IN THE $F_{\lambda}/R$ -DOC CORRELATION METHOD

Although a highly significant correlation has been found to exist between  $F_{\lambda}/R$  and DOC, these regression data cannot be used to provide a precise prediction of DOC concentration for other water bodies using airborne measurements of  $F_{\lambda}/R$  because of the relatively wide scatter in the distribution of DOC with  $F_{\lambda}/R$ , as illustrated by the data in Figures 7 and 8.

A number of these outlying data points can be explained on the basis of poor experimental methodology. Six samples were found to have DOC values greater than their corresponding TOC values and, in the three of these cases where the differences were large, the DOC data points were among the 10 most extreme outliers, whereas the corresponding data points for TOC versus  $F_{\max}/R$  lay significantly closer to the regression line. This suggests the existence of a problem with the DOC analyses, probably involving contamination during filtration of the samples.

Problems with adsorption of COC (colloidal organic carbon) onto the glass fiber filters during preparation of the DOC samples do not appear to have made a significant contribution to this scatter. This can be concluded because of the good DOC reproducibility obtained on 30 replicates of a single Lake Mead sample, and also because the scatter present in the plot of DOC versus  $F_{\max}/R$  is also present in the plot of TOC versus  $F_{\max}/R$ , although on a somewhat smaller scale. In particular, six of the ten most extreme outliers in Figure 7 with high DOC values correspond with six of the ten most extreme outliers in Figure 8 with high TOC values.

The principal reasons for the less than ideal correlation between DOC and a given fluorescence parameter, say  $F_R/R$ , can be understood by representing each parameter as a summation of its constituent parts where these parts are the product of the concentration of each individual substance and an appropriate conversion factor. A general expression for the concentration of DOC can be written in the form:

$$\text{DOC} = \sum_{i=1}^q \begin{pmatrix} D, F \\ n_i \quad b_i \end{pmatrix} + \sum_{i=q+1}^t \begin{pmatrix} D, NF \\ n_i \quad b_i \end{pmatrix} \quad (9)$$

where  $n_i$  is the concentration of the  $i^{\text{th}}$  organic chemical substance,  $b_i$  is a factor that converts  $n_i$  to an equivalent carbon value, superscripts F and NF denote whether the substance is respectively either fluorescent or nonfluorescent, and D is a superscript denoting a dissolved substance. The number of terms in the fluorescent DOC and nonfluorescent DOC series, respectively  $q$  and  $t-q$ , will depend critically on the type and pore size of the filter used to separate the DOC fraction from the POC fraction. It is likely that both  $q$  and  $(t-q)$  are significantly larger when using filters known to be nonadsorbing rather than adsorbing for the purpose of separating the POC and DOC fractions. Similarly,  $F_R/R$  can be written as:

$$\frac{F_R}{R} = A \left\{ \sum_{i=1}^q \left( \frac{D, F}{n_i \sigma_i} \right) + \sum_{i=q+1}^s \left( \frac{P, F}{n_i \sigma_i} \right) \right\} \quad (10)$$

where  $A$  is a proportionality constant that accounts for system and environmental factors such as attenuation coefficients, fields of view, system efficiencies, etc.,  $\sigma_i$  is the excitation cross section for the  $i^{\text{th}}$  substance for fluorescence emission at Raman wavelength  $\lambda_R$  when excited at wavelength  $\lambda_L$ , and  $P$  is a superscript denoting a particulate substance. As the fluorescence measurements, whether measured from an airborne platform or in the laboratory, are obtained on unfiltered samples, the division of this expression into two parts representing the dissolved and particulate fractions is arbitrary, and is made solely to aid in the comparison with the similar expression for DOC. Consequently the dissolved fraction is composed of the contributions from  $q$  substances whereas the particulate fraction is composed of the contributions from  $(s-q)$  substances where  $s$  is the total number of fluorescent substances present in the sample, both particulate and dissolved. It is assumed in the formulation of Equation 10, that the fluorescence from inorganic fluorophors is negligible. As noted earlier, the fluorescence of water samples undergoes a large reduction after passage of the samples through an activated carbon filter, indicating that the fluorescence originates predominantly from dissolved organics rather than from inorganic substances.

From an initial examination of these two equations, it is surprising that a correlation of any significance exists between  $F_R/R$  and DOC, particularly as the conversion factors  $b_i$  and  $\sigma_i$  are considered to be unrelated. The most likely set of circumstances that supports the observed correlation between  $F_R/R$  and DOC ( $r = 0.78$ ) are that:

(a) the second (and presumable larger) term in Equation 9, representing the nonfluorescent DOC, varies in unison with the first term representing the fluorescent DOC,

(b) the second term in Equation 10 representing the particulate fluorophors is significantly smaller than the first term representing the dissolved fluorophors,

and

(c) the first term in Equation 10 varies as the first term in Equation 9.

If all of these conditions are met, then Equations 9 and 10 can be combined, and reduced to a form similar to Equation 5 where  $n_f$  is equivalent to DOC.

It should be noted that for condition (c) to be valid, the conversion factors  $b_i$  and  $\sigma_i$  must either remain essentially constant or vary in unison, or alternatively the averaging effect of large values for  $n_i$  in combination with small values for  $b_i$  and  $\sigma_i$  for a large number of substances must be such that the first term in Equation 9 varies closely as the first term in Equation 10. These conditions are most likely to be met for water within a given drainage basin or lake system where the percentage contribution from each organic substance or group of substances remains nearly constant. It is therefore significant that the samples corresponding to 6 of the 10 extreme outliers in Figures 7 and 8 with high DOC and TOC values respectively, were collected at sites in swampland regions of the Atchafalaya Basin outside the levees that define the floodway. Samples from these regions, unlike those obtained from within the levees, were generally characterized by relatively high levels of chlorophyll a and relatively low turbidity.

The data corresponding to the samples from Lakes Mead and Mohave, apparent in Figures 7 and 8 as the discrete group of points at the low end of the fluorescence scale, are somewhat more anomalous in that these samples exhibit considerable variability in TOC and particularly DOC for essentially constant fluorescence. In addition, all the outliers with high values of DOC or TOC correspond to samples collected from Lake Mead, although the highest DOC value in this group can probably be discounted as it exceeds the corresponding TOC value.

Although there are no obvious explanations for the variability in the Lake Mead data, particularly in view of the essentially constant fluorescence data, several possibilities are discussed. Pleasure craft introduce oil and gasoline residues onto the lake surface, but these substances can be discounted as a reason for this variability as it is well established that petroleum based hydrocarbons are highly fluorescent.

Lake Mead, being surrounded by desert low in vegetation and having low annual rainfall, receives very little organic carbon through runoff from natural vegetation. In addition, examination of the TOC and DOC data in relation to the sampling sites suggests that Las Vegas Wash does not introduce significant levels of organic carbon into Lake Mead.

Another possible source for this variability, particularly in the DOC data, is the phytoplankton population. It is known that both marine and freshwater algae exude large amounts of DOC during photosynthesis, principally in the form of carbohydrates, and release similar amounts on their death and decomposition, and that this algae-related DOC is often a large fraction of the total DOC level (Wangersky, 1972; 1978). Further amounts of DOC are also likely to be produced by zooplankton grazing.

Although planktonic chlorophyll a measurements were not made on the samples from Lakes Mead and Mohave, it was noticed that the samples corresponding to the six principal outliers in this group were collected at sites that are possibly associated with anomalously high levels of chlorophyll a in relation to nearby deep water sampling sites. Three sites, located close to a cove, a recreational beach and an island, support significant populations of benthic algae, whereas the other three sites were located close to anchored navigation buoys that are known to support colonies of periphytonic algae.

If this explanation for the DOC variability for the Lake Mead samples is to be accepted, then it is necessary to assume that this algae-related DOC is essentially nonfluorescent, such that it makes a significant contribution to the second term in Equation 9 without making a corresponding contribution to Equation 10. Samples taken from other water bodies that are characterized by significant spatial variability in the phytoplankton population might then be expected to exhibit similar variability in the distribution of DOC while maintaining a nearly constant fluorescence emission signal.

This suggestion is highly tentative and is based on the unsubstantiated assumption that algae-related DOC is nonfluorescent. Clearly an investigation should be made to establish the fluorescence properties of the DOC fraction associated with the phytoplankton community before any firm conclusions can be reached.

In relation to this anomaly, it is worth noting that the chlorophyll a and DOC data for the Atchafalaya Basin samples did not exhibit a direct relationship. The most likely explanation for the negative correlation ( $r = -0.25$ ) is probably the presence of high levels of detrital organic matter in many of the Mississippi Floodway samples that is closely related to the DOC levels. This same detrital matter, manifest as high sample turbidity, severely limits light penetration, which in turn inhibits photosynthesis resulting in depressed chlorophyll a levels. Under these circumstances it is likely that tendencies towards a direct relationship between algae-related DOC and chlorophyll a are being masked.

Finally, the possibility exists that the relatively high variability in the DOC data (in relation to the TOC data) was caused by some shortcoming in the DOC analysis, particularly, as has already been noted, the extreme outlier for the Lake Mead data had a DOC value greater than the corresponding TOC value. In spite of careful preparations, sample contamination can always occur during either the handling, acidification, filtration or analysis of the samples, or alternatively by sample leakage past the filter.

#### CALIBRATION OF AIRBORNE $F_R/R$ DATA IN TERMS OF DOC CONCENTRATION

The obvious inconsistencies between Equations 9 and 10 constitute an inherent limitation to the determination of a universal relationship between  $F_R/R$  and DOC. This conclusion is not surprising in view of the wide diversity of organic substances, both natural and manmade, that are present in the aquatic environment.



It is suggested that the impact of these differences on the potential for remote sensing organic carbon be minimized by treating each water body as a separate entity with its own unique conversion factor relating  $F_R/R$  to the DOC concentration. This approach is justified on the assumption that, within a given water body, the fluorescent organics change in concentration but not in character. However, this can lead to ambiguities in the interpretation of the airborne data whereby changes in  $F_R/R$  may result from changes in DOC or, alternatively, be caused by the presence of organics with anomalous fluorescent properties.

In any event, such a situation, involving large or sudden changes in  $F_R/R$  over a short distance, would demand that the anomaly be subjected to more intensive investigation by conventional sampling and analytical techniques. Clearly the determination of a conversion factor for each water body by means of an extensive ground truth survey is not only time-consuming and costly but negates any advantages to be gained from a subsequent remote sensing survey. Rather, the airborne measurements for  $F_R/R$  must be calibrated directly in terms of DOC by collecting samples for DOC analysis at a number of key reference sites under the sensor flight path concurrent with the airborne mission. On receipt of this ground truth DOC data, it will then be possible to calibrate the airborne survey data for use in preparing maps of the water surface indicating lines of constant DOC concentration. Because of the possibility of ambiguities in the interpretation of the data as mentioned earlier, it is suggested that these maps be employed in a general purpose screening role to indicate trends and anomalies in the distribution of surface water organics that can then be used to investigate these anomalies in more detail by direct sampling methods.

This direct calibration approach has its limitations; first, it requires that a limited ground truth capability be made available for every airborne mission, and second, this in situ calibration is still subject to the influence of anomalous samples that can produce excessively weak or strong fluorescence emission for a given DOC level.

However, these limitations are more than offset by three significant advantages to be gained by direct calibration of the airborne data at the time and place of a particular survey. First, as the calibration is obtained at the same place and time as the survey, it corresponds exactly to the particular distribution of organics present and to the environmental conditions to which these organics are being subjected. Second, direct calibration of the airborne fluorescence data in terms of DOC avoids the requirement for performing laboratory fluorescence analyses on the reference samples. This is advantageous because  $F_\lambda/R$  is known to be sensitive to variations in sample temperature and pH, which will change between field and laboratory, and because of the problems encountered in converting the  $F_\lambda/R$  data measured on a specific laboratory spectrofluorometer to values equivalent to those measured using a specific airborne laser fluorosensor. Finally, direct calibration of the airborne data at the time of a specific survey eliminates any limitations that might be incurred by using laboratory calibration data. In particular, it now becomes possible to use different excitation wavelengths, subject of course to the availability of a laser with the desired wavelength.

A number of conflicting factors must be considered when selecting the laser (excitation) wavelength in addition to laser performance parameters such as the pulse energy, width, and repetition rate, and the beam divergence. Reasons for choosing near UV excitation (in the region of 337 nm) are:

(a) 337 nm lies close to the optimum wavelength for exciting fluorescence in the dissolved organics present in most fresh waters. The maxima for the fluorescence emission spectra obtained on the 161 fresh water samples of this survey with excitation at 337 nm were located in a relatively narrow (24-nm wide) band centered at 428 nm. With excitation shifted to the blue region, the fluorescence emission spectra will become severely attenuated and truncated in relation to those produced by near UV excitation such as that for the Lake Mead sample shown in Figure 2. This produces a marked shift in  $\lambda_{\max}$  to longer wavelengths together with a marked reduction in  $F_{\max}$ .

(b) The intensity of the Raman emission exhibits a  $\lambda_L^{-4}$  dependence on the excitation wavelength.

(c) Photomultipliers, which are used to detect the fluorescence and Raman signals, are generally more sensitive in the near UV and blue spectral regions.

On the other hand, several reasons exist for employing lasers that operate in the blue spectral region. These are:

(a) Laser excitation in the blue region results in attenuation coefficients for the laser, Raman and fluorescence wavelengths that have values closer to the minimum for attenuation in natural waters than do the coefficients for near UV excitation. Although these reductions in  $k_L$ ,  $k_R$  and  $k_F$  are not expected to effect a significant change in  $F_\lambda/R$ , they will increase  $F_\lambda$  and  $R$ , as predicted by, respectively, Equations 1 and 2. This, in turn, results in an increase in the sensitivity with which  $F_\lambda/R$  can be measured.

(b) By choice of a suitable blue wavelength, the Raman band can be shifted to the peak of the fluorescence band. The separation of  $F_R$  and  $R$  by the process of linear interpolation using three spectral measurements is more reliably performed when the narrow Raman band lies at the peak of the relatively broad fluorescence band than if it were located on the side of the fluorescence band as occurs in Figure 2. In addition, the preferred parameter,  $F_R/R$ , becomes equivalent to  $F_{\max}/R$  under these circumstances.

(c) Visible rather than UV excitation results in reduced atmospheric scattering losses to the laser, Raman and fluorescence signals.

(d) Visible rather than UV excitation generally tends to reduce the background fluorescence induced in the optics and other materials of construction used in the laser fluorosensor.

(e) By employing excitation in the blue spectral region, it is possible to use the laser fluorosensor to monitor phytoplanktonic chlorophyll a as well

as DOC. The optimum wavelength for exciting chlorophyll a lies in the region of 436 nm with emission of 685 nm. Both fluorescence signals can then be corrected for variations in optical attenuation using the same Raman signal.

#### IMPROVEMENTS IN EXPERIMENTAL METHODOLOGY

In addition to the inherent limitations to the fluorescence organic carbon correlation technique described above, it is likely that a number of shortcomings in experimental methodology have tended to reduce the degree of correlation between  $F_R/R$  and DOC, particularly with regard to the DOC analyses. These factors together with possible corrective action are discussed as follows:

- (i) Use of (Whatman GF/F) glass fiber filters in the preparation of the DOC samples may lead to variability in the DOC data due to adsorption of COC. It is suggested that this problem can be avoided by using nonadsorbing 0.8- $\mu$ m pore size silver membrane filters.

This expedient also has the advantage of including the potentially fluorescent COC material in the DOC fraction.

- (ii) HCl added to the DOC and TOC samples for driving off inorganic carbon (in form of  $CO_2$ ) and arresting bacterial activity was seen to introduce a carbon background on the order of 0.4 mg/l. It is suggested that high purity phosphoric acid be used instead of HCl (Gordon and Sutcliffe, 1973).

- (iii) The polyethylene bottles used for transporting and storing the TOC and DOC samples introduced a carbon background on the order of 0.05 mg/l per day. Delhez (1960) has noted that the UV absorption of distilled water stored in polyethylene bottles increases with time, suggesting that soluble organics are being leached from the plastic. Symons et al. (1975) have suggested that this problem be avoided by using glass sample vials that are sealed with PTFE-lined caps, and muffled prior to use at 400°C for at least one hour to drive off any organic matter that might interfere with the TOC or DOC analyses. Alternatively, sample contamination can be avoided by immediately sealing the samples in clean glass ampoules at the collection site, particularly when the samples must be transported over large distances or stored for extended periods of time prior to analysis. The latter expedient will eliminate all possibility of contamination prior to analysis and will also allow the volatile organic fraction to be retained for those situations that allow for their inclusion in the analysis.

- (iv) A nonuniform distribution of POC in the master sample prior to partitioning into subsamples for the TOC, DOC and fluorescence analyses can produce errors in the TOC measurements. Care must be taken to ensure that the master sample is thoroughly stirred or homogenized prior to subsampling.

- (v) The reproducibility of the TOC and DOC determinations, presently on the order of  $\pm 0.1$  mg/l at the 1 mg/l level, can be improved to  $\pm 0.01$  mg/l by using TOC analyzers that employ 1-ml sample injections instead of the 10- $\mu$ l sample injections used by the TOC analyzer in the present study. However, higher precision also demands that extreme care be taken to avoid contamination of the samples or the TOC analyzer.
- (vi) Problems associated with contamination of the filters (glass fiber or silver membrane), which can occur during manufacture or during preparation of the DOC samples, should be avoided by precombustion and careful handling.
- (vii) Leakage of undispersed stray light from the excitation monochromator is not a problem when examining the fluorescence of clear liquid samples. However, when turbid samples are being examined, a significant background signal is produced by scattering from the suspended particulates. As the concentration of these particulates is generally unrelated to the intensity of the sample fluorescence, this background signal can make a marked and random contribution to  $F_\lambda$ , particularly in the region close to the excitation wavelength. This is seen to produce a reduction in the degree of correlation between  $F_\lambda/R$  and DOC, particularly at shorter wavelengths; as this background is relatively broad, it does not influence the measurement of R.

This background signal can be eliminated by inserting a narrow passband filter into the excitation beam centered at the excitation wavelength. Alternatively the intensity of this stray light can be reduced by improved baffling within the excitation monochromator or by using a double monochromator.

Elimination of this background signal by removal of the sample particulates is, unfortunately, not practicable as the samples would no longer be representative of those seen by an airborne laser fluorosensor. First, filtration will remove fluorescent particulate material from the sample and, second, even if non-adsorbing silver membrane filters were used to avoid loss of potentially fluorescent COC, the suspended colloidal material passing the filter would still produce a scattered background signal.

## DETAILED PRESENTATION OF CONCLUSIONS

A number of important findings that have implications in the design and operation of an airborne laser fluorosensor for monitoring surface water organics are presented together with a brief discussion of the reasoning involved.

- (i) It has been shown that the fluorescence data must be normalized using the concurrent water Raman intensity data in order to correct

for sample-to-sample variations in optical attenuation and to make the fluorescence data independent of variations in spectrofluorometer sensitivity. In an airborne laser fluorosensor application, this data correction procedure becomes an absolute necessity because of large variations in optical attenuation that occur from place to place and also because of significant variations that can occur with system sensitivity, particularly those involving laser output power.

Use of the concurrent water Raman return as a measure of the variation in laser beam penetration is ideal because it requires no information concerning the theoretical form of the attenuation coefficient, whether it be the beam attenuation coefficient, the diffuse attenuation coefficient or some intermediate model. Also, the Raman emission emanates from essentially the same sample volume as the fluorescence emission and therefore makes an accurate correction for changes in the attenuation properties, particularly when using  $F_R/R$  as an indicator of DOC. Also,  $F_\lambda/R$ , unlike  $F_\lambda$ , is independent of  $1/H^2$  variations in received signal intensity produced by changes in  $H$ , the elevation of the sensor above the water surface.

- (ii) As already suggested, the airborne measurement of  $R$  can be used to provide a continuous measurement of  $k_\lambda$  provided that the airborne data are calibrated by making a number of concurrent ground truth measurements of  $k_\lambda$  at reference sites under the aircraft flight path. In addition, if a sufficiently wide range of  $k_\lambda$  values is encountered, it might also be possible to determine whether  $k_\lambda$ , the attenuation coefficient used in the laser fluorosensor equations, is more appropriately described by the diffuse attenuation coefficient or by the beam attenuation coefficient.
- (iii) On the basis of the reported correlation data, the fluorescence signal to Raman signal ratio,  $F_\lambda/R$ , appears to be the fluorescence parameter offering the most promise as a remote sensing indicator of waterborne organic carbon, specifically DOC. The significantly lower correlations between  $F_\lambda/R$  and TOC appear to be due to the variability in POC concentration in relation to that for DOC in combination with the fact that the POC fraction appears to be less fluorescent than the accompanying DOC. The ability to remotely monitor DOC rather than TOC may be an advantage as the presence of DOC in untreated sources of drinking water is currently generating much concern. In the absence of specific procedures for their removal, natural dissolved organics such as the humic and fulvic acids are able to penetrate through a drinking water treatment plant and undergo conversion into potentially carcinogenic trihalomethanes during routine chlorination (Youssefi et al., 1978).
- (iv) Although  $F_{\max}/R$  exhibits the highest correlation with DOC ( $r = 0.83$ ), there are compelling reasons for preferring  $F_R/R$  as the chosen remote sensing parameter for characterizing surface water organic carbon. The correlation between  $F_R/R$  and DOC ( $r = 0.78$ ), which is not significantly different from that involving  $F_{\max}/R$  at

the 5 percent level, was shown to be lower due to the interference from an instrumental artifact in which undispersed stray light that leaks from the excitation monochromator is scattered by sample particulates and becomes irretrievably mixed with the fluorescence emission. The influence of this relatively broadband background was most marked in the fluorescence data obtained in the near UV region, which includes the Raman band wavelength at 381 nm, but was considered to be insignificant at the wavelength of maximum emission close to 430 nm; this broadband background does not, however, affect the measurement of  $R$ , the intensity for the relatively narrow Raman emission band. It is likely that, in the absence of this near-UV background,  $F_R/R$  will exhibit the same degree of correlation with DOC as does  $F_{\max}/R$ .

There are two significant advantages to using  $F_R/R$  over  $F_{\max}/R$  as a measure of surface water DOC in remote sensing applications. First, because both  $F_R$  and  $R$  are measured at the same wavelength, interference by differential spectral absorption and scattering does not occur. The same is not true for  $F_{\max}/R$  as differential spectral effects between the measurements made at  $\lambda_R$  and  $\lambda_{\max}$  are known to be present by virtue of the strong correlation between  $F_{\max}/F_R$  and DOC ( $r = 0.78$ ). The second advantage concerns the fact that, in an airborne laser fluorosensor system employing discrete detector and recording channels for each spectral measurement, the determination of  $F_R/R$  requires only three spectral detector channels whereas that for  $F_{\max}/R$  requires four such channels.

## REFERENCES

- Almgren, T., B. Joseffson and G. Nyquist. 1975. A Fluorescence Method for Studies of Spent Sulfite Liquor and Humic Substances in Sea Water. *Anal. Chim. Acta*, 78:411-422.
- Andelman, J. B. and M. J. Suess. 1970. Polynuclear Aromatic Hydrocarbons in the Water Environment. *Bull. Wld. Hlth. Org.* 43:479-508.
- Austin, R. W. 1974. Problems in Measuring Turbidity as a Water Quality Parameter. Proceedings of Seminar on Methodology for Monitoring the Marine Environment, Seattle, Washington. October 16-18, 1973. Report No. EPA-600/4-74-004, October 1974, Office of Monitoring Systems, U.S. Environmental Protection Agency, Washington, D.C.
- Averso, S. J. 1976. Glass-Fiber Filter Paper. *American Laboratory* 8:97-104.
- Baumgartner, D. J., M. H. Feldman and C. L. Gibbons. 1971. A Procedure for Tracing Kraft Mill Effluent from an Ocean Outfall by Constituent Fluorescence. *Water Research*, 5:533-544.
- Black, A. P. and R. F. Christman. 1963. Characteristics of Colored Surface Waters. *Jour. A.W.W.A.* 55:753-770.
- Bowker, D. E. and W. G. Witte. 1977. The Use of LANDSAT for Monitoring Water Parameters in the Coastal Zone. Proc. of AIAA 1977 Joint Conference on Satellite Applications of Marine Operations, New Orleans, Louisiana, November 15-18, 1977.
- Briggs, R., J. W. Schofield and P. A. Gorton. 1976. Instrumental Methods of Monitoring Organic Pollution. *Wat. Pollut. Control*, 75:47-57.
- Bristow, M. P. F. 1979. Fluorescence of Short Wavelength Cutoff Filters. *Appl. Optics* 18:952-955.
- Bristow, M. P. F. 1978. Airborne Monitoring of Surface Water Pollutants by Fluorescence Spectroscopy. *Remote Sensing of Environment* 7:105-127.
- Bristow, M., D. Nielsen and R. Furtek. 1979. A Laser-Fluorosensor Technique for Water Quality Assessment. Proceedings of the 13th International Symposium on Remote Sensing of the Environment. Environmental Research Institute of Michigan, Ann Arbor, Michigan. April 23-27, 1979, pp. 397-417.

- Browell, E. V. 1977. Analysis of Laser Fluorosensor Systems for Remote Algae Detection and Quantification. NASA Technical Note TN D-8447, NASA, Washington, D.C., June 1977.
- Buelow, R. W., J. K. Carswell and J. M. Symons. 1973. An Improved Method for Determining Organics by Activated Carbon Adsorption and Solvent Extraction-Part I. Jour. A.W.W.A. 65:57-72.
- Cahn, R. D. 1967. Detergents in Membrane Filters. Science, 155:195-196
- Chandler, R. L., J. C. O'Shaughnessy and F. C. Blanc. 1976. Pollution Monitoring with Total Organic Carbon Analysis. Jour. Water Poll. Control Fed. 48:2803-2791.
- Chang, C. H. and L. A. Young. 1974. Seawater Temperature Measurement from Raman Spectra. AVCO Research Note 960, January, 1974. AVCO Everett Research Laboratory, Inc., Everett, Massachusetts.
- Christman, R. F. and R. A. Minear. 1967. Fluorometric Detection of Lignin Sulfonates. Trend in Eng. 19:3-7.
- Constable, T. W. and E. R. McBean. 1979. BOD/TOC Correlations and Their Application to Water Quality Evaluation. Water, Air and Soil Pollution. 11:363-375.
- Davis, E. M. and W. J. Fosbury. 1973. Application of Selected Methods of Remote Sensing for Detecting Carbonaceous Water Pollution. Canada Centre for Inland Waters: Hamilton, Ontario. June 1973. Proceedings #17: Remote Sensing and Water Resources Management (Edited by K. P. B. Thompson, R. K. Lane and S. C. Csallany); American Water Resources Association, Urbana, Illinois, 1973.
- Delhez, R. 1960. Ultraviolet Absorption Spectrum of Water Stored in Polyethylene Bottles. Chemist-Analyst 49:20-21.
- DeMent, J. and H. C. Dake. 1942. Fluorescent Chemicals and their Applications. Chemical Publishing Co., Inc. New York.
- Dienert, F. 1910. De la recherche des substances fluorescent dans le controle de la sterilisation des eaux. Compt. Rend. Acad. Sci. (Paris) 150:487-488.
- Dishman, R. A. 1979. Automation of Laboratory Organic Carbon Analysis. Am. Lab. 11:97-111.
- Dixon, W. J. 1975. Biomedical Computer Programs (BMDP). University of California Press, Berkeley.
- Dobbs, R. A., R. H. Wise and R. B. Dean. 1972. The Use of Ultra-Violet Absorbance for Monitoring the Total Organic Carbon Content of Water and Wastewater. Water Research 6:1173-1180.



- Duurmsa, E. K. 1974. The Fluorescence of Dissolved Organic Matter in the Sea. Chapter 11 in Optical Aspects of Oceanography. Edited by N. G. Jerlov and E. Steeman Nielsen. Academic Press, New York.
- Fantasia, J. F. and H. C. Ingrao. 1974. Development of an Experimental Airborne Laser Remote Sensing System for the Detection and Classification of Oil Spills. Proceedings of the 9th International Symposium on Remote Sensing of the Environment, Environmental Research Institute of Michigan, Ann Arbor, Michigan, April 15-19, 1974, pp. 1711-1745.
- Farmer, F. H., C. A. Brown, O. Jarrett, J. W. Campbell and W. Staton. 1979. Remote Sensing of Phytoplankton Density and Diversity in Narragansett Bay using an Airborne Fluorosensor. Proceedings of the 13th International Symposium on Remote Sensing of the Environment. Environmental Research Institute of Michigan, Ann Arbor, Michigan, April 23-27, 1979. pp. 1793-1805.
- Friedman, E. J. and Hickman, G. D. 1972. Laser Induced Fluorescence in Algae: A New Technique for Remote Detection. Final Report, October 1972. Sponsored by NASA Wallops Island under Contract No. NAS 6-2081. Sparcom, Inc., Alexandria, Virginia.
- Gasith, A. and A. D. Hasler. 1976. Airborne Litterfall as a Source of Organic Matter in Lakes. Limnol. Oceanogr. 21:253-258.
- Gilson, T. R. and P. J. Hendra. 1970. Laser Raman Spectrometry. Wiley-Interscience, New York.
- Gordon, D. C. and W. H. Sutcliffe. 1973. A New Dry Combustion Method for the Simultaneous Determination of Total Organic Carbon and Nitrogen in Seawater. Marine Chemistry, 1:231-244.
- Gordon, D. D. and W. H. Sutcliffe. 1974. Filtration of Seawater using Silver Filters for Particulate Nitrogen and Carbon Analysis. Limnol. Oceanogr. 19:989-993.
- Goulden, P. D. 1976. Automated Determination of Carbon in Natural Waters. Water Research. 10:487-490.
- Guillard, R. R. L. and P. J. Wangersky. 1958. The Production of Extracellular Carbohydrates by Some Marine Flagellates. Limnol. Oceanogr. 3:449-454.
- Hall, K. J. and G. F. Lee. 1974. Molecular Size and Spectral Characterization of Organic Matter in a Meromictic Lake. Water Research, 8:239-251.
- Huro, K., T. Tanaka and A. Kawahara. 1977. Measurement of Organic Pollutants in Coastal Sea Water by Fluorescence Method. Bunseki Kagaku 26:574-575. In Japanese. (Translation obtained from F. E. Hoge, NASA Wallops, Wallops Island, Virginia)

- Hwang, C. P., T. H. Lockie and R. R. Munch. 1979. Correction for Total Organic Carbon, Nitrate, and Chemical Oxygen Demand when Using the MF-Millipore Filter. *Environ. Sci. Technol.* 13:871-872.
- Jerlov, N. G. 1976. *Marine Optics*, Elsevier/North Holland Inc., New York.
- Johnson, R. W., I. W. Duedall, R. M., Glasgow, J. R. Proni and T. A. Nelsen. 1977. Quantitative Mapping of Suspended Solids in Wastewater Sludge Plumes in the New York Bight Apex. *Jour. Water Poll. Control Fed.* 49:2063-2073.
- Johnson, R. W. 1978. Mapping of Chlorophyll a Distributions in Coastal Zones. *Photogrammetric Engineering and Remote Sensing.* 44:617-624.
- Kalle, K. 1966. The Problem of Gelbstoff in the Sea. *Oceanogr. Mar. Biol. Ann. Rev.* 4:91-104.
- Kehoe, T. J. 1977. Determining TOC in Waters. *Environ. Sci. Technology* 11:137-139.
- Kerfoot, W. B. and E. C. Brainard. 1978. Septic Tank Leachate Detection. A Technological Breakthrough for Shoreline On-lot System Performance Evaluation. In: *State of Knowledge in Land Treatment of Wastewater.* Edited by H. L. McKim. International Symposium at the Cold Regions Research and Engineering Laboratory, Hanover, New Hampshire, pp. 325-334.
- Kim, H. H. and G. D. Hickman. 1975. An Airborne Laser Fluorosensor for the Detection of Oil on Water. In: *The Use of Lasers for Hydrographic Studies*, NASA Wallops Island, Virginia, September 12, 1973. NASA Special Publication SP 375, Washington, D.C. pp. 197-202.
- Lakshman, G. 1975. Monitoring Agricultural Pollution Using Natural Fluorescence. *Water Resources Research* 11:705-708.
- Lammers, W. T. 1971. Insoluble Material in Natural Waters. In: *Water and Water Pollution Handbook*, Vol. 2. Edited by L. J. Ciaccio. Marcel Dekker Inc., New York. pp. 593-635.
- Levesque, M. 1972. Fluorescence and Gel Filtration of Humic Compounds. *Soil Science* 113:346-353.
- Lock, M. A., P. M. Wallis and H. B. N. Hynes. 1977. Colloidal Organic Carbon in Running Waters. *Oikos*, 29:1-4.
- MacKinnon, M. D. 1979. The Measurement of the Volatile Organic Fraction of TOC in Seawater. *Marine Chemistry* 8:143-162.
- Maier, W. J. and W. R. Swain. 1978. Organic Carbon - A Non Specific Water Quality Indicator for Lake Superior. *Water Research* 12:523-529.
- Mattson, J. S., C. A. Smith, T. T. Jones and S. M. Gerchakov. 1974. Continuous Monitoring of Dissolved Organic Matter by UV-Visible Photometry. *Limnol. Oceanogr.* 19:530-535.

- McLean, R. A. and M. L. Speas. 1946. Fluorescence of Drinking Waters as Evidence of Sewage Pollution. Jour. A.W.W.A., 38:355-360.
- Meakin, J. C. and M. C. Pratt. 1972. Whatman Manual of Laboratory Filtration. W. and R. Balston Ltd., Maidstone, England.
- Measures, R. M., J. Garlick, W. R. Houston and D. G. Stephenson. 1975. Laser Induced Spectral Signatures of Relevance to Environmental Sensing. Can. Remote Sensing Journal, 1:95-102.
- Michalek, S. A., R. A. Dishman and R. B. Thayer. 1977. Capabilities of On-Line TOC and TOD Analyzers. Progr. Wat. Tech. 9:87-92. Pergamon Press, Oxford.
- Miller, J. R., S. C. Jain, N. T. O'Neill, W. R. McNeil and K. P. B. Thompson. 1977. Interpretation of Airborne Spectral Reflectance Measurements over Georgian Bay. Remote Sensing of Environment 5:183-200.
- Montalvo, J. G. and C. G. Lee. 1976. Analytical Notes - Removal of Organics from Water: Evaluating Activated Carbon. Jour. A.W.W.A. 68:211-215.
- Morel, A. and L. Prieur. 1977. Analysis of Variations in Ocean Color. Limnol. Oceanogr. 22:709-722.
- Nriagu, J. O. and R. D. Coker. 1980. Trace Metals in Humic and Fulvic Acids from Lake Ontario Sediments. Env. Sci. Technol. 4:443-446.
- Ogner, G. and M. Schnitzer. 1970. Humic Substances: Fulvic Acid-Dialkyl Phthalate Complexes and their Role in Pollution. Science, 170:317-318.
- O'Neil, R., L. Buja-Bijunas, and D. M. Rayner, 1980. Field performance of a laserfluoresensor for the detection of oil spills. Appl Opt. 19:863-870.
- O'Neil, R. A., A. R. Davis, H. G. Gross and J. Kruus. 1975. A Remote Sensing Laser Fluorometer. Water Quality Parameters. ASTM STP 573, American Society for Testing Materials. pp. 424-436.
- Parker, B. C. 1967. Influence of Method for Removal of Seston on the Dissolved Organic Matter. J. Phycol., 3:166-173.
- Porro, T. J., R. E. Anacreon, P. S. Flandreau and I. S. Fagerson. 1973. Corrected Fluorescence Spectra of Polynuclear Materials and their Principal Applications. Journal of the A.O.A.C. 56:607-620.
- Radley, J. A. and J. Grant. 1935. Fluorescence Analysis in Ultra-Violet Light. Chapman Hall Ltd., London.
- Reiswig, H. M. 1972. The Spectrum of Particulate Organic Matter of Shallow-Bottom Boundary Waters of Jamaica. Limnol. Oceanogr., 17:341-348.
- Riley, G. A. 1970. Particulate Organic Matter in Sea Water. Adv. Mar. Biol. 8:1-118.

- Rook, J. J. 1977. Chlorination Reactions of Fulvic Acids in Natural Waters. *Env. Sci. Technol.* 11:478-482.
- Salonen, K. 1979. Comparison of Different Glass Fibre and Silver Metal Filters for the Determination of Particulate Organic Carbon. *Hydrobiologia* 67:29-32.
- Schnitzer, M. 1971. Metal-Organic Matter Interactions in Soils and Waters. Chapter 13. In: *Organic Compounds in Aquatic Environments* (Edited by S. J. Faust and J. V. Hunter). pp. 297-313. Marcel Dekker, New York.
- Seal, B. K., K. B. Roy and S. K. Mukherjee. 1964. Fluorescence Emission Spectra and Structure of Humic and Fulvic Acids. *Jour. Indian Chem. Soc.* 41:212-214.
- Sharp, J. H. 1973. Size Classes of Organic Carbon in Seawater. *Limnol. Oceanogr.*, 18:441-447.
- Sharp, J. H. 1974. Improved Analysis for "Particulate" Organic Carbon and Nitrogen from Seawater. *Limnol. Oceanogr.* 19:984-989.
- Sheldon, R. W. 1972. Size Separation of Marine Seston by Membrane and Glass-Fiber Filters. *Limnol. Oceanogr.* 17:494-498.
- Smart, P. L., B. L. Finlayson, W. D. Rylands and C. M. Ball. 1976. The Relation of Fluorescence to Dissolved Organic Carbon in Surface Waters. *Water Research*, 10:805-811.
- Sontheimer, H. 1977. Samples of Rhine Water Reveal Organic Carbon Content. *Water and Wastes Engineering* 14:24-27.
- Stevens, A. A. and J. M. Symons. 1974. Measurement of Organics in Drinking Water. *Proceedings A.W.W.A. Water Quality Technology Conference*. pp. xxiii-1-xxiii-25, December 2-3, 1973, Cincinnati, Ohio. A.W.W.A., Denver, Colorado.
- Sydor, M., K. R. Stortz and W. R. Swain. 1978. Identification of Contaminants in Lake Superior through Landsat I Data. *J. Great Lakes Res.* 4:142-148.
- Sylvia, A. E. 1973. Detection and Measurement of Microorganics in Drinking Water. *Jour. New England Water Works Assoc.* 87:183-199.
- Sylvia, A. E., D. A. Bancroft and J. D. Miller. 1974. Detection and Measurement of Microorganics in Drinking Water by Fluorescence. In *Proc. A.W.W.A. Water Quality Technology Conference*, Dallas, Texas, December 2-3, 1974.
- Sylvia, A. E., D. A. Bancroft and J. D. Miller. 1977. Analytical Note-A Method for Evaluating Granular Activated Carbon Adsorption Efficiency. *Jour. A.W.W.A.*, 69:99-102.

Symons, J. M., T. A. Bellar, J. K. Carswell, J. DeMarco, K. L. Kropp, G. G. Robeck, D. R. Seeger, C. J. Slocum, B. L. Smith and A. A. Stevens. 1975. National Organics Reconnaissance Survey for Halogenated Organics. Jour. A.W.W.A., 67:634-647.

Tardiff, R. G. 1977. Health Effects of Organics: Risk and Hazard Assessment of Ingested Chloroform. Jour. A.W.W.A. 69:658-661.

Thruston, A. D. 1970. A Fluorometric Method for the Determination of Lignin Sulfonates in Natural Waters. J. Wat. Pollut. Control Fed. 42:1551-1555.

Trussell, R. R. and M. D. Umphres. 1978. The Formation of Trihalomethanes. Jour. A.W.W.A. 70:604-612.

Wakeham, S. G. 1977. Synchronous Fluorescence Spectroscopy and its Application to Indigenous and Petroleum-Derived Hydrocarbons in Lacustrine Sediments. Environ. Sci. Technology, 11:272-276.

Walden, C. C. 1976. The Toxicity of Pulp and Paper Mill Effluents and Corresponding Measurement Procedures. Water Research 10:639-664.

Walrafen, G. E. 1967. Raman Spectral Studies of the Effects of Temperature on Water Structure. J. Chem. Phys. 47:114-126.

Wangersky, P. J. 1972. The Cycle of Organic Carbon in Sea Water. Chimia, 26:559-564.

Wangersky, P. J. 1975. Measurement of Organic Carbon in Seawater. In: Analytical Methods in Oceanography. Edited by T.R.P. Gibb, Jr. Advances in Chemistry Series, 147:148-162. American Chemical Society, Washington, D.C.

Wangersky, P. J. 1978. Production of Dissolved Organic Matter. In: Marine Ecology, Volume IV, Dynamics, Edited by Otto Kinne. Wiley Interscience, New York.

Wilander, A., H. Kvarnas and T. Lindell. 1974. A Modified Fluorometric Method for Measurement of Lignin Sulfonates and its in situ application in natural waters. Water Research, 8:1037-1045.

Wilson, W. H., R. W. Austin and R. C. Smith. 1978. Optical Remote Sensing of Chlorophyll in Ocean Waters. Proceedings of the 12th International Symposium on Remote Sensing of the Environment, April 20-25, 1978, Manila, Philippines. Environmental Research Institute of Michigan, Ann Arbor, Michigan.

Youssefi, M., S. T. Zenchelsky and S. D. Faust. 1978. Chlorination of Naturally Occuring Organic Compounds in Water. J. Environ. Sci. Health A13:629-637.

Zimmerman, A. and A. R. Bandy. 1975. The Application of Laser Raman Scattering to Remote Sensing of Salinity and Turbidity. Final Technical Report under NASA Contract NAS1-1107, August 1975.

<b>TECHNICAL REPORT DATA</b> <i>(Please read instructions on the reverse before completing)</i>		
1. REPORT NO. EPA-600/4-81-001	2.	3. RECIPIENT'S ACCESSION NO.
4. TITLE AND SUBTITLE REMOTE MONITORING OF ORGANIC CARBON IN SURFACE WATERS	5. REPORT DATE February 1981	6. PERFORMING ORGANIZATION CODE
7. AUTHOR(S) Michael Bristow and David Nielsen	8. PERFORMING ORGANIZATION REPORT NO.	
9. PERFORMING ORGANIZATION NAME AND ADDRESS Environmental Monitoring Systems Laboratory Office of Research and Development U.S. Environmental Protection Agency Las Vegas, Nevada 89114	10. PROGRAM ELEMENT NO.	11. CONTRACT/GRANT NO.
12. SPONSORING AGENCY NAME AND ADDRESS U.S. Environmental Protection Agency-Las Vegas, NV Office of Research and Development Environmental Monitoring Systems Laboratory Las Vegas, NV 89114	13. TYPE OF REPORT AND PERIOD COVERED	14. SPONSORING AGENCY CODE EPA/600/07
15. SUPPLEMENTARY NOTES		
16. ABSTRACT <p>This study shows that the intensity of the Raman normalized fluorescence emission induced in surface waters by ultraviolet radiation can be used to provide a unique remote sensing capability for airborne monitoring the concentration of dissolved organic carbon (DOC). Trace concentrations of hydrocarbons, both manmade and natural in origin, are the predominant source for this fluorescence. Water, on the other hand, is nonfluorescent under UV irradiation, but emits an intense Raman band of constant amplitude relative to the incident light. This Raman emission can be used as an internal reference or normalizing standard with which to correct the fluorescence emission for the effects of attenuation, for variations in system sensitivity, and for changes in sensor elevation. It is suggested that a direct calibration of the airborne fluorescence data in terms of equivalent DOC concentration be accomplished by making DOC measurements on samples obtained at a small number of reference sites under the aircraft flight path at the time of the airborne survey.</p> <p>Airborne laser fluorosensors that utilize this principle will provide a synoptic survey capability for rapidly and cost-effectively producing isopleth maps that show concentrations of surface water DOC. These isopleths can be used for delineating gradients, temporal changes and anomalies in the distribution of total dissolved organics in the surface layers of rivers, lakes and costal waters.</p>		
17. KEY WORDS AND DOCUMENT ANALYSIS		
a. DESCRIPTORS	b. IDENTIFIERS/OPEN ENDED TERMS	c. COSATI Field/Group
hydrocarbons surface water ultraviolet irradiation water pollution	laser fluorosensing airborne platforms	48G 63C 68D
18. DISTRIBUTION STATEMENT RELEASE TO PUBLIC	19. SECURITY CLASS (This Report) UNCLASSIFIED	21. NO. OF PAGES 93
	20. SECURITY CLASS (This page) UNCLASSIFIED	22. PRICE